Biotransformation Capacity of Reconstructed Human Skin versus Human Skin *ex vivo* - analysing Prednicarbate and Testosterone as Example

DISSERTATION

Zur Erlangung des akademischen Grades

des Doktors der Naturwissenschaften (Dr. rer. nat.)

eingereicht im Fachbereich Biologie, Chemie, Pharmazie

der Freien Universität Berlin

vorgelegt von

Wiebke Antonia Klipper

aus Lüdinghausen

Berlin, November 2013

1. Gutachter: Frau Professor Dr. Monika Schäfer-Korting

Institut für Pharmazie, Pharmakologie

Freie Universität Berlin

Königin-Luise-Straße 2 + 4

14195 Berlin

2. Gutachter: Frau Professor Dr. Maria Kristina Parr

Institut für Pharmazie, Medizinische Chemie

Freie Universität Berlin

Königin-Luise-Straße 2 + 4

14195 Berlin

Datum der Disputation: 7. April 2014

Die vorliegende Arbeit wurde auf Anregung und unter Anleitung von

Frau Professor Dr. Monika Schäfer-Korting

in der Abteilung für Pharmakologie und Toxikologie des Instituts für Pharmazie der Freien Universität Berlin im Zeitraum von März 2009 bis November 2011 angefertigt.

Für

meine Familie

DANKSAGUNG

Mein besonderer Dank gilt Frau Professor Dr. Monika Schäfer-Korting für die Vergabe des äußerst interessanten Dissertationsthemas, die unentwegte Unterstützung im Verlauf der Arbeit sowie ihre Bereitschaft zu vielen anregenden Diskussionen. Ihre wissenschaftliche Kompetenz und Gesprächsbereitschaft haben wesentlich zur erfolgreichen Durchführung dieser Dissertation beigetragen.

Frau Professor Dr. Maria Kristina Parr möchte ich herzlich für die Erstellung des Zweitgutachtens danken.

Herrn Professor Dr. Günther Weindl danke ich ganz herzlich für die stete und zuverlässige Unterstützung, die vielen konstruktiven Anregungen und Hinweise sowie sein stets überaus großes Engagement und die geduldige, zuverlässige Hilfsbereitschaft!

Herrn Professor Dr. Hans-Christian Korting, Dermatologische Klinik und Poliklinik, Ludwig-Maximilians-Universität, München, danke ich für seine Kooperation innerhalb des Projektes und seine freundliche Unterstützung der Arbeit, insbesondere bei histologischen Fragestellungen.

Danken möchte ich ferner Herrn Dr. med. Uwe von Fritschen, Chefarzt der Klinik für Plastische und Ästhetische Chirurgie, HELIOS Klinikum Emil von Behring Berlin- Zehlendorf, für die Überlassung der exzidierten Humanhaut. Ohne die gute Zusammenarbeit und sein Engagement wäre diese Arbeit in der vorliegenden Form nicht möglich gewesen.

Allen Mitgliedern des Arbeitskreises danke ich herzlich für die vielen hilfreichen Diskussionen, fachlichen Ratschläge sowie das freundschaftliche Arbeitsklima und die angenehme Zusammenarbeit. Hervorzuheben ist mein Dank insbesondere gegenüber

- Frau Dr. Sarah Heilmann, in der ich nicht nur eine zuverlässige Kollegin, sondern auch eine sehr gute Freundin gefunden habe! Vielen Dank für die vielen Diskussionen, Ratschläge, für dein stets offenes Ohr in beruflichen sowie privaten Bereichen sowie die privaten Aktivitäten außerhalb der Forschung, liebe Sarah!
- Frau Dominika Henkes, Frau Nhung Do-Sydow und Frau Maja Natek für wissenschaftliche und private Diskussionen und ihre stets liebenswürdige Art, mit der sie mir die Mittagspausen und sehr viele weitere Momente, auch außerhalb des wissenschaftlichen Arbeitens, versüßt haben!
- Frau Franzisca Marie Bätz für die gute Zusammenarbeit innerhalb des Projektes und besonders für ihre grenzenlose Geduld, die sie mitunter auf mich übertragen konnte.
- Frau Gabriele Roggenbuck-Kosch für Ihr stets offenes Ohr und ihre Hilfsbereitschaft in allen Lebenslagen!

- Frau Barbara Brüggener für die technische Unterstützung bei der Erstellung der Veröffentlichungen.
- Frau Hannelore Gonska, der ich für die Hilfe bei der Isolierung und Kultivierung humaner Hautzellen und darüber hinaus für viele aufmunternde Worte danke.
- Herrn Matthias Worch danke ich für die tatkräftige Unterstützung bei allen EDV-relevanten Fragen.

Herrn Dr. Dr. Andreas Luch, Herrn Dr. Frank Henkler und Herrn Dr. Joep Brinkmann vom Bundesinstitut für Risikobewertung, Frau Dr. Kerstin Reisinger (Henkel AG, Düsseldorf), Herrn Dr. Robert Landsiedel, Frau Dr. Christine Jäckh und Frau Katharina Guth (BASF SE) sowie allen weiteren hier nicht explizit namentlich benannten Mitarbeitern des BMBF-Projektes danke herzlich ich für die stets gute Zusammenarbeit und die interessanten wissenschaftlichen Diskussionen.

Frau Johanna Laude und Frau Andrea Kieslinger, Dermatologische Klinik und Poliklinik, Ludwig-Maximilians-Universität, München, danke ich sehr für die Unterstützung der histologischen Untersuchungen.

Für die finanzielle Förderung der vorliegenden Arbeit danke ich dem Bundesministerium für Bildung und Forschung, Förderkennzeichen 0315226B.

Herrn Rainer Kembügler, Berthold Technologies, danke ich für die technische Hilfestellung bei der Einarbeitung des Flowstars.

Für die Durchsicht der Arbeit möchte ich mich bei Frau Dr. Sarah Heilmann herzlich bedanken.

Frau Barbara Heynen-Kaiser möchte ich sehr dafür danken, dass Sie mir mit großer Flexibilität vieles erleichtert hat.

Mein größter Dank gilt schließlich meiner Familie, insbesondere meiner Mutter, Frau Edith Klipper und meiner Schwester, Frau Angelika Franke, die mir den Weg bis zur Promotion ermöglicht und erleichtert haben, sowie Jörg Löbker - für die liebevolle, grenzenlose Unterstützung, die vielen aufmunternden Worte und Gesten und den ewigen Rückhalt, den ich bei euch finde!

Abbreviations

α	Separation factor
Ac	Acetonitrile
AD	Androstanedione
ADH	Alcohol dehydrogenase
ALDH	Aldehyde dehydrogenase
ADT	Androsterone
ALI	Air-liquid-interface
AST2000	Advanced Skin Test 2000
AUC	Area under the curve
$b_{0.5}$	Half height peak width
BM	Betamethasone
BMBF	Bundesministerium für Bildung und Forschung
BNPP	Bis(4-Nitro Phenyl) Phosphate
BPE	Bovine Pituitary Extract
BSA	Bovine Serum Albumin
Ca^{2+}	Calcium
$CaCl_2$	Caclium chloride
CE	Carboxylesterase
Cort.	Corticosterone
COX	Cyclooxygenase
cp	crossing points
CPM	Counts per Minute
C.V.	Coefficient of variation
CYP	Cytochrome P
D	Diameter
Da	Dalton
DEPC	Diethylpyrocarbonate

DHEA	Dehydroepiandrosterone
DHT	Dihydrotestosterone
dNTP	Deoxynucleotide(s)
ds-DNA	Double-stranded DNA
3-DIOL	Androstanediole
4-DIONE	Androstenedione
DMEM	Dulbecco´s Modified Eagle´s Medium
DMSO	Dimethylsulfoxide
E	Eserin (Physostigmine)
E_1	Estrone
E_2	17β-Estradiole
EC	European Commission
ECHA	European Chemical Agency
EDTA	Disodium ethylene-diamine tetraacetic acid
ELISA	Enzyme-linked Immunosorbent Assay
EURL ECVAM	European Union Reference Laboratory for Alternatives to Animal Testing
EU	Euopean Union
FBM	Fibroblasts Basal Medium
FCS	Foetal Calf Serum
FDA	Fluorescein diacetate
FGM	Fibroblasts Growth Medium
FMO	Flavin Monooxygenase
FT	Full thickness
GST	Gluthatione-S-transferase
HaCaT	Human adult keratinocytes, kept under low calcium and elevated temperature - spontaneously transformed keratinocyte cell line
HCl	Hydrogen chloride
hEGF	human Epidermal Growth Factor

HOT	6β-Hydroxytestosterone
3α-HSD	3α-Hydroxysteroid Dehydrogenase
3β-HSD	3β-Hydroxysteroid Dehydrogenase
17β-HSD	17β-Hydroxysteroid Dehydrogenase
HPLC	High Performance Liquid Chromatography
IL	Interleukin
I.S.	Internal Standard
IU	International Units
κ´	Retention factor
KBM	Keratinocytes Basal Medium
KCl	Potassium chloride
KGM	Keratinocytes Growth Medium
KH_2PO_4	Potassium dihydrogen orthophosphate
l	litre
LDH	Lactate Dehydrogenase
LLOQ	Lowest Limit of Quantification
LOD	Limit of Detection
Log P	Octanol-water partition coefficient
M	Molar mass
MEME	Minimum Essential Medium Eagle
Mg^+	Magnesium
M-MuLV reverse transcriptase	Moloney murine leukemia virus reverse transcriptase
mRNA	Messenger RNA
MTT	3-(4,5-dimethylthiazol-2-yl)-2,5-diphenyl tetrazolium bromide
min	minutes
NaF	Sodium fluoride
Na_2HPO_4	Disodium hydrogenphosphate

NaOH	Sodium hydroxide
NAT	N-Acetyltransferase
NC-IUBMB	Nomenclature Committee of the International Union of Biochemistry and Molecular Biology
NEMI	N-Ethylmaleimide
NHDF	Normal human dermal fibroblast(s)
NHK	Normal human keratinocyte(s)
OECD	Organisation for Economic Co-operation and Development
p	Passage
P17EC	Prednisolone 17-ethylcarbonate
P21EC	Prednisolone 21-ethylcarbonate
PBS	Phosphate buffered saline
PC	Prednicarbate (Prednisolone 17-ethylcarbonate, -21-propionate)
PMSF	Phenylmethanesulfonyl fluoride
(rt-)PCR	(Real time) polymerase chain reaction
PD	Prednisolone
PON	Arlyesterase
r^2	Correlation coefficient
5α–R	Steroid 5α–Reductase
Radio-HPLC	High Perfomance Liquid Chromatography with Radiodetection
REACH	Regulation on Registration, Evaluation, Authorisation and Restriction of Chemicals
RHE	Reconstructed Human Epidermis
RHS	Reconstructed (full thickness) Human Skin
R_S	Resolution
RT	Room temperature
SDHA	Succinat Dehydrogenase subunit A

SDS	Sodium dodecyl sulfate
SEM	Standard error of the mean
SKALP	Skin derived antileukoproteinase
SPRP	Small prolin rich protein
SOP	Standard Operating Procedure
SULT	Sulfotransferase
T	Testosterone
TBS	Tris-buffered Saline
TG	Test Guideline
TGD	Test Guidance Document
THF	Tetrahydrofuran
TMB	Tetramethylbenzidine
t_m	retention time – dead time (or breakthrough time)
t_r	(Total) retention time
Tris	Tris(hydroxymethyl)aminomethane
t_s	(Net) retention time
UDG	Uracil-DNA Glycosylase
UGT	UDP-glucuronosyltransferase
ULOQ	Upper Limit of Quantification
U/l	Units/l
UV	Ultraviolet

Publications

Manuscripts

F. Bätz*, W. Klipper*, H. C. Korting, F. Henkler, R. Landsiedel, A., U. von Fritschen, G. Weindl and M. Schäfer-Korting: Esterase Activity in Excised and Reconstructed Human Skin - Biotransformation of Prednicarbate and the Model Dye Fluorescein Diacetate. European Journal of Pharmaceutics and Biopharmaceutics 2013 Jun;84(2):374-85. Epub 2012 Nov 29.

**These authors contributed equally to this work*

Poster presentations

W. Klipper, G. Weindl, M. Schäfer- Korting: Biotransformation of Prednicarbate in Reconstructed Human Skin Models Compared to Excised Human Skin. Skin in Vitro Annual Meeting, Frankfurt-Main/Germany, June 2010

W. Klipper, F. M. Baetz, G. Weindl, M. Schäfer- Korting: Comparative Analysis of Esterase Activity in Reconstructed Human Skin Models and Excised Human Skin. 40th Annual ESDR Meeting, Helsinki/Finland, September 2010

D. Henkes, W. Klipper, H.C. Korting, M. Schäfer-Korting, S. Küchler: Investigating the Impact of Filaggrin on Skin Barrier Function in Vitro - A Step in the Direction of a Skin Model Mimicking Atopic Dermatitis? Perspectives in Percutanous Penetration 13th International Conference, La Grande Motte/France, April 2012

G. Weindl, F. M. Bätz, W. Klipper, F. Henkler, R. Landsiedel, A. Luch, U. von Fritschen, H. C. Korting, M. Schäfer-Korting: Esterase Activity in Excised and Reconstructed Human Skin - Biotransformation of Prednicarbate and the Model Dye Fluorescein Diacetate. EUSAAT 2012 - 14th Annual Congress of EUSAAT/Linz 2012 - 17th European Congress on Alternatives to Animal Testing, Linz/Austria, September 2012

Lecture

W. Klipper, G. Weindl, M. Schäfer- Korting: Biotransformation of Prednicarbate in Reconstructed Human Skin Models Compared to Excised Human. DPhG Jahrestagung Landesgruppe Berlin-Brandenburg, Berlin/Germany, May 2010

TABLE OF CONTENTS

1 Introduction

1 Introduction

1.1 Human skin

1.1.1 Skin structure and its barrier function

Human skin is the largest organ of the body (1.73 m^2 surface area and almost 10 % of entire body weight) and the boundary between body and environment [1]. Skin is well suited as target for application of cosmetics and in particular pharmaceuticals in sense of epidermal, dermal and transdermal delivery avoiding severe adverse events due to systemic application and avoidance of the hepatical first-pass effect. Its main function is the protection of the body against pathogens and the prevention of water loss. Important enzyme-dependent metabolic processes take place inside human skin. Furthermore, skin represents an organ of immune responses [2]. In terms of anatomy, human skin can be divided into the following layers: Epidermis, dermis (= *cutis*), separated by a basement membrane, and hypodermis (= subcutis; fig. 1).

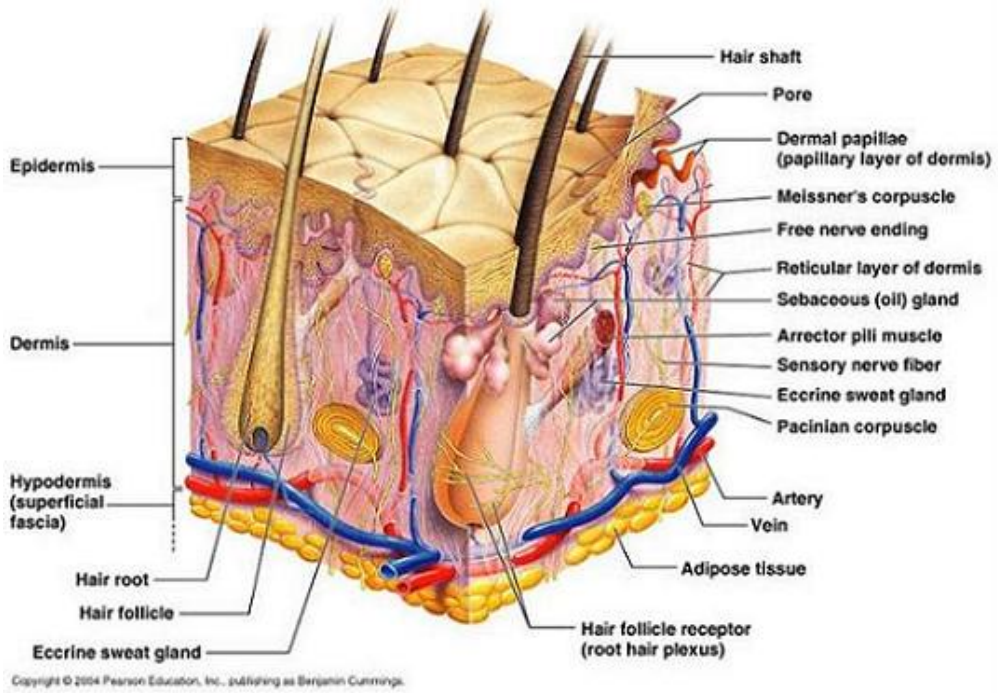

available on: http://www.osovo.com/diagram/skindiagram.htm

Fig. 1: Natural structure of human skin and its appendages.

Depending on the body region, the overall thickness of human skin ranges from 1 to 4 mm (with a general higher thickness in men) and decreases with age [3]. The thickness of epidermis, dermis and underlying fat tissue as well as varying distribution of glands or hair follicles influence physiological properties of human skin and percutaneous penetration.

Epidermis

The human epidermis (fig. 2), a highly specialized squamous stratified epithelium, forms the outermost layer of the human skin. With a total thickness of 50 µm to 1.5 mm, the epidermis is the thinnest skin layer. Differences in thickness are due to mechanical stress to the body surface and the consequent effects on various keratinization of the skin. Especially in the palms of the hands as well as foot sole, keratinization is particularly pronounced, since these regions require accessorily protection. The dominating cells of human epidermis are keratinocytes. Furthermore, Langerhans cells, lymphocytes, Merkel cells and melanocytes are present. The keratinocytes are organized in multiple layers ("strata"), building an adhesive interconnected system to establish a functional barrier: the stratum basale, stratum spinosum, stratum granulosum, (stratum lucidum only in palm of the hand and foot sole) and the stratum corneum. These layers comprise specific cytoskeletal and cell-cell connections like actin associated adherens junctions, gap junctions, desmosomes, tight junctions and the junction components (mainly keratin, desmogleins and cadherins) essential for the epidermal barrier function and immune surveillance [4].

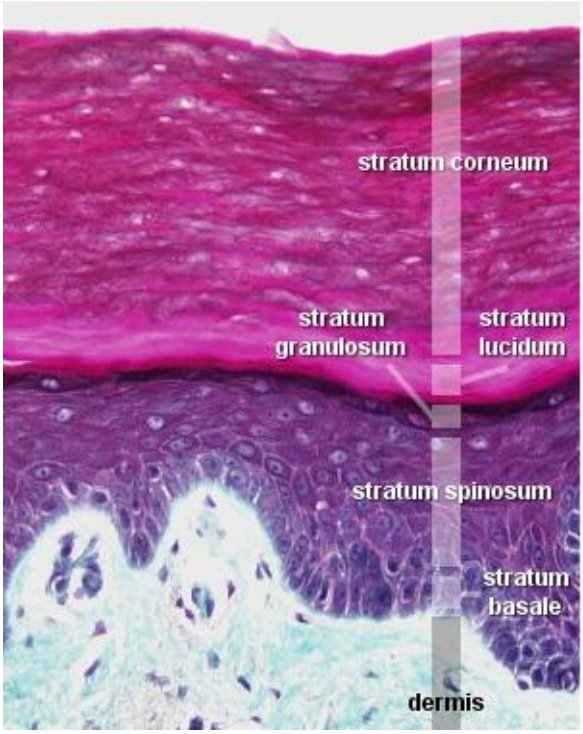

available on: http://www.nku.edu/~dempseyd/SKIN.htm

Fig. 2: Morphology of human epidermis.
The human epidermis is divided into different cell layers: stratum corneum, stratum lucidum (only in the palms of the hand and foot sole), stratum granulosum, stratum spinosum and stratum basale. The stratum corneum, the outermost layer of the human epidermis, consists of anuclear cells (corneocytes) and forms a barrier to protect underlying skin layers. The deeper strata (= viable epidermis) are responsible for the generation of the outermost skin layer, the stratum corneum. The basal, proliferating cell layer (stratum basale) is in contact with the dermis through integrin-based adhesions and hemidesmosomes.

The epidermis is an ongoing self-regenerating tissue: The loss of cells from the skin surface of the stratum corneum, desquamation, is compensated by cell growth in the inner part of the epidermis [5], taking almost two weeks for cell migration and differentiation from stratum basale to stratum granulosum and further four weeks to cross the stratum corneum. The stratum basale is attached to the dermis by hemidesmosomes and integrin-based adhesions on a basement membrane. This stratum represents the innermost layer of proliferating basal cells, organized as cylindrical cells. It is responsible for the regeneration of the skin [6]. Integrins probably crosstalk with epidermal growth factor receptors (EGFR) inducing cell proliferation in the stratum basale [4]. During migration, keratinocytes undergo multiple stages of differentiation and changes in structure and composition. In the stratum spinosum adjacent polyhedral keratinocytes become connected through desmosomes and begin to synthesize keratinosomes (= secretory organelles; odland bodies), enriched with polar lipids (mainly phospholipids), glycosphingolipids, free sterols and metabolizing enzymes like proteases, acid phosphatases and lipases [4]. These secretory organelles exert a central role in stratum corneum formation: They function as carriers of barrier lipid prequels. Further differentiation products present in the stratum spinosum are keratin filaments and structural proteins like involucrin and loricrin [4]. In the adjoining cell layer - the stratum granulosum - the cytoplasm of keratinocytes contains keratohyalin granules, a multiprotein structure promoting the aggregation and cross-linking of keratin. The granules are mainly composed of the histidine-rich protein profilaggrin. After cleavage to filaggrin, this protein promotes the aggregation of keratin filaments in the upper layers stabilizing the keratin network responsible for the mechanical stability of the skin. In the uppermost granular cell layers, lipids are released into the intercellular spaces at the stratum granulosom-stratum corneum boundary surface [7]. Those polar lipids are then enzymatically converted into non-polar lipids: Ceramides are the result of enzymatic hydrolysis of glycolipids. Phosphatase-cleavage delivers free fatty acids, which are arranged into short- and long-periodicity lamellar structures parallel to the cell surface surrounding the corneocytes [8]. In the upper stratum granulosum, keratinocyte proteins like involucrin and loricrin are linked by transglutaminases. Furthermore, released lysosomal enzymes (proteases including specialized caspase) are responsible for the degradation of the cell nucleus and cell organelles as response to keratinization [4]. As a consequence keratinocytes flatten and transform into corneocytes [4]. The stratum corneum plays an important role in protection of underlying tissues from dehydration, infection as well as chemical and mechanical exposure and forms the most effective barrier of human skin [7]. 10-30 µm thick stratum corneum cell layers of polyhedral corneocytes contribute to total human skin consistency.

Corneocytes are the final result of keratinocyte differentiation. These anucleated terminally differentiated flat cells produce proteins and lipids acting as precusors of the water-impermeable barrier of the stratum corneum [4]. Cornified cells are attached among themselves by corneodesmosomes responsible for the stratum corneum cohesiveness. Furthermore, corneocytes are surrounded by stacked layers of proteins, the cornified envelope proteins. These cross-linked protein envelope reduces the absorption of topically applied substances [4]. A lipid monolayer (lipid envelope) linked to the densely packed protein envelope serves as interface between the hydrophilic corneocytes and the non-polar lipids of the surrounding extracellular room. Dominating lipids of the stratum corneum are cholesterols, cholesteryl esters, ceramides and free fatty acids [8, 9]. The water content of stratum corneum accounts for 20 % [7]. The duly composition and arrangement of the lipid lamellae is responsible for the skin barrier function [7]. Furthermore, the stratum corneum represents a reservoir for e.g. glucocorticoids responsible for a constant drug release [10].

Dermis

With a total thickness of 1 to 2 mm, the human dermis is structurally divided in two layers, the stratum papillare and the stratum reticulare. Structual components of the dermis are collagen, elastic fibres (mainly composed of elastin) and extrafibrillar matrix, composed of glycosaminoglycans (e.g. hyaluron), proteoglycans and glycoproteins. The dermis also contains skin appendages like hair follicles and glands, lymphatic vessels as well as macrophages and mast cells. Furthermore, the dermis harbours mechanoreceptors providing the sense of touch and heat. The superficial stratum papillare, a loose connective tissue, is anchored through the basement membrane with the epidermis (stratum basale). It consists of blood vessels, responsible for an adequate nourishment and waste removal from its own cells and the epidermis. Furthermore, it enables accession of transdermal drugs into circulation. In contrast, the usually much thicker stratum reticulare is composed of a tight connective tissue and dermal fibroblasts responsible for secretion of collagen, elastin and proteoglycanes and hence the strength and elasticity of the human skin [7].

Hypodermis

The hypodermis layer (subcutis) underlines the dermis and is attached to it by collagen and elastic fibres. The hypodermis preponderantly consists of a loose connective tissue and elastin. The dominating cell types are adipocytes, arranged as fat tissue lobules, fibroblasts and lymphocytes. Blood vessels and nerves are present, too. Depending on the body region and nutritional condition, the thickness of this subcutaneous fat layer is variable. The

hypodermis is not part of the skin; it mainly acts as energy reserve. Furthermore, it is responsible for the attachment of the skin to underlying muscles and bones and its supply with blood vessels and nerves.

Skin Appendages

Skin appendages include primarily eccrine and apocrine sweat glands as well as sebaceous glands, hair follicles and nails. Sweat glands are tubular structures of the skin producing and excreting sweat. Eccrine sweat glands are smaller than apocrine glands. Distributed all over the body except from lips and fingers with varying density depending on body region, eccrine sweat glands serve as coiled tubular glands discharging their secretions directly onto the skin surface. Furthermore, they are involved in thermoregulation as well as protection by preserving the skin´s acid mantle protecting the skin surface from colonisation of pathogenic organism. Apocrine sweat glands are limited to axilla and perianal regions and discharge in the canals of hair follicles. Sebaceous glands usually found in hair-covered regions, secrete a mixture of triglycerides, free fatty acids and squalene, called sebum, to prevent human skin from drying out. Sebaceous lipids contribute to maintenance of the skin barrier integrity and expression of pro-inflammatory and anti-inflammatory properties [11]. The glands transfer sebum to the skin surface along the hair shaft. The pore size of sebaceous and sweat glands and production of sebum/sweat in men is higher compared to women [12] influencing the acidity and microflora of the skin [13, 14].
Hairs are long horn fibres composed of keratin growing all over the external body except for mucous membranes, palms and soles. A hair consists of a visible part, the hair shaft and hair follicle found in the dermis. The structure, growth rate and hair density differs depending on body site and sex with a general higher density in male. Skin appendages, especially hair follicles, can influence percutaneous penetration ([15, 16]); chapter 1.1.2).

1.1.2 Dermal absorption and penetration pathways through the skin

For the toxicological assessment of substances with contact to the skin surface, sufficient knowledge of dermal absorption and subsequent uptake into systemic circulation is an important factor. After contact with the intact surface of the skin, compounds can penetrate into the stratum corneum of the epidermis and in the further course attain the viable epidermis, dermis and blood vessels for subsequently distribution.

There are two main pathways [17]:

I. transepidermal route including intercellular and transcellular penetration

II. via skin appendages- shunt routes.

The intercellular pathway seems to be the major route of penetration [18]. By this route, compounds pass through the small spaces between the keratinocytes, making the route more tortuous. Transcellular route means a direct pathway through both the phospholipids membranes and the cytoplasm of the corneocytes, whose lipid content is low. Although this is the pathway of shortest distance, drugs encounter significant resistance to permeation. They have to cross the lipophilic membrane of each cell, followed by the polar cellular components containing hydrated keratin, and again the phospholipid bilayer of the cell. This series of steps is repeated numerous times to traverse the full thickness of the stratum corneum [19].

The penetration pathway via skin appendages like sweat glands and hair follicles with their associated sebaceous glands contributes only to a minor extent to drug penetration because skin appendages account for around 0.1 % of the skin area [17]. However, it should be considered that the follicular surface area depends on the site of the body [15] and influences penetration behaviour in intensively haired regions [20].

Permeation of small molecular compounds through the skin is mainly due to passive diffusion [18] mainly following Fick´s law of diffusion; active transport appears to be of minor relevance. Skin permeation of macromolecular compounds is very difficult and hence almost impossible. The penetration rate of a topically applied compound across the skin layers is controlled by its physicochemical characteristics (molecular weight, lipophilicity, melting point) and chemical structure (number of hydrogen bonding acceptor capacity). Moreover, the properties of formulation, its vehicle compounds (vehicle itself, addition of penetration enhancers, surfactants or solvents) and interactions between the test compound or vehicle and the skin [15, 21, 22] can influence penetration and permeation. In general, good conditions for penetration and permeation are a molecular weight < 500 Da, number of H-bond donors/-acceptors < 5/10 and moderate octanol-water partition coefficient (log P) between 1-3 [23]. Beside physicochemical properties of a topically applied compound, anatomical site and health state of the skin influence penetration behaviour. In wounded or diseased skin, for example, an impaired barrier function leads to enhanced penetration. Furthermore, biotransformation in the skin influences penetration and permeation of topically applied xenobiotics and functions as a further, biochemical skin barrier ([24-26]; chapter 1.3). Thus, cutaneous metabolism during percutaneous absorption besides physicochemical properties needs to be taken into account in penetration studies.

1.2 Alternatives to animal skin in *in vitro* tests for toxicity evaluation and drug development

Due to its large contact surface human skin is exposed to various biological and chemical compounds (e.g. as ingredients of pharmaceuticals, cosmetics, chemicals or clothing). To protect human health, compounds (potentially) exposed to human skin have to be assessed by standardized toxicological analysis. For the development of pharmaceuticals intended for dermal application skin absorption and general toxicity evaluation is mandatory. This holds true for the safety evaluation of cosmetics, too. The assessment of skin corrosion - the production of irreversible tissue damage in the skin following the application of a test compound [27] - is a legal prerequisite for all chemicals put into circulation. *In vitro* tests are important tools for toxicity analysis. For hazard assessment of substances with dermal absorption *in vitro* methods must reflect the *in vivo* situation as precisely as possible. Human skin is the most suitable model for such *in vitro* toxicity testing and recommended by OECD Technical Guidances [28, 29]. Due to the limited availability of human skin (sources are cosmetic surgery or cadaver skin) animals have been used for this purpose, too. [30-35] However, there are ethical as well as legal crucial points regarding the use of human and animal tissues. Thus, alternatives to animal and human skin are required. The following regulations and directives promote the use of alternative test methods.

1.2.1 Legal basis

EU Cosmetic Directive

The 7th Amendment to the EU Cosmetics Directive bans animal tests for cosmetics and their ingredients in total from 2013 on. Required toxicological analysis should be performed without the use of animals. Since July 2013, the Cosmetics Directive prohibits the marketing of cosmeticals or ingredients of cosmetics tested on animals.

Registration, Evaluation, Authorization and Restriction of Chemicals (REACH)

Due to the implementation of the Registration, Evaluation, Authorization and Restriction of Chemicals (REACH) legislation (Regulation (EC) No. 1907/2006), all companies manufacturing or importing chemical substances into the European Union in quantities of ≥ 1 tonne per year need to register these substances by the European Chemicals Agency (ECHA). They have to provide data regarding physicochemical properties of chemicals. More importantly, hazard assessment is required. Information on properties such as toxicity after long-term exposure, the potential carcinogenicity or toxicity to the reproductive functions is often not available. The closing of these information gaps probably requires new studies

using animals. REACH promotes two approaches to restrict the use of animal testing to a minimum:

- The regulation states that it is necessary to replace, reduce or refine testing on animals. Implementation of this regulation should be based on the use of alternative test methods suitable for hazard assessment of chemicals wherever possible. Testing on animals may be performed only as a last resort to obtain missing information about a substance and to meet the information requirements of REACH. ECHA shall examine all proposals to control whether reliable and appropriate data are obtained and to avoid unnecessary animal testing.
- In order to avoid duplication of work, and in particular to reduce testing involving animals, the provisions concerning preparation and submission of registrations and updates should require sharing of information where this is requested by any registrant. For this purpose Substance Information Exchange Forums (SIEFs) were performed. Providing of existing test results on animals is mandatory.

Pharmaceutical directive (Directive 2001/83/EC)

The assessment of quality, efficacy and safety of pharmaceuticals for human use is regulated by the pharmaceutical direcitve. In preclinial drug development studies on animals are required. However, the directive states that *in vitro* test systems can replace tests on animals for toxicological (safety) analysis if they are of comparable quality and usefulness for the purpose of safety evaluation (Annex 1).

1.2.2 Reconstructed Human Epidermis and full thickness Human Skin

Amongst others due to the prohibition of animal use for toxicological analysis of cosmcetics alternatives for animal use in drug development and hazard assessment of substances with dermal absorption have to be established and validated. *In vitro* toxicity tests can only be accepted for regulatory purposes and for a broader use after successful validation [27, 36, 37]. In Europe, the European Union Reference Laboratory for Alternatives to Animal Testing (EURL ECVAM) promotes the scientific and regulatory acceptance of non-animal tests, which are of importance to biomedical sciences, through research, test development and validation. Frequently, *in vitro* tests in hazard analysis are based on (immortalised) cell lines. However, due to the lack of physiological cell-cell-interaction and a qualified barrier, monolayer cell cultures frequently have a tendency to overpredict toxic effects.

Normal human-cell derived reconstructed human epidermis (RHE) and reconstructed full thickness human skin (RHS) mimicking native human skin have become increasingly

important as alternative approach. Reconstructed human tissues are based on normal (non-transformed), human-derived foreskin (EpiDerm, Phenion FT) or breast (EPISKIN®) epidermal keratinocytes (NHK) and in case of RHS of normal human-derived dermal fibroblasts (NHDF), too. RHE are produced by seeding keratinocytes on the surface of a polycarbonate or cellulose acetate membrane to form a multi-layered matrix. After proliferation, the cells are exposed to the air (air-liquid interface) to induce the differentitation. In case of RHS, fibroblasts are embedded in collagen matrix representing the dermis and keratinocytes are seeded on the surface of the matrix. Differentitation is performed as decribed for RHE. A first full-thickness skin model was described in 1981 based on rat skin cells on a collagen matrix [38]. Ten years later a comparable reconstructed tissue based on human-derived dermal cells was introduced [39]. Some of these artificial human skin constructs - with varying levels of differentiation - are commercially available like the reconstructed human epidermis EpiDerm™ (EpiDerm; Mattek Corp., USA), SkinEthic®, EPISKIN® (L`Oréal, France) and the reconstructed full thickness human skin EpiDerm-FT™ (EpiDerm-FT; Mattek Corp.), Advanced Skin Test AST2000 (CellSystems®, Germany) and Phenion® Full Thickness Skin Model (Phenion FT; Henkel, Germany). Most of these reconstructed tissues have been characterized for morphology, lipid composition, biochemical markers and barrier function [32, 35, 40-43]. Recent studies have expanded our knowledge of phase I and II metabolizing enzyme expression in RHE [44-47] and RHS [48, 49]. To some extent, enzyme activity has been described, too [24, 50-54]. Besides reconstructed human epidermis and full thickness skin representing native human skin, reconstructed tissues mimicking skin diseases like atopic dermatitis are under development [55]. Initially created as artificial skin to substitute injured skin, these reconstructed tissues nowadays are used as an *in vivo*-like system for dermato-toxic analysis of chemicals, cosmetical products and their ingredients [56]. The OECD Test Guideline 428 and accompanied Technical Guidance Document (TGD) 28 defining principles for skin absorption testing in risk assessment state that RHE can replace human skin in *in vitro* tests for percutaneous uptake and hazard analysis, respectively, if data obtained with RHE are equivalent to results obtained with human or animal skin [28]. RHE-based test procedures have been validated and are OECD adopted like *in vitro* tests for percutaneous absorption [35, 42, 57], skin irritation [36, 58, 59] and phototoxicity [60, 61]. The protocol for percutaneous absorption of compounds in aqueous solution using RHE is also applicable for the assessment in RHS [62, 63] and to compare various formulations [57, 63-66]. Yet *in vitro* testing for sensitization and genotoxicity is still a challenge: among others the risks are linked to (still insufficiently known) cutaneous biotransformation [67-70]. An important prerequisite for using RHE/RHS as alternative to animal experiments is not only a high similarity to

human skin morphology, barrier function and hence penetration and permeation: An equivalent biotransformation capacity is of relevance, too. However, comprehensive information about biotransformation capacity of RHE/RHS is still not available.

1.2.3 Morphology, barrier characteristics and differentiation markers of RHE and RHS

The morphological examination of several commercially available reconstructed human epidermis like EpiDerm, SkinEthic® and EPISKIN® and full thickness skin [71] demonstrated high similarity to human skin [41] with formation of a multilayered stratified epithelium including stratum basale, stratum spinosum, stratum granulosum and a stratum corneum [40, 41]. However, not all RHE revealed a fully developed basement membrane and presence of hemidesmosomes [41, 72]. The number of viable epidermal, stratum corneum layers and total epidermal thickness of most RHE were less pronounced compared to native human skin [41] with differences in cell organization and irregular cellular shape. Contrary to native human skin, intracellular lipid droplets were found in all strata, especially in the stratum basale and stratum corneum [41]. Incompletely transformed lamellar bodies in the stratum corneum of RHE were detected. Thus, the physiological extrusion at the stratum granulosum-stratum corneum interface of RHE is disturbed [41]. Elastin mRNA expression and elastic fibres responsible for the flexibility of the skin were detected in RHS correlating with native human skin [71]. Unlike native human skin, blood vessels and skin appendages like hair follicles or glands are not present in reconstructed tissues.

The expression of terminal differentiation markers is necessary for the correct differentiation of the epidermis and the formation of a competent barrier [41]. Differentiation markers keratin 1 and 10 are expressed in all suprabasal layers of reconstructed tissues just as in native human skin [40]. Loricrin and SPRR 2 (small prolin rich protein) expression in the stratum granulosum corresponds with human skin. Involucrin, also precursor of the cornified envelope, is present in all suprabasal layers of RHE. In human skin expression is limited to the stratum granulosum [42]. The same holds true for expression of transglutaminase [40]. Further differences in expression and localization of several markers in reconstructed tissues compared to native human skin were observed. Contrary to native human skin keratin 6, SKALP (skin derived antileukoproteinase) and SPRR 3 are expressed in several reconstructed tissues [40]. Keratin 6 is associated with hyperproliferation and wound healing. SKALP is involved in the regulation of cutaneous inflammatory processes. For example, psoriasis patients showed latent SKALP activity [73].

These differences in precursor protein expression and localization probably contribute to

imbalances between proliferation and differentitation and hence to the well-known lower barrier function of reconstructed human epidermis and skin.

1.2.4 Lipid composition and organisation of RHE and RHS compared to native human skin

The lipid composition of various RHE/RHS differs slightly from human skin. All epidermal lipid classes are present in RHE, including ceramides, phosholipids, cholesterol, cholesterol sulfates and esters, sphingolipids, triglycerides and free fatty acids. However, the proportions occasionally differ significantly. In contrast to equimolar glucosylsphingolipid amounts, the low content of free fatty acids (26 - 40 % of normal epidermis; [15]), especially long chain fatty acids, and cholesterol esters differs from those found in native human skin. Relative amounts of ceramides were considerably higher in reconstructed tissues (approx. 200 - 240 % of normal epidermis; [15]). The ceramide profiles of analysed RHE deviate from native human skin with a much higher content of ceramide 2 and significantly lower amounts of polar ceramides 5 and 6 [42]. In contrast to native human skin, ceramide 7 is not present in commercially available RHE/RHS [41, 42]. Lanosterol, a precursor of cholesterol, is present in reconstructed skin but not in native human skin [40, 41]. There is a higher amount of triglyerides in reconstructed tissues, too. With respect to the arrangement and distribution of elastin-containing fibres in the dermis RHS are very close to human skin [71].
Deviations in lipid lamellar organization with only long-range lipid lamellar phases compared to presence of both short- and long-range lamellars in native human skin might be mainly due to differences in free fatty acids profiles and contents resulting in a lower barrier function of RHE/RHS compared to native human skin [40, 41].

1.3 Metabolism in the skin

Skin is a metabolically active organ. Less is known about cutaneous metabolism compared to well known drug-metabolizing organs such as the liver and extrahepatic organs like the lung, kidney and the intestine. However, skin contributes to phase I (oxidation, reduction or hydrolysis) and subsequent phase II (conjugation with hydrophilic co-factors like glucuronic acid or sulfate) reactions [26, 53, 74, 75]. The biotransformation capacity of human skin is mainly described by mRNA levels but less by protein levels and functionality [44, 54]. Localization and activity of various cutaneous enzymes are mainly in the epidermis but also

take place in the dermis and skin appendages, especially sebaceous glands and hair follicles [76-80]. The expression level and biotransformation capacity of several enzymes present in the skin are highly variable. They differ between body site regions and can be influenced by various attributes (chapter 1.3.2). The biotransformation can lead to detoxification of foreign compounds. Excretion of more polar metabolites is faciliated. Yet the formation of mutagenic and sensitizing metabolites or intermediates in the skin can occur, too. Bioactivation of topically applied pro-drugs is possible [53] influencing drug absorption and efficacy [65]. Due to the enhancement of dermal absorption lipophilic and bioconvertible (pro-)drugs such as (carboxylic acid) esters are often used in the topical treatment of skin diseases. Following absorption of the ester prodrug through the stratum corneum, ester cleavage by cutaneous esterases to the active ingredient occurs in the skin. This demonstrates that for evaluation of drug efficacy and especially toxicity sufficient knowledge about (cutaneous) biotransformation is of high relevance.

1.3.1 Drug-metabolizing enzymes of human skin

The focus of this thesis is on cutaneous ester cleavage of the diester prednicarbate as well as bioconversion of the androgen testosterone. With this purpose in mind, primarily the enzyme expression and/or activity responsible for the cutaneous biotransformation of these compounds are described in detail. Further enzymes are mentioned briefly only for completeness.

1.3.1.1 Esterases

Mammilian esterases are members of the α/β hydrolase fold family cleaving several ester- and amide-containing substances. Thus, the capacity of cutaneous ester hydrolysis [51, 52, 81] is of particular importance for efficacy and safety especially of glucocorticoid esters like prednicarbate or betamethasone 17-valerate for dermal use [82-85]. Esterases are classified based on their substrate specificity according to the recommendations of the Nomenclatur Commitee of the International Union of Biochemistry and Molecular Biology (NC-IUBMB). However, the individual hydrolases (EC3) exhibit properties of several catalytic activities. Carboxylic ester hydrolases (EC3.1.1) for example also catalyse hydrolytic reactions of lipases, lysophospholipases or amidases beside carboxylesterase activities. Carboxylesterases (CE; EC3.1.1.1), part of the serine superfamily of (carboxylic) esterases, play an important role in biotransformation of ester (pro)drugs [86, 87]. According to the homology of the amino acid sequence of the encoding genes CE are classified into five

families (CE1-CE5). The CE1 and CE2 families include the major forms of CE isozymes [88]. Differences between CE1 and CE2 families mainly regard substrate specifity and tissue distribution. CE1 preferentially hydrolyse compounds with large acyl moieties esterified by small alcohols, while CE2 subtrates are small acyl compounds esterified by relatively large alcohols [86, 88]. CE are expressed in liver, lung and small intestine [89] but little is knowm about expression and activity in human skin. CE are present in keratinocytes [90] and sweat glands [91] of human skin. Only CE2 mRNA is expressed in HaCaT [92]. Further esterases like arylesterase isoenzymes 2 and 3 (PON 2 and PON3) are expressed in human skin and HaCaT, too [93]. Some acetylcholinesterase activity in human skin was described, too [94]. However, intensive ester hydrolysis of the prednisolone diester prednicarbate occurs in human skin indicating relevant cutaneous esterase activity [66, 95].

1.3.1.2 Cutaneous prednicarbate biotransformation

Prednicarbate (PC) is the 17-ethylcarbonate, 21-propionate double ester of the non-halogenated glucocorticoid prednisolone (PD). Topically applied in the therapy of acute atopic dermatitis and contact dermatitis, PC induces strong anti-inflammatory activity [83, 96] with a low risk of typically glucocorticoid adverse events of skin thinning due to antiproliferative impacts on fibroblasts [95, 97]. The lipophilic PC penetrates into the skin very quickly. In human skin and mainly in the epidermis the double ester is enzymatically hydrolysed by esterases [95] to the more potent monoester prednisolone 17-ethylcarbonate (P17EC; fig. 3). P17EC exerts a higher receptor affinity than native PC and reveals also high atrophogenic potential [95, 98]. After non-enzymatic acylmigration to the monoester prednisolone 21-ethylcarbonate (P21EC; fig. 3), an intermediate without receptor affinity, further significant hydrolysis of this monoester results in formation of the non-esterificated PD. PD formation is a result of detoxofication since PD exerts low glucocorticoid receptor affinity. As a consequence the antiinflammatory effect of PC and P17EC decreases and hence the risk of skin thinning due to antiproliferative effects.

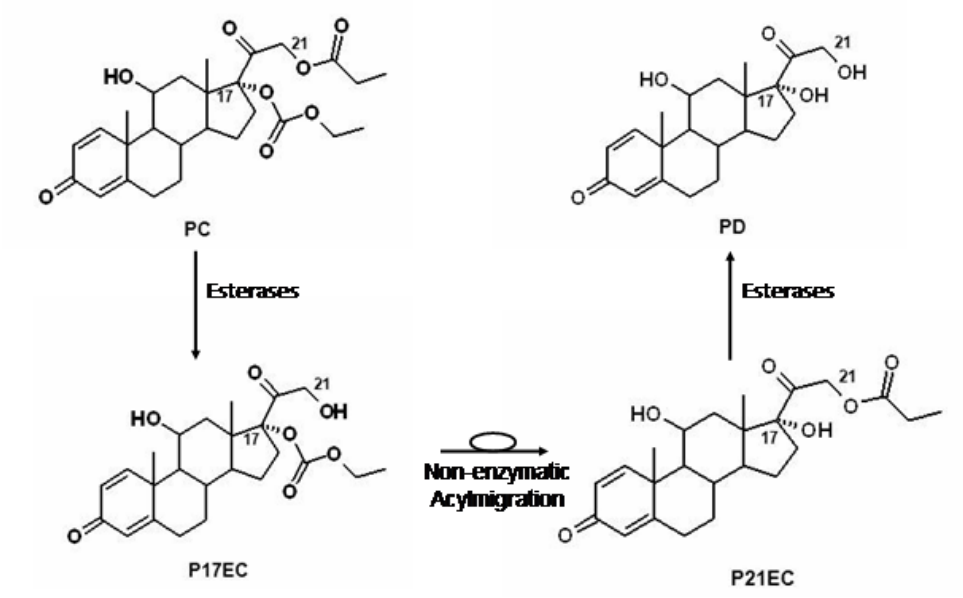

Fig. 3: Cutaneous biotransformation of the glucocorticoid double ester Prednicarbate (PC). After esteratic hydrolysis in position 21 to the monoester prednisolone 17-ethylcarbonate (P17EC) and non-enzymatic acylmigration to position 21, the rate limiting step of PC transformation, the intermediate prednisolone 21-proprionate (P21EC) is again cleaved by esterases to prednisolone (PD). Esteratic activity dominates in the epidermal compartment and is rather low in dermal fibroblasts [95].

1.3.1.3 Androgen metabolizing enzymes

In human skin androgen synthesis occurs since enzymes required are present in human skin and skin appendages including hair follicles, sebaceous and sweat glands [99]. Furthermore, biotransformation to more potent androgens or inactivation of androgens occurs. The steroid 5α-reductase (5α-R), 17β-hydroxyteroid dehydrogenase (17β-HSD) types 3 and 5 as well as 3β-hydroxysteroid dehydrogenase (3β-HSD) type 1 are responsible for the formation of potent androgens. Contrary, aromatase (product of *CYP19* gene; [99]), 17β-HSD type 2 and 3α–hydroxysteroid dehydrogenase (3α-HSD) inactivate androgens to achieve androgen homeostasis [100]. Furthermore, Cytochrome P450 enzymes (CYP3A4/CYP3A5) and to a less extent phase II related enzymes (UDP-glucuronosyltransferases (UGT), sulfotransferase (SULT)) can contribute to inactivation and excretion of androgens [101] .

In human skin, 5α-R type 1 and type 2 is detectable with type 1 being the more abundant isoform in the skin of all body regions [99, 100, 102] but predominantly in neonatal foreskin keratinocytes and sebaceous glands from face and scalp. 5α-R is also expressed in

fibroblasts, hair dermal papilla cells and melanocytes [103]. 17β-HSD mRNA expression (types 1, 2 and 4) dominates in keratinocytes and the pilosebaceous unit [99], whereas only type 2 is detectable in the HaCaT cell line [100]. In human sebaceous glands and outer rooth sheath cells, type 2 is strongly expressed. 17β-HSD type 3 activity is present in sebaceous glands but not in keratinocytes. Reductive activity in facial sebaceous glands exceeds activity in acne non-prone body regions [100, 104]. Only in sebocytes 3β-hydroxysteroid dehydrogenase (3β-HSD) type 1 activity - the oxidation of the 3-β-hydroxy-steroids like dehydroepiandrosterone (DHEA) to corresponding 3-keto-steroids as essential step in endogenous androgen formation - is present [100]. Aromatase expression and/or activity was observed in fibroblasts from both genital and non-genital human skin and adipose tissues as well as keratinocytes cultured in serum-free medium [105-107]. CYP3A4/CYP3A5 are mainly localized within the epidermis and the sebaceous glands [75, 78, 108, 109] but are also detectable in Langerhans cells, fibroblasts, dendritic cells and melanocytes [75, 110, 111] at high inter-individually varying amounts [109]. 3α–hydroxysteroid dehydrogenase (3α-HSD) is expressed in cultured human fibroblasts, keratinocytes, sebocytes and melanocytes [99, 112]. UGT enzymes are expressed only in traces [113, 114]. In human skin and cultured keratinocytes mRNA of several SULT isoforms (e.g. SULT1A1, SULT1A3 and SULT1E1) are slightly expressed [53].

1.3.1.4 Cutaneous testosterone biotransformation

The androgen testosterone is not only OECD accepted as lipophilic standard compound in skin absorption testing [28] but also therapeutically used for transdermal treatment of hypogonadism [115]. The dermal biotransformation differs depending on body site (e.g. genital and non-genital region). Sex related differences were described, too [99, 102, 116]. 5α-R activates testosterone irreversibly to the most potent androgen 5α–dihydrotestosterone (DHT; fig. 4) in human foreskin fibroblasts and keratinocytes, female breast skin keratinocytes and male skalp skin. Furthermore, formation to DHT takes place in skin appendages, especially sebaceous and sweat glands [100, 102, 116]. 17β-HSD types 2 and 4 oxidatively inactivate testosterone and DHT to androstenedione (4-DIONE) and androstanedione (AD), respectively. Contrary, 17β-HSD type 3 and 5 catalyze the transformation of 4-DIONE and AD, respectively, in an opposite direction to the more potent androgens testosterone and DHT [102]. Subsequently, 4-DIONE is irreversibly converted by 5α-R to AD (fig. 4). AD and DHT are enzymatically inactivated by 3α–HSD to

androstanediole (3-DIOL) and androsterone (ADT), respectively. Furthermore, CYP related formation of testosterone occurs. CYP3A4/5 is responsible for the hydroxylation of testosterone to 6β-hydroxytestosterone (HOT). Aromatisation of testosterone and 4-DIONE to the estrogens 17β-estradiole (E_2) and estrone (E_1), respectively, is catalysed by CYP19A1 (aromatase) [117]. 17β-HSD (types 1, 7 and 12) contributes to formation of E_1 to E_2. In contrast, 17β-HSD type 2 catalyses the formation in an opposite direction (E_2 to E_1; [118]). UGT2B7, UGT2B15 and UGT2B17 and sulfotranfserases are involved in phase II glucuronidation of 3-hydroxysteroid metabolites like 3-DIOL and ADT [101, 119]. However, due to only negligible expression in human skin, glucuronidation and sulfation contribute only slightly to testosterone formation, if at all [48, 113].

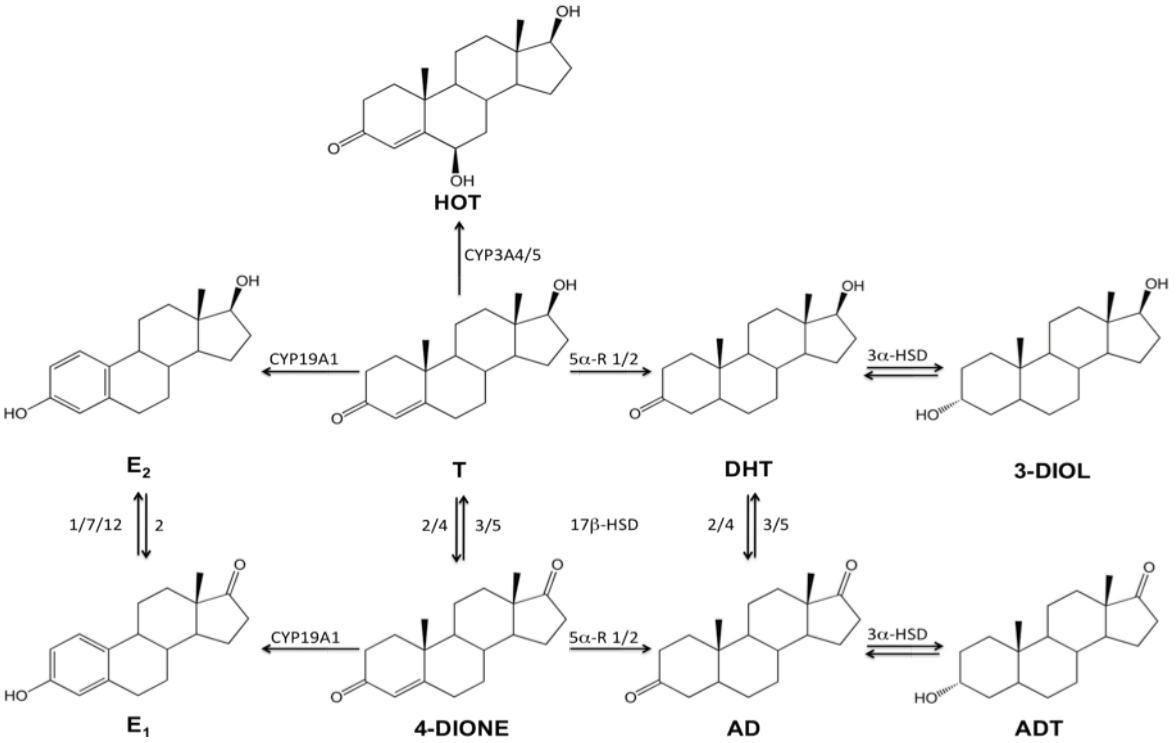

Fig. 4: Schematic representation of cutaneous phase I testosterone biotransformation and corresponding relevant enzymes. CYP 450-dependent enzymes CYP3A4/5 are involved in hydroxylation of testosterone (T) to 6β-hydroxytestosterone (HOT). 5α-Reductase (5α-R) activates T irreversibly to the most potent androgen 5α-dihydrotestosterone (DHT) and after oxidative conversion of testosterone to androstenedione (4-DIONE) by 17β-hydrosteroid dehydrogenases (17β-HSD) types 2 and 4, 5α-R catalyses the conversion of 4-DIONE to androstanedione (AD). AD and DHT are reversibly converted by 3α-hydroxysteroid dehydrogenase (3α-HSD) to androsterone (ADT) and androstanediole (3-DIOL), respectively. Aromatase (CYP19A1) catalyzes the aromatization of testosterone and 4-DIONE to the estrogens 17β-estradiole (E_2) and estrone (E_1), respectively.

1.3.1.5 Further enzymes of human skin

Phase I metabolizing enzymes

Another oxidizing enzyme family present in human skin in similar amounts like CYP [120] is flavin-dependent monooxygenase (FMO), catalysing oxidation of several drugs and pesticides like organophosphates and carbamates. In human breast skin, mRNA expression of FMO (types 1, 3, 4 and 5) is present with inter-interindividual levels [109]. FMO 1 is selectively expressed in the epidermis. FMO 3 is restricted to the dermis and FMO 4 and 5 are evenly spread across the hole skin [44, 48]. Furthermore, cyclooxygenases (COX) 1 and 2 as well as alcohol (ADH) and aldehyde dehydrogenase (ALDH) are expressed in human skin [75], especially in the epidermis, sebaceous glands and hair follicles [121].

Phase II metabolizing enzymes

Beside negligible expression of UGT in human skin as decribed, N-acetyltransferase (NAT) and gluthatione-s-transferase (GST) expression or activity was found [75]. Responsible for the important detoxification of aromatic amines, NAT1 mRNA is detectable in neonatal and adult human keratinocytes [122]. In cultured human keratinocytes, only GST π (pi) is expressed with increasing activity due to higher differentiation status [123], whereas other isoforms might be of non-keratinocyte origin [75].

1.3.2 Influences on enzyme expression and biotransformation capacity

Cutaneous biotransformation can strongly be influenced by various factors mainly comprising sex, age, body site, cell differentiation status and culture conditions. It is scarcely surprising that androgen biotransformation, for example, is strongly influenced by sex/age since enzymes involved in transformation are responsible for the endogenous synthesis and regulation of sex hormones. Due to the general insufficient knowledge of cutaneous biotransformation it cannot be ruled out if this generally applies to cutaneous enzymes. Furthermore, it cannot generally be estimated with any degree, which factors exert the strongest influence on biotransformation and what the relationship between those factors is. Thus, when evaluating biotransformation and toxicity of substances exposed to human skin these factors of probable influence must be taken into account.

Sex related differences

17β-HSD expression level, for example, differs between male and female with lower expression in women [124]. In addition, 17β-HSD isoenzymes substrate specifity differs between male and female skin. In male skin the reductive 17β-HSD substrate affinity (inactivation of estrogens) exceeded female skin affinity [118]. Contrary, female skin tends to oxidative 17β-HSD activity and thus formation to strong estrogens [118]. 5α-R type 2 enzyme activity in occipital and frontal scalp hair follicles and sebaceous glands of male donors exceed up to three times the activity of those in female follicles [125]. Contrary, aromatase expression in women´s front hair follicles is six times greater than in men [126].

Origin of cells (body site)

Differences are especially pronounced with cells from genital and from non-genital areas. 3α-HSD and 5α-R type 1 activity in genital fibroblasts or foreskin keratinocytes, respectively, is high, yet missing in skin of legs or arms [112]. Furthermore, 5α-R activity of sebocytes from facial regions exceeds activity of sebocytes from non-facial areas. The expression of aromatase is intense in regions of hair growth like scalp and beard [127].

Age

Age related varieties affect amongst others the expression of androgen metabolizing enzymes like aromatase and 17β-HSD. Contrary to adult skin, aromatase is only detectable in melanocytes but not in anagen hair follicles fetal skin. In addition, expression level of epidermal aromatase decreases with increasing age [128]. 17β–HSD is expressed in high amounts before 2 years age and again during teenage years [102]. Besides testosterone, age related differences were detected in biotransformation of the ester ethyl nicotinate in rat skin. Activity continuously increases during childhood and becomes constant in the adult [129].

Culture conditions and skin handling

Cryoconservation of skin (storage at -20° C) may result in partial or complete enzyme degradation [33, 130, 131] due to decrease of cell viability. Moreover, culture conditions like composition of cell culture medium can influence biotransformation by extent and metabolism profile. For example, cultured in medium with high calcium concentrations, CYP activity is increased [132]: The up-regulation of several CYP enzyme expression levels (e.g. CYP3A4/5) corresponds with increasing differentiation status [133, 134]. This also holds true for 5α-R and 17β-HSD activity [135, 136]. Glucocorticoids like hydrocortisone, a frequently used supplement of cell culture growth medium, stimulate aromatase activity [105]. Other

steroids like dexamethasone and testosterone act as inductors of CYP expression and activity [48, 79, 137]. Bovine serum albumin (BSA) recommended by the OECD as component of receptor media in permeation studies to alleviate solubility of lipophilic compounds strongly inhibits the metabolism of topically applied prednicarbate in reconstructed epidermis due to toxic effects on keratinocytes [138, 139]. Fetal calf serum (FCS), a frequently used supplement of media for cell or tissue cultivation, contains ~6% BSA [139] shifting testosterone formation in keratinocytes to higher androstanediole formation instead of androstenedione [140].

The inducibility/inhibitability in the skin could be important for the local bioavailability of cytotoxic compounds and hence for the formation of sensitizing and/or mutagenic biotransformation intermediates or products. However, the effect of enzyme induction/inhibition in general can be used for effective drug development and medicinal treatment. For example, benign prostate hyperplasia or androgenic alopecia can be treated with finasteride due to selective inhibition of 5α-R type 2 [141]. In addition, inhibitors offer the ability to limit which (iso-)enzymes are involved in biotransformation. The choice of probable inhibitors is based on the structural conditions that are of importance for metabolism.

Diseased skin

Another factor influencing dermal biotransformation is the general health condition of the skin. Wounded skin for example offers a more permeable barrier. Thus, substances with dermal absorption might be transformed considerably faster and to a greater extent. Furthermore, enzyme expression level can also be altered. In patients with acne 3β-HSD and 5α-R activity is increased due to elevated sebaceous gland volume [142, 143]. In psoriatric skin, several CYP isoforms mRNA expression levels are increased [2].

1.3.3 Differences in enzyme expression and metabolism between human and animal skin

Several studies comparing metabolism in human and animal skin revealed considerable higher metabolic capacity of animal skin, in particular of mouse and rat skin. Furthermore, differences in metabolic profiles in animal skin especially skin of mouse and rat compared to human skin were found. This holds true for esterases [144] and androgen metabolism, too [33]. The esterase activity of hairless or hairy rat, rabbit and hairless mouse skin exceeded actitiy of human skin by far [145]. Significant differences in the biotransformation profile of the double ester PC in human and various mammalians resulted after topical application: In rat

blood, nearly 20 metabolites were found [146]. Although some of them also include hepatic metabolites, these differences are noticeable because in human skin and liver the hydrolysis to P17EC and PD clearly dominates (fig. 3; [95, 146-148]. Interestingly, metabolism of prednisolone farnesylate in skin of hairless mouse increased with the distance from skin surface indicating that responsible esterases are mainly localised in lower skin layers. In contrast, human skin ester hydrolysis mainly takes place in the epidermis [10, 80, 149]. Procain ester hydrolysis was comparable for human and porcine skin, whereas rat skin demonstrated higher hydrolysis activity [144]. This holds also true for epoxide hydratase with up to 10 times faster epoxide hydrolysis [150]. Mouse and rabbit skin showed highest testosterone transformation rate of animals tested (mouse, rat, rabbit, hamster and pig) with primary formation of intensively permeated testosterone to polar metabolites and DHT [151]. In contrast, incubation of porcine skin with testosterone revealed a higher transformation rate compared to human skin with nearly solely formation of non-polar metabolites [33]. With respect to CYP expression profile and activity, porcine skin showed similarity to human skin, whereas rat skin showed rather low CYP activity. Mouse revealed highest dermal CYP activity [152]. In mouse skin, 17β-HSD type 6 and 8 mRNA expression is present but no expression of these isoforms is detectable in human skin. Moreover, 17β-HSD of human and rodent skin reveals different substrate specifities; in rat and mouse skin, six isoforms of hydroxysteroid sulfotransferases were observed in contrast to human skin with just two detectable isoforms [153].

To summarise, the varying biotransformation capacity of human and animal skin with mainly higher biotransformation activity of animal skin, especially rat skin, amongst others is probably due to differences in enzyme expression levels. In addition, differences in skin morphology and thickness of the epidermis [154] as well as unequal distribution of metabolic active skin appendages potentially contribute to differences in biotransformation [155]. In general, animal skin is more permeable than human skin. Porcine skin corresponds better with human skin than furry animals with respect to skin structure; the xenobiotic penetration through pig and human skin is more limited as with rodent skin [156-160]. Due to the differences in penetration and biotransformation and also the high level of interindividual variability the correlation between animal data and human skin and hence tranferability to human skin is questionable.

1.3.4 Enzyme expression and activity in RHE and RHS

The expression of various phase I and phase II metabolizing enzymes identified in native human skin was also demonstrated in several reconstructed tissues but with occasionally

different expression levels [44, 45, 48]. As with native human skin investigations primary are based on mRNA expression levels supported by limited available analysis of enzyme activity. Again, in the following the focus is on expression and activity of relevant enzymes for ester cleavage and androgen metabolism (see also chapter 1.3).

1.3.4.1 Esterases

Enzyme expression and activity of esterases in reconstructed tissues has yet not been addressed systematically. However, data are available with respect to biotransformation of the double ester PC and the monoester betametasone 17-valerate. Esteratic activity in reconstructed tissues (e.g. EpiDerm) exceeded hydrolysis of PC and betamethasone 17-valerate in monolayers of NHK/NHDF as well as human skin [10, 52, 65, 66, 95, 161, 162]. In addition, biotransformation of naltrexon esters revealed slightly higher hydrolytic activity in the RHE EpiDerm compared to human skin [163]. Expression of CE1 and CE2 are similar or even slightly higher in reconstructed epidermis EpiDerm and the reconstructed skin EpiDerm-FT and Phenion FT compared to human skin. Arylesterase expression (PON2 and PON3) in the RHE EpiDerm is comparable to human skin. Contrary, expression level in human exceeded expression in RHS EpiDerm-FT and Phenion FT. PON1 is not expressed in reconstructed tissues but slightly in human skin [93].

1.3.4.2 Androgen metabolizing enzymes

Comparable amounts of steroid sulfatase, 3α-HSD type 3 and 20α-HSD were found in reconstructed tissues and female human breast skin [48]. The expression levels of other steroidogenic and steroid-inactivating enzymes like 5α-R, 17β-HSD isotypes and 20α-HSD in RHE are comparable with human epidermis [45]. Furthermore, the metabolic profile of DHEA and 4-DIONE metabolism in EPISKIN® supports the functionality of steroid transforming enzymes in RHE [45]. The general CYP expression levels are low in reconstructed human epidermis and full thickness skin (EpiDerm, EPISKIN®, and Phenion FT) with increasing levels due to higher differentiation status [49] as described for human skin (chapter 1.3.2). The expression of CYP3A5 is comparably low as seen with human skin [48]. Various CYP expression levels of reconstructed full thickness skin were closer to native human epidemis than expression levels of RHE. This holds true amongst others for CYP3A5 [48]. CYP3A activity in RHE EpiDerm is very similar to human skin [47].

1.3.4.3 Further enzymes

Phase I metabolizing enzymes

The expression level of FMO varies significantly between native human skin and reconstructed tissues: In native human skin, FMO 1 and 5 are predominantly present in the epidermis but are not present in RHE EPISKIN®. In EpiDerm a lower expression level of FMO1 and a significantly stronger expression of FMO 5 compared to human breast skin was observed [44]. In contrast, FMO 2 is highly expressed in EPISKIN® RHE and RHS but not in native human skin [48]. The enzyme activity of FMO 1, 3 in microsomal fractions of EpiDerm and Phenion FT revealed similar activities in RHE and RHS [54]. Aldehyd dehydrogenase 1B is expressed in high levels in human dermis, the absence in human epidermis corresponds with lack of expression in EPISKIN® RHE/RHS [48].

Phase II metabolizing enzymes

With respect to phase II metabolizing enzymes, the expression levels of GST 1, various UGT 1 and UGT2 subfamilies as well as NAT1 and NAT5 are slightly higher [48] in reconstructed epidermis [123]. As with human skin, no NAT2 is detectable in reconstructed epidermis and skin. This holds also true for isoforms 1A1 and 1B1 of sulfotransferase [45]. The high expression level of SULT2B1B in RHE/RHS is similar to human skin, too [48].

1.4 Scientific aim

On the basis of the current legal situation the efforts to develop and validate non-animal approaches for hazard assessment have become very urgent. In addition, there is a clear need for efficient methods in preclinical drug development based on human-derived materials to overcome species differences. For this purpose, reconstructed human epidermis (RHE) and full thickness human skin (RHS) based on human-derived cells resembling native human skin have been developed. With respect to morphology and barrier function various commercially available constructs (e.g. EpiDerm, EpiSkin, SkinEthic) are well characterized. For regulatory purposes *in vitro* tests can only be accepted after experimental standardization and validation studies demonstrating equivalence to results gained with animal experiments [37]. Several RHE-based test procedures have been validated and adopted by the OECD (e.g. *in vitro* test protocols for precutaneous absorption, skin corrosion, skin irritation and phototoxicity).

In view of the already described impact of cutaneous biotransformation on the toxical properties of substances with dermal absorption (chapter 1.1.2; 1.3), for accurate toxicity assessment sufficient knowledge of cutaneous biotransformation is required together with validated RHE/RHS mimicking native human skin not only with respect to penetration behaviour but also to biotransformation capacity.
As a consequence of the still inadequate knowledge of the biotransformation capacity of reconstructed human epidermis and skin, the focus of this thesis was on the evaluation of three commercially available RHS (EpiDerm-FT, Phenion FT and AST2000) composed of differentiating NHK and NHDF embedded into a collagen matrix. The RHE EpiDerm formed by differentiating NHK without dermal equivalent was compared to human skin ex-vivo in view of the epidermal biotransformation competence, too. Since dermal cells contribute differently to esteratic, oxidative/reductive phase I biotransformation, cultured human keratinocytes and dermal fibroblasts were need for reference, too. In addition, impact of experimental setup on dermal biotransformation and hence skin viability is examined by mounting skin to Franz diffusion cells (the standard technique for penetration/permeation studies) and placing skin in tissue culture inserts (membrane insert approach).

Thus, this thesis aimed at the following task:

- Characterisation of prednicarbate biotransformation for the assessment of esteratic cleavage in reconstructed human epidermis and full thickness skin compared to human skin *ex vivo* in consideration of differences in enzyme activity of dermal cells

- Quantitative determination of testosterone biotransformation in reconstructed human tissues (RHE and RHS) compared to human skin *ex vivo* under consideration of biotransformation in isolated NHK/NHDF

This necessitated the following:

- Development and *in house* validation of an analytical HPLC-radiodetection method for the separation and quantification of testosterone and biotransformation products extracted from biological materials (monolayer cell cultures, tissues and corresponding receptor media)

- Evaluation of the quality of the reconstructed tissues and determination of resiliency to experimental conditions

For a more detailed insight into cutaneous biotransformation, the following analyses were performed:

- Evaluation of prednicarbate biotransformation in the immortalized keratinocyte cell line HaCaT to complete the knowledge of prednicarbate biotransformation by dermal cells
- Influences of experimental setup (Franz diffusion cell technique vs. membrane insert approach) as well as storage conditions (cryoconservation) on cutaneous biotransformation
- Determination of sex-specific differences in esteratic activity of human skin ex vivo

2 Materials and Methods

2 Materials and Methods

2.1 Monolayer cell cultures and native human skin

Monolayer cell cultures

The following table (tbl. 1) provides an overview of the applied cell lines:

Cells	Description	(Biological) Origin of cells
NHK	Normal human keratinocytes, passages (p) 1 - 3	Isolation from juvenile human foreskin taken from circumcision surgery (with ethical consent by the Medical Association Berlin)
NHDF	Normal human dermal fibroblasts, p 1 - 5	Isolation from juvenile human foreskin taken from circumcision surgery
HaCaT	Human adult keratinocytes, kept under low calcium and elevated temperature - spontaneously transformed keratinocyte cell line p 60 - 65	CLS Cell Lines Service, Eppelheim/ DKFZ, Heidelberg, Germany
HepG2	Human caucasian hepatocellular liver carcinoma cell line	European collection of cell cultures (ECACC), Salisbury (UK)

Tbl. 1: Overview of applied cell lines for biotransformation experiments and enzyme expression analysis by Polymerase Chain Reaction (PCR).

Native Human Skin

Human skin samples were obtained from aesthetic-plastic surgeries (Helios Klinikum Emil von Behring Berlin, Germany) with informed consent of the donors and general permission by the Medical Association Berlin (Ärztekammer Berlin). Donors of abdomen (19 donors) and breast skin (4 donors) were mainly female patients (3 male donors, abdomen skin) of different age and unknown pharmacological background.

2.2 Reconstructed Human Epidermis and Skin

Reconstructed tissues were the RHE EpiDerm™ (Epi-200) and the respective RHS EpiDerm-FT™ (EFT-400) from MatTek (Ashland, MA, USA). RHS were also the Phenion® Full Thickness Skin Model (Phenion FT; Henkel AG, Düsseldorf, Germany) and Advanced Skin Test 2000 (AST2000; CellSystems® Biotechnologie Vertrieb GmbH, Troisdorf, Germany). The corresponding culture media were provided by the manufacturer. Tissues as well as culture media are tested for viral (Hepatitis B/C, HIV) and mycoplasma contamination by the supplier. For shipment at approximately 4 - 6° C, tissues in their inserts are embedded in an agarose gel containing nutrient. Basic characteristics of the RHE and RHS are summarized in tbl. 2.

RHE/RHS	Manufacturer	(Biological) Origin of cells	Tissue Surface	Specification (insert type/ culture conditions)
EpiDerm™ (Epi-200)	MatTek Corporation, Ashland, MA, USA	Single donor normal human epidermal keratinocytes, isolated from neonatal foreskin	0.637 cm^2	cultured in tissue culture inserts with a chemically modified, collagen-coated membrane using serum free medium on an average of 10 days
EpiDerm-FT™ (EFT-400)	MatTek Corporation, Ashland, MA, USA	Single donor normal human epidermal keratinocytes and fibroblasts, isolated from neonatal foreksin	1.00 cm^2	cultured on specially prepared cell culture inserts using serum free medium; dermal compartment is composed of a collagen matrix containing fibroblasts

RHE/RHS	Manufacturer	(Biological) Origin of cells	Tissue Surface	Specification (insert type/ culture conditions)
Phenion® Full Thickness Skin Model (Phenion® FT)	Henkel AG & Co. KGaA, Düsseldorf, Germany	Non-pooled normal human keratinocytes and fibroblasts from the same donor, isolated from neonatal foreskin	1.30 cm^2	9 - 12 days cultivation period at the air-liquid-interface
Advanced Skin Test 2000 (AST2000)	CellSystems® Biotechnologie Vertrieb GmbH, Troisdorf, Germany	Human primary skin cells from healthy donors	0.60 cm^2	14 days cultivation in inserts with a polycarbonate membrane (0.8 µm pore size)

Tbl. 2: Basic attributes of Reconstructed Human Epidermis (EpiDerm) and Full-Thickness Skin (EpiDerm-FT, Phenion FT and AST2000).

2.3 Technical equipment

For the experiments the following appliances were used:

Analytical and precision balances	Sartorius AG, Göttingen, Germany
Autoclave	Systec, Wettenberg, Germany
BetaCounter 1450 Microbeta Plus LSC	Wallak, Freiburg, Germany
BioDocAnalyze	Biometra, Göttingen, Germany
Biometra Powerpack P25	Biometra, Göttingen, Germany
Centrifuge	
Eppendorf 5415 C	Eppendorf, Hamburg, Germany
Megafuge 1.0 R	Haraeus, Hanau, Germany

Pico 17 Centrifuge	Thermo Scientific, Langenselbold, Germany
Climatic chamber WTB	Binder, Tuttlingen, Germany
Dermatom Acculan 3Ti	Aesculap, Tuttlingen, Germany
Flowstar LB 513	Berthold Technologies, Bad Wildbad, Germany
Fluostar optima	BMG Labtech, Offenburg, Germany
Franz diffusion cells, d= 15 mm, volume of receptor chamber= 12 ml	PermeGear, Bethlehem, Pa., USA
Gel electrophoresis chambers	Biometra, Göttingen, Germany
Heidolph Titramax 100	Heidolph Instruments GmbH & Co. KG, Schwabach, Germany
HPLC LaChrom®	Merck, Darmstadt, Germany
Autosampler L-7250	
Interface D-7000	
Pump L-7100	
UV detector L-7400	
HPLC Pump LB-5035	Berthold Technologies, Bad Wildbad, Germany
Incubator BB6220	Heraeus, Hanau, Germany
Jetstream 2 HPLC Peltier Column thermostat	WO Industrial electronics, Langenzersdorf, Austria
LaminAir® Flow Hood Hera-safe	Heraeus, Hanau, Germany
LightCycler 480®	Roche, Mannheim, Germany
Liquid Scintillator Mixing Flow Cell Z-500- 4, 500 µl	Berthold Technologies, Bad Wildbad, Germany
Microtom Frigocut® 2800 N	Leica, Bensheim, Germany
Microtom Leica CM 1510 S-1	Leica, Bensheim, Germany
Mikroscope Axiovert 135	Zeiss, Jena, Germany
Nalgene® Cryo 1° Freezing Container	Nalgene, Rochester, USA
Neubauer counting chamber ($0.00225mm^2$/0.1mm)	Zeiss, Jena, Germany

Pipettes Eppendorf Reference	Eppendorf, Hamburg, Germany
Pipetting controller Pipetboy®	Integra Biosciences, Fernwald, Germany
Punch 10 mm	Bauhaus, Berlin, Germany
Punch 25 mm	Bauhaus, Berlin, Germany
RO 10 power IKAMAG	IKA® Werke GmbH & Co. KG, Staufen, Germany
Savant SC 210A, Speed Vac concentrator	Thermo Scientific, Langenselbold, Germany
Scalpells	C. Roth, Karlsruhe, Germany
SG-Labostar 2-DI/-UV	SG Wasseraufbereitung und Regenierstation GmbH, Barsbüttel, Germany
Software Radiostar V 4.6	Berthold Technologies, Bad Wildbad, Germany
Speed Vac plus SC 110 A	Savant, NY, USA
Standard Power Pack P25	Biometra, Göttingen, Germany
T-Gradient	Biometra, Göttingen, Germany
Thermoblock	Biometra, Göttingen, Germany
Thermo HAAKE P5	Haake, Karlsruhe, Germany
Thermostat HAAKE DC 10	Haake, Karlsruhe, Germany
Tissue lyser II	Quiagen, Retsch GmbH, Haan, Germany
T-mixer	Berthold Technologies, Bad Wildbad, Germany
Tweezers	C. Roth, Karlsruhe, Germany
Ultrasonic bath SONOREX RK100	Bandelin, Berlin, Germany
Universal vacuum system plus UVS400A	Savant, NY, USA
Universal vacuum system UVS400A	Thermo Scientific, Langenselbold
UV- cuvettes mikro 15 mm	Brand, Wertheim, Germany
UV-Meter WPA Biowave DNA	Biochrom Ltd., Cambridge, UK
Volumetric flask (50ml, 100 ml, 500 ml, 1 l)	Brand, Wertheim, Germany
Vortex	Bender & Hobein, Zürich, Switzerland
Water Bath DC3/W26	Haake, Karlsruhe, Germany

2.4 Reagents and expendable items

The following reagents and expendable items were used:

Acetic acid	C. Roth, Karlsruhe, Germany
Acetone	Sigma-Aldrich, Schnelldorf, Germany
Acetonitrile, HPLC grade	Fisher Scientific, Schwerte, Germany
Acetonitrile, HPLC grade	Prolabo, VWR, Darmstadt, Germany
Acetonitrile, LiChrosolv® HPLC grade	Merck, Darmstadt, Germany
Agarose	C. Roth, Karlsruhe, Germany
Aluminium foil	
[1,2,6,7-^{3}H]-Androstenedione in toluene:ethanol 9:1 (v/v) specific activity: 3.15 TBq/mmol (> 99.1%)	GE Healthcare, Buckinghamshire, UK
Androstanediol	Sigma-Aldrich, Schnelldorf, Germany
Androstanedione	Sequoia Research, Berkshire, UK
Androstenedione	Sigma-Aldrich, Schnelldorf, Germany
Androsterone	Sigma-Aldrich, Schnelldorf, Germany
Aqua bidest., sterile filtered, degased	
AST2000 Maintanance Medium	CellSystems® Biotechnologie Vertrieb GmbH, Troisdorf, Germany
Benzil	Sigma-Aldrich, Schnelldorf, Germany
Betamethasone (> 98%)	Sigma-Aldrich, Schnelldorf, Germany
Bis(4-nitrophenyl) phosphate (BNPP)	Sigma-Aldrich, Schnelldorf, Germany
Boric acid	VWR Merck, Darmstadt, Germany
Bovine Serum albumin (BSA), protease-free	C. Roth, Karlsruhe, Germany
Braun Dermatom® Blades	Braun, Tuttlingen, Germany
Bromphenol blue	Sigma-Aldrich, Schnelldorf, Germany
Calcium chloride	Sigma-Aldrich, Schnelldorf, Germany
Cell culture dishes (5, 10 cm)	TPP, Trasadingen, Switzerland
Cell culture plates (6-Well)	BD Biosciences,NJ, USA

Cell culture plates (6-Well, 96-Well)	TPP, Trasadingen, Switzerland
Centrifuge tubes 15 ml, 50 ml	TPP, Trasadingen, Switzerland
Centrifuge tubes® Borosilicat glass 16x125 mm	VWR, Darmstadt, Germany
Chloroform, anhydricum (> 99%)	Sigma-Aldrich, Schnelldorf, Germany
Citric acid, monohydrate	C. Roth, Karlsruhe, Germany
[1,2,6,7-^{3}H]-Corticosterone in toluene:ethanol 9:1 (v/v) specific activity: 2.89 TBq/mmol (> 95.9%)	GE Healthcare, Buckinghamshire, UK
Corticosterone (> 98.5%)	Sigma-Aldrich, Schnelldorf, Germany
Cover slip 24 x 50 mm	C. Roth, Karlsruhe, Germany
Cryo tubes, 1.8 ml	Biochrom, Berlin, Germany
Culture Tubes, AP Glass, 100 x 16 mm, Duran Group	VWR, Darmstadt, Germany
Diethylpyrocarbonate	C. Roth, Karlsruhe, Germany
Diethylether Chromasolv® for HPLC (>99.9%)	Sigma-Aldrich, Schnelldorf, Germany
5α–Dihydro[1,2,4,5,6,7-^{3}H]testosterone in toluene:ethanol 9:1 (v/v) specific activity: 3.74 Tbq/mmol (> 98.8%)	GE Healthcare, Buckinghamshire, UK
Dihydrotestosterone (> 97.5%)	Sigma, Schnelldorf, Germany
Dimethylsulfoxide (DMSO)	Merck, Darmstadt, Germany
Disodium hydrogenphoshate (Na_2HPO_4)	Merck, Darmstadt, Germany
Dispase II	Roche Diagnostics, Mannheim, Germany
DNase I, Amplification grade, AMPD1	Sigma-Aldrich, Schnelldorf, Germany
Dulbecco´s modified Eagle´s medium (DMEM)	Sigma-Aldrich, Schnelldorf, Germany
Dulbecco´s modified Eagle´s medium high glucose (DMEM high glucose)	Sigma-Aldrich, Schnelldorf, Germany
Dulbecco´s PBS (1x) without Ca& Mg	Sigma-Aldrich, Schnelldorf, Germany
DuoSet Elisa IL-8 (Human CXCL8/IL-8)	R&D Systems, Abingdon, UK
Eosin solution 0.5 %	C. Roth, Karlsruhe, Germany
EpiDerm™ maintenance medium (Epi-100-ASY)	MatTek Corporation, Ashland, MA, USA

EpiDerm-FT™ maintenance medium (EFT-400-ASY)	MatTek Corporation, Ashland, MA, USA
Eppendorf tubes (0.5; 1.5; 2 ml)	Eppendorf, Hamburg, Germany
Eserin (Physostigmine)	Sigma-Aldrich, Schnelldorf, Germany
17β-Estradiole (min. 98%)	Sigma-Aldrich, Schnelldorf, Germany
Estron	Sigma-Aldrich, Schnelldorf, Germany
Ethanol, absolute, HPLC grade	Merck, Darmstadt, Germany
Ethyl acetate Chromasolv® plus	Sigma-Aldrich, Schnelldorf, Germany
Ethylene-diamine-tetraacetic acid (EDTA)	Sigma, Schnelldorf, Germany
Fluorescence phase contrast microscope Biozero BZ-8000	Keyence, Neu Isenburg, Germany
Foetal Calf Serum (FCS)	Biochrom, Berlin, Germany
Formaldehyde	C. Roth, Karlsruhe, Germany
GelRed™ Nucleic Acid Gel Stain, 10.000x in water	Biotium, Hayward, Californien USA
Gelred™ Nucleic Acid Stain	Biotrend, Cologne, Germany
GeneRuler 50 bp DNA ladder	Fermentas, St. Leon-Rot, Germany
Gentamicin sulfate	C. Roth, Karlsruhe, Germany
Glutaraldehyde	C. Roth, Karlsruhe, Germany
Glycerol 85%	C. Roth, Karlsruhe, Germany
HPLC- supplies	VWR international, Darmstadt, Germany
Micro insert, 0.1 ml clear glass	
Vials, threaded, 1.5 ml, 32x11.6 mm	
Srew cap, 8 mm slitted	
Septum 8 mm, Silicone white/PTFE blue, 60°, slitted	
Column guard: Lichrocart® 4-4, Lichrospher®100, RP 18 (5 µm)	Merck Darmstadt, Germany
Column: Lichrospher, Lichrocart® cartridges, d= 4mm, RP18, 100A°, 125x4mm	Merck, Darmstadt, Germany
Hydrogen peroxide, 30%	C. Roth, Karlsruhe, Germany

6β−Hydroxytestosterone	Sigma-Aldrich, Schnelldorf, Germany
Keratinocytes Basal Medium and Supplements for Growth Medium	Lonza, Berlin, Germany
L-Glutamine	Biochrom, Berlin, Germany
Lactate dehydrogenase IFC Version 2	Roche Diagnostics, Mannheim, Germany
LightCycler 480 96-well plates plus sealing foil	Roche Diagnostics, Mannheim, Germany
LightCycler 480 SYBR Green I Master	Roche Diagnostics, Mannheim, Germany
Mayer´s Hematoxylin solution for microscopy	C. Roth, Karlsruhe, Germany
Membrane Filter attachment 250 ml PES Membrane 0.22 µm	TPP, Trasadingen, Switzerland
Methanol, **HI**P**S**OLV CHROMANORM®, HPLC grade	VWR, Darmstadt, Germany
Methanol, HPLC grade	Merck, Darmstadt, Germany
Microplate, 96 well	Greiner BioOne GmbH, Frickenhausen, Germany
Microscopes slides Superfrost Ultra plus	Thermo Scientific, Langenselbold, Germany
N-Ethylmaleimide (NEMI)	Sigma-Aldrich, Schnelldorf, Germany
Nitrogen, liquid	Air Liquide, Berlin, Germany
NucleoSpin RNA II	Macherey-Nagel, Düren, Germany
Nylon mesh, (Monofil) pore size 150 µm	Neolab, Heidelberg, Germany
Optiflow plus	Berthold Technologies, Bad Wildbad, Germany
Orange G	C. Roth, Karlsruhe, Germany
PAA Dulbecco´s PBS (1x) without Calcium and Magnesium	PAA Laboratories GmbH, Cölbe, Germany
Parafilm® M	Brand GmbH & Co, Wertheim, Germany
Penicillin/Streptomycin	Biochrom, Berlin, Germany
Phenion® FT ALI-medium	Henkel AG & Co. KgaA, Dusseldorf
Pipette Biosphere® Filter Tips DNA/RNAse free Type Eppendorf/Gilson	Sarstedt, Nümbrecht, Germany

Pipette Tips	Sarstedt, Nümbrecht, Germany
Phenylmethanesulfonyl fluoride (PMSF)	Sigma-Aldrich, Schnelldorf, Germany
Polyurethane foam	
Potassium chloride	Merck, Darmstadt, Germany
Potassium dihydrogen phosphate	C. Roth, Karlsruhe, Germany
Potassium hydroxide	Merck, Darmstadt, Germany
Prednicarbate	Sanofi- Aventis, Frankfurt, Germany
Primer	Tib Molbiol, Berlin, Germany
RevertAid First Strand cDNA Synthesis Kit	Fermentas, St. Leon-Rot, Germany
Roti®-Histokit fixing agent	C. Roth, Karlsruhe, Germany
SafeSeal tubes (0.5; 1.5; 2 ml)	Sarstedt, Nümbrecht, Germany
Scalpel blades	C. Roth, Karlsruhe, Germany
Single-use needles (0.8/80 mm)	VWR, Darmstadt, Germany
Single-use syringes (5 ml/20 ml)	VWR, Darmstadt, Germany
Sodium dihydrogen phosphate	Merck, Darmstadt, Germany
Sodium dodecyl sulfate (SDS)	Merck, Darmstadt, Germany
Sodium fluoride (pro analysi)	Merck, Darmstadt, Germany
Sodium nitrite	C. Roth, Karlsruhe, Germany
Stainless steel beads for Tissue lyser II (d= 5 mm)	Quiagen, Retsch GmbH, Haan, Germany
Sterile filter Pur S plus, 0.2 µm	Sarstedt, Nümbrecht, Germany
Streptomycin	Biochrom, Berlin, Germany
Sulfuric acid	Merck, Darmstadt, Germany
[1,2,6,7-^{3}H(N)]-Testosterone in ethanol specific activity: 2.59 TBq/mmol (> 97%)	Perkin Elmer, Boston, MA, USA
[1,2,6,7-^{3}H(N)]-Testosterone in toluene:ethanol 9:1 (v/v) specific activity: 2.74 TBq/mmol (>98%)	GE HealthCare, Buckinghamshire, UK
Testosterone (> 98%)	Sigma-Aldrich, Schnelldorf, Germany
Tetramethylbenzidine	C. Roth, Karlsruhe, Germany

Tissue culture flasks (25 cm^2, 75 cm^2)	TPP, Trasadingen, Switzerland
Tissue culture inserts, 0.4 µm, polycarbonate membrane	Nunc, Roskilde, Danmark/ VWR, Darmstadt, Germany
Tissue freezing medium	Leica Microsystem, Nussbach, Germany
Tris-Hcl	Sigma-Aldrich, Schnelldorf, Germany
Tris Base	Sigma-Aldrich, Schnelldorf, Germany
Trypsin	Biochrom, Berlin, Germany
Tween® 20	C. Roth, Karlsruhe, Germany
UV-cuvettes micro Z 15 mm	Brand GmbH, Wertheim, Germany
Xylene cyanol	Sigma-Aldrich, Schnelldorf, Germany

2.5 Media and solutions

The following media and solutions were used for cell and tissue cultivation as well as all accomplished experiments. If necessary, media and solutions were prepared under aseptic conditions.

2.5.1 Cell culture media

Keratinocytes Growth Medium (KGM)

Keratinocytes Basal Medium (KBM) 500 ml
+ Human epidermal growth factor (hEGF)
+ Insulin
+ Bovine pituitary extract (BPE)
+ Hydrocortisone
+ Gentamycin sulfate/Amphotericin B
in concentrations provided by the manufacturer (Lonza).

Keratinocytes Test Medium

Keratinocytes Basal Medium (KBM) 500 ml
+ Human epidermal growth factor (hEGF)
+ Insulin

in concentrations provided by the manufacturer (Lonza).

For cultivation and experiments with NHDF, respectively, Dulbecco´s Modified Eagle Medium (DMEM) was supplemented as followed:

Fibroblasts Growth Medium

DMEM

+ L-Glutamin	2mM
+ Foetal calf serum (FCS)	10 % (v/v)
+ Penicillin	100 I.E./ml
+ Streptomycin	100 µg/ml

Fibroblasts Test Medium

DMEM

+ L-Glutamin	2 mM

For cultivation as well as experiments with HaCaT cell line, DMEM was prepared as followed:

HaCaT Growth Medium

DMEM high glucose

+ L-Glutamin	2 mM
+ FCS	10 % (v/v)
+ Penicillin	100 I.E./ml
+ Streptomycin	100 µg/ml

HaCaT Test Medium

DMEM high glucose

+ L-Glutamin	2 mM

All Media were stored at 4° C for a maximum of 4 weeks.

2.5.2 Solutions for cell isolation and cultivation

Transport Medium

DMEM

+ Penicillin	100 I.E./ml
+ Streptomycin	100 µg/ml

Stop Medium

DMEM

+ FCS	10 % (v/v)
+ Penicillin	100 I.E./ml
+ Streptomycin	100 µg/ml

Phosphate buffered saline (PBS)

KCl	0.2 g/l
+ NaCl	8.0 g/l
+ KH_2PO_4	0.2 g/l
+ Na_2HPO_4	1.44 g/l

in Aqua bidest.

pH value was adjusted to pH = 7.4 with NaOH or HCl, respectively. This was followed by autoclaving.

Dispase II stock solution

Dispase II (1 U/mg)	1 mg
+ Phosphate buffered saline (PBS)	ad 100 ml

Following sterile filtration (0.2 µm), stock solution was stored at -20° C.

Trypsin-EDTA solution

PBS

+ Trypsin	1.67 mg/ml
+ EDTA	0.67 mg/ml

0.05 % EDTA solution

Dulbecco´s PBS (1x) without Ca&Mg

+ EDTA	0.05 %

Freezing Medium

DMEM

+ FCS	10 % (v/v)
+ DMSO	10 % (v/v)

Cell lysis buffer

SDS 0.5 %

in aqua bidest.

All solutions were stored at +4° C.

2.5.3 Media for excised native human skin

Transport Medium

DMEM

+ Penicillin	100 I.E./ml
+ Streptomycin	100 µg/ml

Test Medium for biotransformation experiments

KBM

+ Calcium chloride 1.4 mM

2.5.4 Media for RHE and RHS

EpiDerm culture medium (Epi-100-ASY)

Dulbecco's Modified Eagle's Medium (DMEM)

+ Epidermal growth factor (EGF)

+ Insulin

+ Gentamycin 5 µg/ml

+ Amphotericin B

+ Phenol red

+ lipid precursors

in concentrations provided by the manufacturer.

EpiDerm-FT culture medium (EFT-400-ASY)

Dulbecco's Modified Eagle's Medium (DMEM)

+ Epidermal growth factor (EGF)

+ Insulin

+ Gentamycin 5 µg/ml

+ Amphotericin B 0.25 µg/ml

+ Phenol red

+ lipid precursors

in concentrations provided by the manufacturer.

Phenion FT medium (ALI-medium)

DMEM + Glutamax/Ham´s F12 medium (3:1)

+ BSA 1.6 mg/ml

+ Hydrocortisone 0.4 µg/ml

+ Insulin 0.12 IU/ml

+ Ascorbic acid 2-phosphate 1 mM

+ Penicillin 100 IU/ml

+ Streptomycin 100 µg/ml

The medium was provided by the manufacturer.

AST2000 medium

The exact composition is known only to the manufacturer.

2.5.5 Further solutions

Solutions for HPLC analysis

Solvents

Water:	For all HPLC analysis aqua bidest. (sterile filtrated (0.2 µm) and degased in ultrasonic bath) was used.
Acetonitrile:	Gradient grade acetonitrile was used constantly for all HPLC analysis.

Wash-solution for the Injection needle

Aqua bidest. 10 (v/v)

Methanol, HPLC grade 90 (v/v)

Sodium fluoride solution, saturated

Sodium fluoride, pro analysi 120 mg/ml

in aqua bidest.

Solutions for esterase inhibition

The various inhibitors (tbl. 3) were dissolved in ethanol (ultrasound bath under refrigeration, 3 min) and diluted with the test medium for biotransformation experiments to achieve the final concentrations (in 500 µl test medium) required for esterase inhibition of human skin homogenates.

Inhibitor	Stock solution (concentration)	mg/ml ethanol or ethanol/test medium (1:4)	Final concentration(s)
BNPP	0.1 M	34.02 mg	10^{-3} M, 10^{-2} M
PMSF	0.1 M	17.42 mg	10^{-3} M, 10^{-2} M
BNPP+PMSF	0.1 M each	34.02 mg/17.42 mg	10^{-3} M, 10^{-2} M each
Eserin	0.1 M	30.32 mg	10^{-5} M
Eserin+BNPP	0.1 M each	30.32 mg/34.02 mg	10^{-5} M 10^{-3} M
Eserin+PMSF	0.1 M each	30.32 mg/17.42 mg	10^{-5} M/10^{-3} M
NEMI	0.1 M	12.5 mg	$2•10^{-4}$ M, $5•10^{-2}$ M
Benzil	0.01 M	2.103 mg	10^{-7} M, 10^{-4} M

Tbl. 3: Inhibitor solutions (individual solutions or combinations) for esterase inhibition experiments and applied concentrations.

Solutions required for Interleukin-8-measurement (ELISA)

Wash buffer

Tween® 20 0.05 %

in PBS

pH value was adjusted to pH =7.4 with NaOH or HCl, respectively.

Tris-buffered saline (TBS)

Aqua bidest.

+ Tris Base 20 mM

+ NaCl 150 mM

pH value was adjusted to pH 7.2-7.4, 0.2 µm sterile filtered.

Block buffer

PBS

+ BSA 1 %

+ NaN_3 0.05 %

Reagent Diluent

TBS

+ BSA 0.1 %

+ Tween® 20 0.05 %

pH value was adjusted to pH 7.2 - 7.4, 0.2 µm sterile filtered.

Citric buffer

Citric acid, monohydrate 21 g

Aqua bidest. ad 1 l

pH value was adjusted to pH= 3.95 with KOH, followed by sterile filtration (0.2 µM).

Solution was stored at 4° C.

TMB-solution

TMB 20 mg

+ DMSO 0.5 ml

+ Ethanol 0.5 ml

After sterile filtration (0.2 µM) solution was stored at 4° C for approx. 4 weeks.

Substrate solution

Citric buffer 11 ml

+ TMB-solution 110 µl

+ Hydrogen peroxide, 30 % 3.3 µl

Solution was prepared immediately before experiments.

Stop solution

2 N H_2SO_4

Solutions for gene expression analysis

DEPC-treated water (DEPC-water)

DEPC 1 ml

+ Aqua bidest. ad 1 l

After incubation at room temperature for 24 h, solution was autoclaved for complete deletion of DEPC.

Ethanol 70 %

Ethanol (96 %)	772.7 µl/ml
+ DEPC-Wasser	227.3 µl/ml

Thermolysin reaction buffer

KCl	24.6 mg
+ NaCl	29.2 mg
+ $CaCl_2 \bullet H_2O$	7.4 mg
+ HEPES	23.83 mg
in DEPC water	10 ml

After sterile filtration (0.2 µM) solution was stored at -20° C for approx. 4 weeks.

Thermolysin solution

Thermolysin	0.5 mg/ml

in Thermolysin reaction buffer

10 mM Tris-HCl, pH 7.5

Tris Base	1.2114 g
DEPC water	900 ml

HCl for pH-value adjustment (pH 7.5)

DEPC water	ad 1 l

0.5 mM Na_2EDTA

EDTA	186.12 g
+ Aqua bidest.	900 ml

+ NaOH for pH value adjustment (pH 8.0)

+ Aqua bidest.	ad 1 l

Solution was sterilized by autoclaving and stored at room temperature.

TBE buffer (10x)

Tris Base	108 g
Boric acid	55 g
Na_2EDTA 0.5 mM	40 ml
+ Aqua bidest.	ad 1 l

Loading buffer (10x)

Bromphenol blue	100 mg
+ Xylene cyanol	100 mg
+ Tris 150 mM	33 ml
+ Glycerol (85 %)	60 ml
+ DEPC water	7 ml

GelRed staining solution

GelRed (10 0000x)	30 µl
in Aqua bidest.	200.0 ml

150 mM Tris pH 7.6

Tris Base	1.817 g
+ DEPC water	90 ml

+ HCl (conc.) for pH value adjustment (pH 7.6)

+ DEPC water	ad 100 ml

Loading buffer (6x)

Orange G	3.6 mg
+ Glycerol (85 %)	6 g
+ 150 mM Tris pH 7.6	ad 10 ml

Agarose gel 1 %

Agarose	0.5 g
+ TBE buffer (1x)	50 ml

Solution was boiled and filled into the electrophoresis chamber.

Agarose gel 2 %

Agarose	1.0 g
+ TBE buffer (1x)	50 ml

Solution was boiled and filled into the electrophoresis chamber.

NucleoSpin® RNA II Lysis buffer

β-mercaptoethanol	10 µl/ml

in NucleoSpin® RNA II RA1 buffer

PCR-Mastermix

Primer_forward	62.5 µl/ml
+ Primer_reversed	62.5 µl/ml
+ SYBR Green I Mix	625 µl/ml

in PCR water

Karnovsky-Stock solution

Formaldehyde p.A. 37 %	72.07 g
+ Na_2HPO_4 x $2H_2O$	9.56 g
+ KH_2PO_4	1.76 g
+ Aqua bidest.	ad 1 l

Karnovsky-Application solution

Karnovsky- Stock solution	7.5 ml
+ Glutaraldehyde 25 %	1.0 ml
+ Aqua bidest.	ad 10.0 ml

2.6 Test compounds and their solutions

2.6.1 Prednicarbate

2.6.1.1 Preparations for HPLC quantification

For the quantification of PC and metabolites P17EC, P21EC and PD as well as internal standard betamethasone by means of HPLC-UV/Vis-detection, stock solutions were prepared at 10^{-2} M in ethanol. Prior to experiments, dilutions for preparation of calibration solutions for standard curves were made with methanol to six final concentrations of 10^{-4} M to $2.5 \cdot 10^{-7}$ M for PC and $5 \cdot 10^{-7}$ M for metabolites and betamethasone, respectively.

Furthermore, the stock solution of bethametasone was diluted with methanol in a ratio of 1:10 to a concentration of 10^{-3} M. This solution was added to each sample obtained in the biotransformation experiments for a final concentration of 10^{-5} M.

Stock solutions were kept at -20° C in aliquots for a maximum period of 4 weeks.

2.6.1.2 Preparations for biotransformation experiments

Monolayer cell cultures

Immediately before biotransformation experiments, PC stock solution was prepared in ethanol at 10^{-3} M and diluted for a final concentration of $2.5 \cdot 10^{-6}$ M with corresponding test medium for cell cultures of NHK, NHDF and HaCaT, respectively (see chapter 2.9.1).

Human skin and RHE/RHS

In order to study biotransformation of PC in human skin and the reconstructed tissues, 5 mg PC were dissolved in 1 ml ethanol and diluted with phosphate buffered saline (PBS) pH 7.4 for a final concentration of 0.25 % PC immediately before the experiment.

2.6.1.3 Preparations for esterase inhibition of skin homogenates

For the enzyme inhibition experiments, 2.5 mg PC were dissolved in 1 ml ethanol and diluted with PBS for a further PC solution with a final concentration of 0.125 % PC.

2.6.2 Testosterone

2.6.2.1 Preparations for HPLC quantification

For the development and *in house* validation of the HPLC-radiodetection (Radio-HPLC) analysis as well as the establishment of calibration solutions (for standard curves) for the quantification of testosterone and metabolites, stock solutions of radiolabelled testosterone, metabolites (tbl. 4) and corticosterone (internal standard) were prepared at concentrations of 3.7 MBq/ml each in ethanol. Steroid stock solutions were diluted with methanol to achieve nine final concentrations (tbl. 4) immediately before starting quantitative Radio-HPLC measurement. Since not all metabolites were available as isotope-labelled substances, non-labelled testosterone, all feasible metabolites and corticosterone (cort.) were subjected to HPLC-UV/VIS analysis for the determination of retention times, too. Stock solutions of non-labelled androgens were prepared at concentrations of 10^{-1} M each in ethanol.
Furthermore, the [^{3}H]-corticosterone stock-solution was diluted 1:10 with methanol and added to each sample for a final corticosterone concentration of 0.037 MBq/ml in each sample before extraction.

Steroids	**Range of concentrations for standard curves**
Androstanediole	10^{-5} M - 10^{-2} M
Androstanedione	10^{-5} M - 10^{-2} M
Androstenedione [^{3}H]-Androstenedione	10^{-5} M - 10^{-2} M 0.0025 - 1 MBq/ml; 0.33 ng/ml - 133.1 ng/ml ($0.75 \cdot 10^{-10}$ M - $3.1 \cdot 10^{-7}$ M)
Androsterone	10^{-5} M - 10^{-2} M
Corticosterone (i.s.) [^{3}H]-Corticosterone	10^{-6} M - 10^{-2} M 0.0025 - 1 MBq/ml; 0.37 ng/ml - 146.8 ng/ml ($0.8 \cdot 10^{-10}$ M - $3.1 \cdot 10^{-7}$ M)
Dihydrotestosterone [^{3}H]-Dihydrotestosterone	10^{-5} M – 10^{-2} M 0.0025 - 1 MBq/ml; 0.38 ng/ml - 155.9 ng/ml ($0.7 \cdot 10^{-10}$ M - $2.7 \cdot 10^{-7}$ M)
17β-Estradiole	10^{-6} M - 10^{-3} M

Steroids	Range of concentrations for standard curves
Estrone	10^{-5} M - 10^{-2} M
6β-Hydroxytestosterone	5 ·10^{-5} M - 10^{-2} M
Testosterone [^{3}H]-Testosterone	10^{-6} M - 10^{-4} M 0.0025 - 1 MBq/ml; 0.27 ng/ml - 102 ng/ml (0.9•10^{-10} M - 3.6•10^{-7} M)

Tbl. 4: Concentration range of non-labelled (in M) and isotope-labelled (in MBq/ml and ng/ml) testosterone, its metabolites and internal standard (i.s.) corticosterone for standard curves.

Stability of radiolabelled solutions

All isotope-labelled original stock solutions (37 MBq/ml) were stored at -20° C. Under these storage conditions the average rate of decomposition of the product is 0.13 - 1 % per week. To avoid falisfication of biotransformation results, solutions for the experiments and standard solutions were prepared immediately prior to experiments / analysis. Stock solutions (3.7 MBq/ml) of radiolabelled substances were stored at -20° C for approx. 5 days.

2.6.2.2 Preparations for biotransformation experiments

Monolayer cell cultures

Immediately before biotransformation experiments, the [^{3}H]-testosterone stock solution (in ethanol) was diluted 1:10 with methanol. Again diluted with corresponding test medium for NHK and NHDF, respectively, a final concentration of 5.69 ng/ml (0.0555 MBq/ml; 2·10^{-8} M) testosterone was achieved.

Excised human skin and RHE/RHS

In order to study biotransformation of testosterone in human skin and the constructs, the [^{3}H-] testosterone stock solution (in ethanol) was diluted in a ratio of 1:3 to achieve a final concentration of 12.33 MBq/ml.

2.7 Methods

2.7.1 Cell cultures

For primary cultures, normal human dermal fibroblasts (NHDF) and normal human keratinocytes (NHK) were isolated from juvenile foreskin [95, 164] obtained from circumcisions with permission by the Medical Association Berlin (Ärztekammer Berlin).

2.7.1.1 Normal human keratinocytes (NHK)

Immediately after transport in the corresponding medium (transport medium), foreskins were washed with PBS. After transfer into a petri dish, the skin was cut into pieces of approximately 5 x 5 mm and placed in a mixture of dispase II (600 U/ml) and 5 ml of PBS at 4° C for at least 20 hours. Then the epidermis was separated from the dermis carefully and placed in a centrifuge tube. After the addition of 2 ml of trypsin/EDTA, the tube containing the epidermis was panned in the water bath (37° C) up to the occurrence of a slight opacity (2 - 3 minutes). The enzymatic reaction was terminated by the addition of stop medium (8 ml). After centrifugation (1000 × g, 5 min, 16° C) and removal of the supernatant, the cell pellet was washed twice with 10 ml PBS. After additional centrifuation, and resuspension in keratinocyte growth medium (KGM), cells were seeded in a cell culture flask (25 or 75 cm^2) containing pre-heated KGM. After overnight incubation (37° C, 5 % CO_2) and PBS wash, the medium was replaced for separation of remaining dead or not sufficiently attached cells and blood cells. In addition, a microscopic examination has been carried out to ensure the presence of a pure keratinocyte cell culture. Any existing fibroblasts were separated by adding 1.5 ml of trypsin/EDTA and incubation (37° C, 5 % CO_2) for 1 minute and then removed by washing with PBS. These cells are cells of the 0th passage.

Every 2nd, no later than every 3rd days the medium was changed. After a confluence of approx. 70 %, the cells were splitted in a ratio of 1:2 to 1:3. For this puropse, cells were washed with 10 ml PBS followed by the addition of 2 ml trypsin/EDTA to dissolve the cell assembly and to release cells from the bottom (37° C for 2 - 4 minutes). The reaction was terminated by the addition of 8 ml stop medium. The cells were transferred into a centrifuge tube and the cell culture flask washed two times with 10 ml of PBS each. The combined cell solutions were centrifuged (1000 × g, 5 min, 16° C) and after resuspension of the cell pellet in 5 ml preheated KGM, cells were used directly for experiments or seeded in fresh tissue culture flasks containing preheated KGM (passage +1 after each splitting process) for cell expansion. Cells were frozen after trypsinization in the Freezing Container at -80° C and addition of 1.5ml freezing medium if not requred immediately. After 24 hours, cells were transferred into a nitrogen tank. Frozen cells were reactivated as follows: After removal from

the nitrogen tank, the cells were thawed quickly in the water bath (37° C). Followed by centrifugation, the cell pellet was reconstituted in KGM and transferred in cell culture flasks containing pre-warmed KGM. The next day, the medium was replaced by pre-warmed KGM.

2.7.1.2 Normal human dermal fibroblasts (NHDF)

For the isolation of fibroblasts, foreskins were cut into pieces of approx. 5 x 5 mm after PBS wash and transferred into a petri dish containing 2 ml Trypsin/EDTA. After 20 hours at 4° C, the enzymatic reaction was terminated by the addition of 8 ml of stop medium. The obtained cellsuspension was centrifuged (1000 x g, 5 min, 16° C), washed two times with 10 ml PBS each and again centrifuged. After resuspension of the cell pellet in fibroblast growth medium (FGM), cells were seeded in tissue culture flasks (25 or 75 cm^2) containing pre-warmed FGM. Media exchange, passaging and the freezing of not immediately required cells was determined analogously to the procedures described for NHK (chapter 2.7.1.1).

2.7.1.3 Cultivation of HaCaT cell line

The cultivation of the HaCaT cell line was accomplished with previously frozen cells. Cells were warmed quickly in a water bath (37° C) and centrifuged (1000 x g, 5 min, 16° C). The obtained cell pellet was washed with PBS and resuspended in the appropriate growth medium. Then, cells were seeded in tissue culture flasks containing pre-warmed growth medium. Every 2 days, the medium was changed. On reaching a confluency of about 80 %, the cells were splitted in a ratio of 1:5 to 1:10. The splitting process was the same as described for NHK (chapter 2.7.1.1).

2.7.2 Handling of Reconstructed Human Epidermis and Skin

All steps were performed under sterile conditions. The corresponding media were stored at 4° C and tempered to approx. 37° C immediately before use if required.
Upon receipt, reconstructed tissues were visually inspected and if physical imperfections were noted, tissues were rejected. All reconstructed tissues were delivered under refrigeration (4 - 6° C) and equilibrated immediately after delivery according to instructions of the supplier:

EpiDerm and EpiDerm-FT

Upon receipt, the unopened 6-well shipping plates containing RHE/RHS were stored in the refrigerator for a rest period of 1 h.

0.9 ml for RHE and 2 ml for RHS, respectively, of the corresponding pre-warmed medium were dispended into each well of a provided 6-well-plate. The Epiderm/EpidermFT in their culture inserts were removed from the transport plate with sterile forceps. Adhering transport agarose on the underside of the insert was stripped carefully and the tissues were transferred to the prepared wells containing the coressponding medium. No air bubbles were allowed under the insert. RHE and RHS were equilibrated at 37° C, 5 % CO_2 overnight (at least for 16 - 18 hours) before the corresponding media were replaced by fresh pre-warmed media.

Phenion® FT

Under a LaminAir three Petri dishes (d = 35 mm) were placed in an outer large Petri dish (d = 100 mm). Then, two sterile metal supports were placed on the bottom of each inner small Petri dish. Sheets of filter paper were put on the top of the pre-placed metal supports. 5 ml of the provided ALI-medium were filled in each inner Petri dish until the medium reaches the upper surface of the filter paper and the papers were soaked with medium. With a sterile pair of tweezers tissues were transferred from the transport plate on top of the filter papers as carefully as possible to avoid mechanical stress. The outer Petri dish was closed and the Phenion FT skin models were equilibrated at 37° C, 5 % CO_2 overnight (16 - 18 hours) and the media were replaced by 5 ml fresh, pre-warmed media.

AST2000

1.5 ml of cold maintenance medium was filled into each well of a 6-well plate. Inserts were lifted with sterile pair of tweezers and transferred into the prepared culture dishes (6-well plates) avoiding transfer of adhering transport agarose and bubbles between the insert and the bottom of the culture dish. Then, tissues were incubated overnight at 37° C, 5 % CO_2 before medium was replaced by 1.5 ml new pre-warmed maintance medium.
After 1 h rest period, all reconstructed tissues were ready for experiments. The media of overnight equilibration of each tissue were retained for the determination of LDH leakage and IL-8 release (chapter 2.10).

2.7.3 Handling of human skin

Surgically discarded female and male human breast or abdominal skin was handled according to standardized procedures [35]. Immediately after surgery, the skin was separated from the underlying fatty tissue to avoid the contamination of the skin surface with

subcutaneous lipids. For preparation a scalpel was applied directly beneath the dermis and the fatty tissue removed by carefully cutting. The resulting pieces of skin were wrapped in surgical drapes and transported to the laboratory under refrigeration. In the laboratory, the skin surface was washed gently with PBS and cotton cloths to get rid of blood. The skin was either used within 24 hours (freshly excised human skin) or alternatively wrapped in aluminum foil and frozen at -20° C for a maximum of 3 month (cryoconserved human skin) to investigate the influences of cryoconservation on biotransformation. Freshly excised or cryoconserved and thawed human skin was dermatomed to 500 ± 25 µm and punched for a surface area of 0.78 cm^2 and 1.95 cm^2 (diameter = 10 mm/25 mm) for biotransformation experiments in tissue culture inserts (membrane insert approach) and Franz diffusion cell (Franz cell technique), respectively. Basal medium supplemented with $CaCl_2$ to a final Ca^{2+} concentration of 1.4 mM was used to preserve cellular and connective tissue structures in the dermal and epidermal compartments [165].
In addition, dermatomed skin (diameter = 10 mm) was disintegrated for esterase inhibition experiments using Tissue Lyser II. Skin samples were frozen in liquid nitrogen for 15 sec and transferred to tubes containing a 5 mm stainless steel bead and 250 µl test medium for biotransformation experiments. The tubes were placed in cooled teflon container and than the skin samples were disintegrated for 10 min at 30 Hz.

2.8 High performance liquid chromatography (HPLC)

The steroid concentrations in cell cultures, reconstructed human tissues and excised human skin were determined with reversed-phase high performance liquid chromatography (RP-HPLC).

2.8.1 Quantification of prednicarbate and metabolites

Chromatographic conditions

For the separation and quantification of PC and its metabolites P17EC, P21EC and PD as well as internal standard an HPLC analysis was used based on a method of Gysler [95].
The mobile phase was a gradient of acetonitrile/water in a ratio of 20/80 to 100/0 v/v within 20 minutes and a flow rate of 1 ml/min. The sample injection was performed using an autosampler and the samples were analysed with on-line UV-detection at 254 nm. Prior to each analysis run, the hplc system was flushed with the mobile phase (20/80 acetonitrile/water) with a flow rate of 1 ml/min for a minimum of 1 h in order to obtain a sufficient signal to noise ratio and a stabie baseline. Before the sample injection, a methanol solution was analysed to eliminate possible adhering material of previous measurements

from the column. After every fifth to tenth measurement the column was washed with the mobile phase for 30 min. The injection needle was washed after each injection. In the stand-by-modus and at the end of each run the column was flushed with a mixture of acetonitrile/water (60/40 v/v; flow rate 0.5 ml/min). The analysis of each measurement was undertaken by means of the integration of the peak areas (LACHROM® HPLC Multi System Manager Software).

Internal standard

To determine the extraction efficiency of each experiment and for the detection of analysis errors during the measuring process, the internal standard betamethasone in a pre-specified quantity (final concentration: 10^{-5} M) was added to each sample.

Calibration curves

In each assay run seven concentrations of PC, its metabolites and the internal standard, respectively, were analysed to obtain a standard curve for the concentration calculation. All concentrations of the standard curve were randomised over the entire assay run in order to detect any possible measurement interferences which may have arisen during the run.

Concentration calculation

The peak areas of the chromatograms of the calibration points were plotted against their corresponding concentrations and the straight line equation determined by linear regression. From the peak areas of the substances the respective concentrations were calculated. The extraction efficiency was calculated by setting the amount of betamethasone in relation to the amount of internal standard used for the extraction. The actual steroid concentration of PC and metabolites was calculated in consideration of the recovery rate (see chapter 2.8.3) from medium and tissue and the extraction efficiency of each individual sample extraction.

2.8.2 Quantification of testosterone and metabolites

Development

For the development of an hplc method for the separation and quantification of [^{3}H]-testosterone and its expected metabolites, in a first step the substances were injected separately for the determination of their retention times (using UV-detection, too, since not all anticipated metabolites were available as isotope-labelled compounds). Since testosterone and its metabolites in general are rather lipophilic substances, an RP-phase hplc column and an isocratic mobile phase consisting of 50 % acetonitrile and 50 % water was used. Mobile phase composition was optimized by increasing the share of acetonitrile subsequently to a

ratio of 60 % acetonitrile and 40 % water at a flow rate of 1 ml/min. The sample injection was performed using an autosampler. Samples were analysed with on-line radio-detection. Prior to detection in the cell, each sample received 2 ml of Optiflow plus Liquid scintillation cocktail by a scintillator pump at 25° C avoiding direct light. The radiodetector (Flow Star LB 513) was equipped with a 500 µl volume Z-500-flow-through cell for HPLC-analysis. The hplc was flushed with the mobile phase (60/40 v/v acetonitrile/water) for a minimum of 1 h prior to each analysis run. Before the samples were injected, a methanol solution was analysed as desrcribed for PC for background substraction. After every fifth to tenth sample analysis the column was flushed with the mobile phase for 30 min. In addition, the injection needle was washed after each injection. In the stand-by-modus and at the end of each run the column was flushed with a mixture of acetonitrile/water (60/40 v/v; flow rate 0.5 ml/min).The final chromatographic conditions for the optimum separation and quantification are summarized in tbl. 5.

Column	LiChroCART® 250-4 RP-18.5 µm
Column guard	LiChroCART® 4-4
Injection	Autosampler
Injection volume	50 µl
Mobile phase Ratio	Acetonitrile/water isocratic 60/40 v/v
Flow rate	1 ml/min
Run time	30 min
Detection	Radiodetection
Liquid Scintillation cocktail	Composition: 1,2,4-Trimethylbenzene 50 - 70 % (Pseudocumole) Butanol 10 - 15 % Ethoxylated alkylphenol 10 - 20 %
Flow rate – scintillator pump	2 ml/min
Peak Integration	RadioStar 4.6 Software

Tbl. 5: Parameters of hplc-analysis for the separation and quantification of testosterone and its metabolites.

Internal standard

As described for PC, an internal standard was added to each sample. In previous publications [166], corticosterone was described as internal standard for the quantification of testosterone and metabolites via HPLC analysis. Its suitability for these testosterone biotransformation experiments was tested.

***In house* validation**

The *in house* validation of the hplc analysis with radiodetection was performed by the determination of the following parameters:

- **separation (retention factor κ', separation factor α, resolution R_S)**
- **selectivity**
- **linearity**
- **intra-day and inter-day variability**
- **limit of detection**
- **limit of quantification**

Concentration calculation

The peak areas of the chromatograms of the calibration points were plotted against their corresponding concentrations and the straight line equation determined by linear regression. From the peak areas of the substances the respective concentrations were calculated. The extraction efficiency was calculated by setting the determined amount of the internal standard corticosterone in relation to the amount of internal standard used for the extraction (4.95 ng/ml; 0.037 MBq/ml) of each sample. The actual concentration of [^{3}H]testosterone and its metabolites was calculated with the aid of the extraction efficiency and [^{3}H]testosterone recovery rate (chapter 2.8.3) from medium and (dissrupted) tissues.

2.8.3 Quality assurance - Recovery

To ensure that the extraction from the biological materials and interactions between the test compounds and e.g. test medium or culture tubes did not falsify the quantification of the biotransformation experiments, the recovery of the test compounds and their corresponding internal standards from the medium, reconstructed tissues and excised human skin was

determined. For this purpose a defined concentration of the test compounds PC/testosterone or the corresponding internal standards were added to test medium and dissrupted tissues (RHE/RHS and excised human skin). After incubation for 1 h, all samples were extracted three times with ethyl acetate as described in chapter 2.9.2 and analysed by HPLC for the quantification of the test compounds recovered. The analytical results for extracted samples were compared with unextracted standards that represent 100 % recovery.
In addition, the concentration of the test compounds remaning in the pipette after application to the tissue surface was examined. After application of 10 µl/cm^2 of the test solutions, the pipettes were washed three times with 50 µl methanol each and analysed for the quantification of the remainder by HPLC analysis.

2.9 Biotransformation experiments

2.9.1 Experimental setup

Monolayer cell cultures

After cultivation as described in chapter 2.7.1, cells from at least three donors were pooled to reduce donor specific properties. Keratinocytes of the 2nd to 3rd passage and fibroblasts of the 2nd to 5th passage were used for the experiments. Immortalized HaCaT cells were of the 60 - 65th passage. 10^5 cells/well were seeded in 6-well plates in 2 mL growth medium (without hydrocortisone) and were allowed to grow for 24 h (37° C, 95 % humidity, 5 % CO_2). After 24 h, the growth medium was removed and the seeded cells washed with 5 ml PBS before test solutions of prednicarbate or testosterone, respectively, were added.

Prednicarbate

For the determination of PC biotransformation, 1 mL of the test medium containing PC $2.5 \cdot 10^{-6}$ M (chapter 2.5.1.2) was added to each well. Cells (NHK, NHDF, HaCaT) were incubated at 37° C, 5 % CO_2 for 0, 3, 6, 9, 12 and 24 h (NHK and HaCaT only), respectively. For the determination of spontaneous ester hydrolysis of prednicarbate during incubation 1ml test medium containing PC $2.5 \cdot 10^{-6}$ M was tested in parallel. To ensure that culture conditions caused no interfering peaks untreated controls were studied, too.

Testosterone

Analogous to the procedure described for PC, 1 ml of the test medium containing 0.0555 MBq/ml (5.69 ng/ml) [^{3}H]-testosterone was added to the seeded cells (NHK and NHDF). For determination of testosterone absorption to the 6 well plates or further non-enzymatic

reactions 1 ml of the testosterone containing test medium was incubated in parallel. Untreated controls were studied, too. Cells were incubated as described for PC for 0, 6 and 24 h, respectively.

Sample collection

After incubation for up to 24 h, the media were completely transferred to tubes (PC samples) or glass centrifuge tubes (testosterone samples) for extraction after addition of the corresponding internal standard. In case of PC biotransformation studies, 500 µl of a sodium fluoride solution was added to culture medium in order to inhibit ongoing enzymatic reaction [95]. Cells were lysed with 400 µl sodium dodecylsulfate (0.5 %). 200 µl sodium fluoride solution was added to the lysed cell suspension (only for PC). Internal standard was added to the cell suspension before extraction.

Native human skin

Membrane insert approach

After preparation as described in chapter 2.7.3, human skin (11 donors of breast (2) and abdomen skin (9) for PC and 8 female donors of breast (3) and adomen skin (5) for testosterone) was mounted in polycarbonate-membrane inserts (tissue culture inserts) with the stratum corneum in contact with the air. Inserts were placed in 6 well plates filled with 1 ml of Ca^{2+}-supplemented keratinocyte basal medium. The tissues were incubated at 37° C and 5 % CO_2 for 1 h. Then, medium was replaced by fresh pre-warmed medium prior to application of the test compounds.

Application of test compounds

10 µl/cm^2 of 0.25 % PC solution (25 µg/cm^2) or 10 µl/cm^2 of 12.3 MBq/ml [^{3}H]-testosterone solution, respectively, were applied to the skin surface and spread homogeneously using a nylon mesh (150 µm pore size). Skin samples were incubated at 37° C, 5 % CO_2 for 6 h (only PC) and 24 h.

Comparison of experimental setup: Membrane insert approach vs. Franz cell technique

For a comparison of experimental setup influences on (esterase) enzymatic activity, biotransformation of PC in human skin was studied using the membrane insert approach and also Franz diffusion cells, the standard experimental setup for penetration/permeation studies. For this purpose, skin from identical donors (in total 3 female donors, abdomen skin)

was analysed with both experimental setups in parallel.
Using Franz cell technique, three skin samples were fixed in static Franz diffusion cell chambers arranged in parallel. The receptor chambers were filled with 12 ml of Ca^{2+}-supplemented keratinocyte basal medium (receptor medium). The tissues were arranged with the stratum corneum side gaining contact with the air. The bottom side of the skin could be flushed with the receptor medium adjusted to 37° C. Application of PC solution was done as described for the membrane insert approach.

Evaluation of influences due to cryconservation

For the determination of influences on biotransformation due to cryoconservtion, experiments were repeated with cryoconserved and thawed human skin (from the same donor, in total 5 female and 1 male donors; abdomen skin). After a freezing period of approx. 3 months skin was exposed to PC (0.25 % solution, 10 µl/cm^2) and testosterone (12.3 MBq/ml, 10 µl/cm^2) for 24 h, respectively, using the membrane insert approach.

Determination of sex-specific differences in cutaneous esteratic activity

Experiments were performed with human skin from both genders (11 female donors of breast/abdomen skin and 3 male donors of abdomen skin) to determine differences in cutaneous esteratic activity. Experiments were conducted under conditions of equality and as described for PC using the membrane insert approach (24 h exposure).

RHE/RHS

For the biotransformation experiments, the reconstructed tissues (RHE/RHS) were used in their inserts and in case of the RHS Phenion FT petri dishes, respectively. After overnight equilibration and 1 h rest period after medium exchange PC or testosterone solution were applied to tissue surface as described for human skin. Then, tissues were incubated for 6 h (only EpiDerm) and 24 h (37° C; 5 % CO_2).

Sample collection (native human skin and RHE/RHS)

Media collection and preparation of each sample were determined analogously to preparation of monolayer culture media.
The tissue surface of human skin or RHE / RHS, respectively, was washed three times with 100 µl PBS each to remove surplus PC or testosterone. The wash solutions were transferred to tubes together with the nylon mesh. Respective internal standard was added to each sample. In addition, 150 µl of a sodium fluoride solution was added to each sample in case of PC biotransformation experiments.

Transferred to tubes containing a 5 mm stainless steel bead and 500 µl PBS or in case of PC biotransformation studies 500 µl sodium fluoride solution, tissues were disintegrated for 30 sec (EpiDerm and EpiDerm-FT), 10 min (Phenion FT) and 12 min (human skin) at 30 Hz using Tissue Lyser II.

Wash solution, filter (of culture inserts or filter paper in case of Phenion FT) in 500 µl PBS wash or sodium fluoride solution, and media were harvested for analysis in separate tubes and extracted for quantitative analysis as described in chapter 2.9.3.

2.9.2 Esterase inhibition of skin homogenates

Human skin homogenates (chapter 2.7.3) were incubated with PC 0.25 % alone or in the present of various solutions of specific or unspecific esterase inhibitors (chapter 2.5.5) for 6 h (37° C, 5 % CO_2). Addition of 250 µl sodium fluoride and extraction was performed as described for biotransformation experiments (chapter 2.9.3). In addition, experiments were done with reduced PC concentration (0.125 %) and exposure time (3 h) to enhance the inhibition efficiency.

2.9.3 Sample preparation - Extraction procedure

For the quantitative HPLC analysis the steroids had to be extracted from the biological materials to avoid interfering peaks and a contamination of the HPLC column. Extraction and quantification by HPLC (chapter 2.8.1 and 2.8.2) was performed immediately after the incubation period (and disruption of tissues) or samples were frozen at -20 °C for at least 5 days for testosterone and for 2 weeks at -80° C in case of PC, respectively.

The samples were extracted three times by equivalent amounts of ethyl acetate (vortex 1.5 min) and centrifuged (1000 rpm, 3 min). The upper organic phase was removed and transferred to a new tube. The combined organic phases of each sample were evaporated by vacuum rotation (Speed Vac SC 210A, Thermo Scientific, Langenselbold, Germany). The remainders were reconstituted and dissloved in 550 µl methanol (ultrasound bath under refrigeration, 3 min) and centrifuged to separate interfering (in methanol slightly soluble) compounds. 500 µL of the supernatant was transferred into a fresh tube and again exsiccated. After resuspension in 150 µl methanol and centrifugation, 100 µl of the supernatant were transferred into HPLC micro inserts and quantified by HPLC-analysis (chapter 2.8).

2.10 Quality of Reconstructed Human Epidermis and Skin

Before entering into the studies of steroid biotransformation, tissue morphology (integrity) and viability of RHE and RHS were analysed to ensure high quality of the constructs after shipment and resiliency to experimental conditions (tbl. 6).

After overnight equilibration (day 0) and at the end of each experiment, histological examination as well as measurement of IL-8 release/LDH leakage of untreated tissues and tissues treated with test compounds PC/testosterone and their solvents (for 24 h) was performed.

Day/ Matrix	**-1**	**0**	**1**	**60 - 90**
RHE/RHS	Arrival and Overnight equilibration	Medium replacement, quality control and recovery from shipment, IL-8/LDH release or incubation with test compounds/solvents and biotransformation studies	Quality control – IL-8/LDH release and histological examination of integrity after incubation with test compounds/solvents	
Human skin fresh		Surgery and biotransformation studies		
Human skin cryoconserved		Surgery and freezing		Biotransformation studies

Tbl. 6: Handling scheme and timeline for quality control (viability and integrity/resiliency of reconstructed tissues) in the context of biotransformation experiments with reconstructed tissues and excised human skin.

2.10.1 Histological examination of RHS/RHS

Toluidine blue staining

Tissues fixed in Karnovsky-application solution were shipped at 4°C to the Department of Dermatology, Ludwig-Maximilians University in Munich. Samples embedded in epoxy resin were sliced (1 - 2 µm sections), stained with 1% toluidine/1% pyronine G and subjected to histological evaluation using light microscopy.

H&E (hematoxylin and eosin) staining

Additionally, cryoconserved tissue samples were cut into halves, embedded in tissue freezing medium and frozen at -80° C. Tissue slides (10-20 µm) were subjected to hematoxylin and eosin (H&E) staining for evaluation by fluorescence microscopy.

2.10.2 Interleukin-8 release

As a result of inflammatori stimuli like chemicals, keratinocytes release the intracelluar accumulated chemokine interleukin-8 (IL-8). The release of IL-8 into the receptor medium of untreated and exposed tissues was determined with a commercial sandwich enzmye linked immunosorbent assay technique with the IL-8 DuoSet kit/R&D Systems) following the instructions of the manufacturer.

2.10.3 Lactat dehydrogenase leakage

The release of lactate dehydrogenase (LDH) from the epidermis and dermis into the receptor medium as a marker of cell membrane damage and thus violation of cell integrity was analysed. Its activity can be measured by determination of NADH formation. The receptor medium was collected at the conclusion of the experiments and assayed spectrophotometrically at the Department of Dermatology, Ludwig-Maximilians University in Munich after shipment under refrigeration (4° C) within 48 h.

2.11 Gene expression analysis

Separation of epidermal tissues from the dermis

For the separation of the epidermal tissue from the underlying dermis the reconstructed tissues were washed two times with PBS (without Ca^{2+} and Mg^{+}), placed in 6-well plates and incubated with 1ml thermolysine (1 h at 4° C). Epidermis and dermis were separated carefully with the help of tweezers and transferred to tubes containing NucleoSpin® lysis buffer for tissue disintegration (as described in chapter 2.7.3). After disintegration, the epidermis was immediately usable for RNA isolation, whereas the dermal homogenate was centrifuged (30 sec at 4° C, 15.700 x g) and the supernatant tranferred to tubes. 300 µl RNAse-free water and 1.6 µl Proteinase K were added for protein degradation. After incubation for 10 min at 55° C and centrifugation (30 sec, 4° C, 15.700 x g) the dermal homogenates were used for RNA isolation.

RNA isolation and purification

The total RNA isolation from cultured cells (NHK, HaCaT, NHDF and HepG2 cells as a positive control) and tissues was determined by using the NucleoSpin RNA II Kit in accordance with the RNA isolation protocol of the manufacturer („Total RNA purification from cultured cells and tissue with NucleoSpin® RNA II“).

4 x 10^5 cells were seeded in 6-well plates containing 1 ml growth medium and incubated for 24 h (5 % CO_2, 37° C) before cells were lysed with 350 µl NucleoSpin lysis buffer. Lysed cells and the tissue homogenates were treated with a mixture of β-mercaptoethanol and RA1-buffer (part of the Nucleo Spin® RNA II Kit; contains guanidinthiocyanat for RNAase inactivation). The lysates were applied on top of the Nucleo Spin® Filter and centrifuged for 1 min at 11.0000 x g to remove solid components (e.g. cell or tissue debris). 350 µl ethanol 70 % was added to the homogenized lysate to achieve optimal binding of the RNA to the silica membrane of the Nucleo Spin® RNA II Column. The column loading with the RNA was obtained by centrifugation for 30 s at 11.000 x g. After DNase digestion (incubation with DNase reaction mixture for 15 min at room temperature) and three washings (with RA2- and RA-3 buffer) the purified RNA was eluted with 60 µl RNAse-free water followed by centrifugation (1 min, 11.0000 x g).

RNA quantification and quality control

The concentration of RNA was determined photospectrophotometrically. The samples were diluted and pH adusted with Tris-HCl 10 mM pH 7.5 in a ratio of 1:40 and the absorbance (A) measured at 260 nm using RNAse-free quartz cuvettes. An absorbance of 1 unit at 260 nm corresponds to 40 µg of RNA per ml (A260 = 1 = 40 µg/ml at pH 7.4 - 7.5).

For quality control, absorbance was analysed at 230 and 280 nm since the ratio between the absorbance values at 230, 260 and 280 nm gives an estimate of RNA purity (A230/260: impurities with polysaccharides, A260/280: alcohol and protein impurities). Furthermore, quality and integrity of isolated total RNA was verfied by gel electrophoresis. For this purpose, 3 µl of RNA was mixed with 2 µl loading buffer (1x) and 5 µl DEPC-water and applied to an agarose gel 1 %. Electrophoresis was determined at 100 V for approx. 45 min with the agarose gel placed in electrophoresis chamber filled with TBE buffer 1x. After staining with Gelred (20µl/100ml) for 20 min, the agarose gel was exposed to UV light (312 nm) and photographed (BioDoc Analyzer). Purity of isolated RNA was assumed if only the 18s and 28s-RNA band was visible. In case of remaining DNA a further DNase digestion with DNase I Amplification grade (DNase I Amplification Kit) was required prior to cDNA synthesis.

cDNA synthesis

For rt-PCR quantification of isolated total RNA, transcription of the RNA into cDNA was required. The cDNA was synthesised by using the cDNA synthesis kit (RevertAid First Strand cDNA syntesis kit) following the instructions of the manufacturer. Briefly, DNase free RNA solution was treated with 1 µl random hexamer Primer (0.2 µg/µl), 4 µl reaction buffer 5x, 1 µl RiboLock^{TM} RNase inhibitor (20 u/µl), 2 µl 10 mM dNTP mix, and 1 µl RevertAid M-MuLV reverse transcriptase (200 u/µl) and incubated for 5 min at 25 °C (pre incubation), 1 h at 40°C (cDNA synthesis) and 5 min at 70°C (termination of reaction). The cDNA was diluted with RNAse-free water in a ratio of 1:1.

Primer

The primer used for rt-PCR were acceeded from the NCPI gene data base (http://www.ncbi.nlm.nih.gov/gene) and are presented in table 7. All primer pairs were exon-intron-spanning in order to prevent amplification of DNA fragments. Primer suitability (with HepG2 cells for positive control) and efficiency were tested before usage for quantification of gene expression. Succinat dehydrogenase subunit A (SDHA) was used as house keeping gene.

Gene	GenBank Accession No.	Primer sequences (5´ to 3´)	Product size (bp)	Efficiency
CYP19A1	NM_000103.3 NM_031226.2	f: acttgggctgcagtgcatcgg r: gccggggcctgacagagcttt	112	1.98
HSD17B1	NM_000413.2	f: gcgtggacgtgctggtgtgta r: accaacacgcgtcccgaacc	169	1.99
HSD17B3	NM_000197.1	f: gccatttcctgaacgcaccgg r: tgcgcacacaaacgccttgga	200	1.93
SDHA	NM_004168.2	f: tgggaaccaagagggcatctg r: ccaccactgcatcaaattcatg	86	1.94

Tbl. 7: Real-time RT-PCR primer sequences, and expected product size (bp) for the target and reference genes. f = forward, r = reverse.

Quantitative real-time polymerase chain reaction

The quantitative real time polymerase chain reaction (rt-PCR) can be used for amplification of DNA sequences and quantification of double-stranded DNA (ds-DNA) by measuring fluorescence at 530 nm with the LightCycler®480. The dye SYBR Green (included in Mastermix SYBR Green I Master) binds to the minor groove of ds-DNA and fluoresces at a much higher intensity when bound to ds-DNA when compared with the dye (SYBR Green) in

free solution. The fluorescence released during PCR is directly proportional to the amount of available target DNA and is measured continuously during amplification by the PCR instrument. The Mastermix SYBR Green I Master includes AmpliTaq® Fast DNA Polymerase, a highly purified DNA polymerase for instant hot start, minimizing non-specific product formation and enabling reactions to be set up at room temperature, SYBR® Green I dye, deoxynucleotides (dNTPs) to maintain optimal PCR results and Uracil-DNA Glycosylase (UDG) to reduce carryover contamination, in an optimized buffer.

For rt-PCR, 8 µl of the prepared mastermix (including the specific primers) and 2 µl cDNA or 2 µl DEPC-water (negatic control) were filled into 96-well plates. The FastStart Taq polymerase was activated by heating at 95° C (preincubation) for 5 min. Gene amplification and fluorescence detection was determined over 45 cycles at different temperatures (10 sec at 95°C for denaturation of ds-DNA, 10 sec at 60° C for primer hybridization and 10 sec at 72° C for DNA elongation). Following the rt-PCR a dissociation curve was determined to exclude formation of primer dimers. Thus, the samples were heated again at 95° C and the decrease in fluorescence (due to ds-DNA separation and hence termination of GYBR Green intercalation) was measured. Each PCR-product has its own characteristic mealting peak. For the quantitative analysis the „crossing points“ (cp, point of amplification curve with inital significant increase of fluorescence compared to background fluorescence) were used. The calculated cDNA quantities are reffered to the quantity of the house keeping gene (reference gene).

Gel electrophoresis of PCR products

For additional (quality) control of the results, PCR products were subjected to electrophoresis in a 2 % agarose gel alongside size markers, positive control and the negative controls from the PCR steps.

2.12 Data analysis and statistics

Arithmetric mean (± SEM) are obtained from at least three independent experiments (each run in triplicate): With respect to reconstructed tissues, in total 10 different batches of RHE EpiDerm (PC = 7, testosterone = 4) and 6 batches of RHS EpiDerm-FT (PC = 6, testosterone = 3) and 6 of Phenion FT (PC = 4, testosterone = 3) were analysed. Human skin was from eleven different donors for PC and seven donors for testosterone biotransformation. With respect to monolayer experiments (4 different donors of NHK and NHDF) steroid amounts in medium and lysed cells were summed. PC/testosterone metabolite formation in human skin and the reconstructed tissues was corrected for uptake rates when comparing biotransformation efficiency. In line with the finite dose approach a mass balance (total

PC/testosterone and metabolites recovered from medium, tissue, filter and supernatant) was calculated. Recovery of metabolites was corrected to PC/testosterone by molecular mass. Experiments were regarded valid, if mass balance was 85 - 115 %.

Data were compared by Mann-Whitney (two data pairs) or Kruskal Wallis test combined with Dunn's multiple comparison test (at least 3 data pairs); $p \leq 0.05$ indicates a difference.

3 Results

3 Results

3.1 Development and *in house* validation of HPLC-analysis for testosterone and metabolite quantification with radiodetection

Internal standard corticosterone

For quantitative analysis, an internal standard in a pre-specified quantity is added to each sample to determine the extraction efficiency of each experiment. Furthermore, detection of analysis errors during the measuring process becomes possible. After the extraction, the real amount of the test compound in each sample can be calculated with the means of the recovery rate of the internal standard. Generally, an internal standard should offer similar structure and physicochemical properties such as the substance to be examined to achieve comparable extraction efficiencies. The internal standard should offer similar retention times compared to the evaluated substances without overlapping of the peaks in the chromatogram. The corticosteroid corticosterone (cort.) demonstrates structural similarities to the test compound testosterone and the metabolites. An important prerequisite for the extraction is fulfilled with similar lipophilicity compared to testosterone (tbl. 8). Thus, the suitability of corticosterone as internal standard was tested.

Compound	Structure	Log P	MW
T	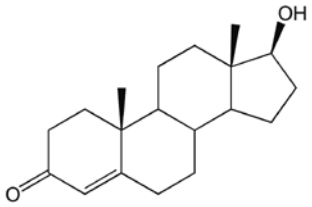	3.334	288.42
DHT	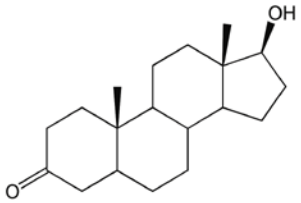	3.553	290.44
4-DIONE	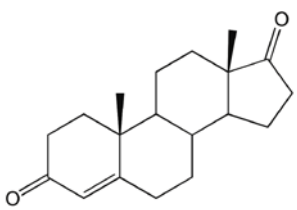	3.007	286.41

Compound	Structure	Log P	MW
AD	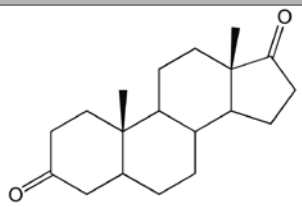	3.151	288.42
ADT	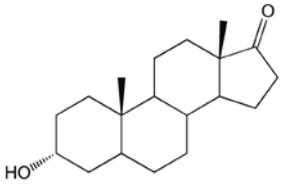	3.553	290.44
HOT	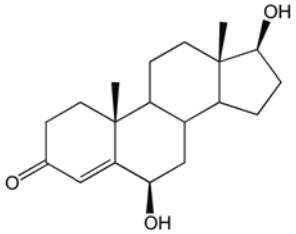	1.793	304.20
E_2	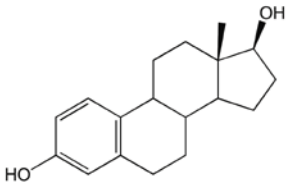	3.784	272.18
E_1	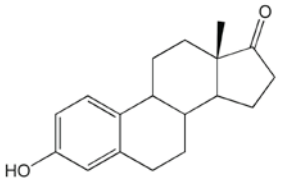	3.130	270.36
Cort. (i.s.)	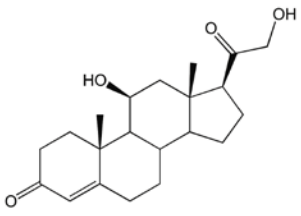	3.409	346.46

Tbl. 8: **Structures, log P and molecular weight of testosterone and potential biotransformation products of excised native.** Structures and calculation of log P by ChemOffice-BioDraw. T = testosterone, DHT = 5α-dihydrotestosterone, 4-DIONE = androstenedione, AD = androstanedione, ADT = androsterone, HOT = 6β-hydroxytestosterone, E_2 = estradiole, E_1 = estron, cort. (i.s.) = corticosterone (internal standard)

Extraction efficiency

The extraction efficiency for testosterone compared to corticosterone was determined by examination of each recovery rate after extraction from test medium containing testosterone and corticosterone in two pre-defined concentration (10^{-6} M, 10^{-5} M). The extraction was tested with chloroforme and ethyl acetate. Extraction with ethyl acetate showed nearly identical extraction behaviour of testosterone and corticosterone (tbl. 9), whereas chloroforme extraction was unequal with high variability.

Solvent	Testosterone % [±SEM]	Corticosterone % [±SEM]
Chloroforme	60.8 ± 15.0 % (10^{-6} M)	65.2 ± 23.0 % (10^{-6} M)
	39.6 ± 8.5 % (10^{-5} M)	47.9 ± 13.3 % (10^{-5} M)
Ethyl acetate	97.3 ± 1.2 % (10^{-6} M)	98.1 ± 1.0 %(10^{-6} M)
	95.7± 3.7 % (10^{-5} M)	95.8 ± 8.1 % (10^{-5} M)

Tbl. 9: Extraction rate (%) of testosterone and the internal standard corticosterone after extraction with chloroforme and ethyl acetate.

Furthermore, almost quantitative extraction of testosterone and corticosterone was achieved with ethyl acetate, whereas recovery rate of both substances was insufficient following chloroforme extraction. Thus, extraction was done with ethyl acetate. Quantification/calculation was performed with corticosterone as internal standard. For each analysis, the extraction efficiency was calculated by setting the determined amount of corticosterone in relation to the amount of internal standard used for the individual sample extraction (0.037 MBq/ml). The actual steroid concentration of T and its metabolites was calculated with the aid of the extraction efficiency.

Method

The sufficient and repeatable separation of testosterone (see fig. 5; tbl. 10), internal standard and the metabolites was achieved with an isocratic method and a mobile phase of acetonitrile/water (60/40 v/v). The run time was 30 min at 25° C and avoiding direct light. The separation was performed with an RP-18 column. The optimal mixture with the scintillation cocktail was obtained with addition of 2 ml of the scintillation cocktail prior to detection in the cell of the radiodetector.

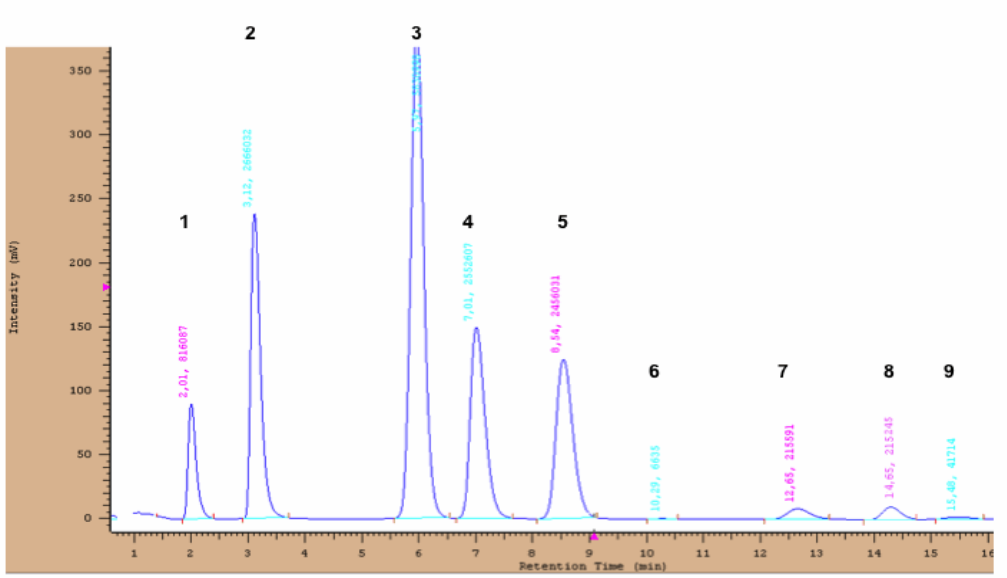

A

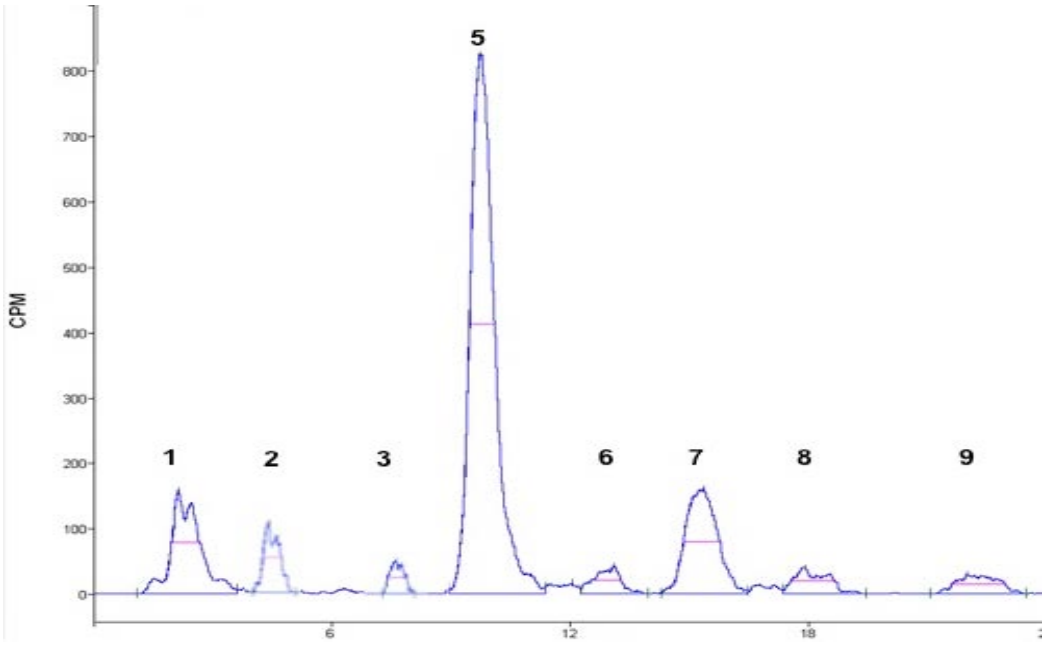

B

Fig. 5: Representative chromatograms of testosterone, internal standard and metabolites obtained after injection of a solution containing non-labelled HOT (1), i.s. cort. (2), E_2 (3), E_1 (4), testosterone (5), 4-DIONE (6), DHT (7), AD (8) and ADT (9) (A; UV-detection for the determination of retention times) and (B) after incubation of biological material with radiodection.

***In house* validation**

Separation

The mean retention times and retention factors for testosterone, its metabolites and cort. were as followed:

Compound	Retention times (t_s), in minutes (min)	Retention factors κ'
T	9.2 ± 0.5	13.3
HOT	2.4 ± 0.2	3.5
E_2	6.7 ± 0.5	9.7
E_1	8.0 ± 0.3	11.6
4-DIONE	11.8 ± 0.4	17.1
DHT	15.1 ± 0.3	21.9
AD	17.4 ± 0.3	25.2
ADT	19.1 ± 0.6	27.6
Cort. (i.s.)	4.4 ± 0.5	6.4
t_m	0.69	-

Tbl. 10: retention times t_s (in minutes) obtained with radiodetection for testosterone, metabolites 6β-hydroxytestosterone (HOT), estradiole (E_2), esterone, (E_1), androstenedione (4-DIONE), dihydrotestosterone (DHT), androstanedione (AD), androsterone (ADT) and internal standard (i.s.) corticosterone. t_m = dead time

The dead time (t_m) was 0.69 min. The retention factor κ' means the relative retention of each peak on the column ($\kappa' = t_s / t_m$). κ' should be > 1.This criterion is fulfilled for all compounds.

Separation factor and Resolution

The separation factors (α) and resolutions (R_S) for the determination of baseline separation were calculated with the following equations:

$\alpha = {}^2t_s / {}^1t_s$

t_s = time it takes for a particular analyte to pass through the system (net retention time)

At α <<1, peaks overlap, with α > 1 the separation is sufficient.

$$Rs = 1.18 \bullet \frac{{}^{2}t_r - {}^{1}t_r}{{}^{2}b_{0.5} + {}^{1}b_{0.5}}$$

R_s = Resolution; t_r = total retention time of a compound; $b_{0.5}$ = half height peak width

The higher the value, the better the different peaks are separated from each other. A baseline separation is given with $R_S \geq 1.5$; with $R_S = 1.5$ the overlap of two peaks is approx. 0.1 %.

The results are summarised in tbl. 11:

Compound	separation factors (α)	Resolutions (R_S)
HOT - t_m	3.5	4.5
HOT - Cort. (i.s.)	1.8	4.4
Cort. (i.s.) - E_2	1.5	2.5
E_2 – E_1	1.2	1.6
E_1 - T	1.2	1.8
T - 4-DIONE	1.3	2.6
4-DIONE - DHT	1.3	4.2
DHT - AD	1.2	4.1
AD - ADT	1.1	5.2

Tbl. 11: Separation factors (α) and resolutions (R_S) for the HPLC-RD analysis for testosterone (T), metabolites 6β-hydroxytestosterone (HOT), estradiole (E_2), androstenedione (4-dione), dihydrotestosterone (DHT), androstanedione (AD), androsterone (ADT) and internal standard corticosterone (cort., i.s.). t_m = dead time

With all $\alpha > 1$ and $R_S >> 1.5$ the separation of each compound from another is sufficient.

Selectivity

Selectivity is the ability of the bioanalytical method to measure unequivocally and to differentiate the analyte(s) from each other and from the matrix in the presence of components which may be expected to be present. Typically, these might include impurities, degradants, matrix components, etc. For the determination of selectify a lack of response in

blank matrices has to be proved. For this purpose, blank matrices (test medium without test compounds and with or without seeded cells, skin homogenates without test compounds, methanol solutions (2.9.1) were analysed. The chromatograms of the blank matrices showed no interfering peaks with testosterone, its metabolites or the internal standard. Thus, selectifity of this method is given.

Linearity

The peak areas of the chromatograms of the calibration points (standard solutions of testosterone and corticosterone) were plotted against their corresponding concentrations and the straight line equation as well as correlation coefficient (R^2) determined by linear regression (fig. 6). Adequate linearity is given with correlation $R^2 > 0.99$ for testosterone and the internal standard cort..

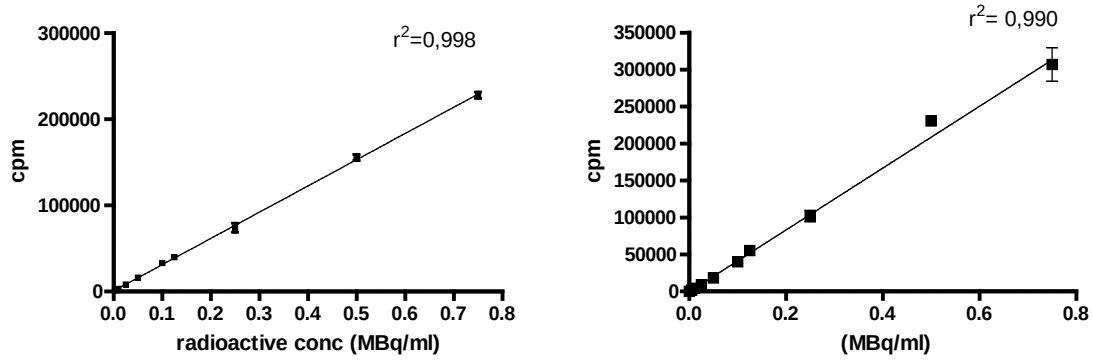

A **B**

Fig. 6: Calibration curves of testosterone (A) and internal standard corticosterone (B) after radiodetection of 9 concentrations (0.005 – 0.75 MBq/ml).

Repeatability

Intra-day and inter-day variability

For the determination of the intra-day variability, the absolute C.V. of the peak areas was calculated. A minimum of three concentrations in the range of expected concentrations is recommended [167]. In table 12 the C.V. of nine concentrations of testosterone and i.s. cort. measured in triplicate at the same day are summarised. Inter-day variability was calculated after measurement of the standard solutions of testosterone and i.s. cort. on three independent days. The results for inter-day variability are summarised in table 12, too.

Conc. (MBq/ml)	C.V. 0.005	0.0075	0.025	0.05	m 0.1	0.125	0.25	0.5	0.75
Intra-day variability									
T	26.8	3.7	10.5	7.8	12.6	4.3	7.0	4.4	5.9
Cort. (i.s.)	6.1	12.0	11.7	11.3	7.9	15.0	12.1	10.0	14.1
Inter-day variability									
T	20.4	2.7	2.2	5.6	5.8	2.4	7.1	2.2	16
Cort. (i.s.)	4.9	10.4	5.8	9.3	6.6	7.1	10.5	14	17.7

Tbl. 12: Variation coefficient (C.V.) of testosterone (T) and internal standard corticosterone (Cort. (i.s.)) for intra-day- and inter-day-variability.

The variability determined at each concentration level should not exceed 15 % of the C.V. except for the lower concentration level, where it should not exceed 20% of the C.V. [167]. Not acceptable variations were observed at concentrations of 0.005 MBq/ml for testosterone and 0.75 MBq/ml for testosterone and corticosterone. With respect to intra-/inter-variability, the method is valid in a concentration range from 0.0075 - 0.5 MBq/ml for T and 0.005 - 0.5 MBq/ml for cort. C.V. was < 15 % within this range. Thus, the method was applicable for this concentration range.

Limit of detection

The limit of detection (LOD) is the lowest concentration of analyte in an sample which can be detected and that the bioanalytical procedure can reliably differentiate from background noise of blank samples (LOD = X_{blank} + 3 • s.d. with X = mean value (blank), s.d. = standard deviation; [168]). The lowest detectable quantity of T and cort. (i.s.) was 0.0025 MBq/ml each.

Limit of quantification (LLOQ and ULOQ)

The lowest limit of quantification (LLOQ) is the lowest amount of a compound in a sample that can be quantitatlvely determined with suitable precision and accuracy and is obtained by the following equation: LLOQ = 3 • LOD. The lowest amount of steroids that can be

quantitatively determined with this method was 0.0075 MBq/ml.
The upper limit of quantification (ULOQ) is the maximum analyte concentration of a sample, that can be quantified with acceptable precision and accuracy. In general the ULOQ is identical with the concentration of the highest calibration standard [169].For testosterone, ULOQ with this method is 0.5 MBq/ml and 0.75 MBq/ml for cort..

3.2 Quality assurance - Recovery from biological materials, mass balance and withhold in pipette

The recovery rates of PC and testosterone after extraction with ethyl acetate from medium and dissrupted tissues compared to results with unextracted standards are summarised in tbl. 13.

Material	PC % [± SEM]	T % [± SEM]
Medium	98.0 ± 4.1	97.3 ± 1.2
Human skin (dissrupted)	80.5 ± 4.5	85.7 ± 2.4
RHE (dissrupted)	87.5 ± 2.5	95.4 ± 1.6
RHS EpiDerm-FT(dissrupted)	83.5[1]	83.7 ± 0.5
Phenion FT(dissrupted)	83.5[1]	96.9 ± 3.2

1 Determination only in duplicate; SEM not calculated

Tbl. 13: Recovery of total prednicarbate (PC) and testosterone (T), respectively, from biological materials after incbuation for 1 h and extraction with ethyl acetate.

For the quantification of the compounds and their metabolites, the results from biotransformation experiments were corrected for the recovery rate. In line with the finite dose approach a mass balance (total PC/testosterone and their metabolites recovered from medium, tissue, filter and supernatant) was calculated, recovery of metabolites was corrected to PC/testosterone by molecular mass. Experiments were regarded valid, if mass balance was 85 – 115 %. With respect to PC, mass balance was 94.7 ± 4.1 %, 93.2 ± 1.8 % for human skin, 93.4 ± 1.7 % for EpiDerm, 95.6 ± 3.1 % for EpiDerm-FT and 97.4 ± 2.3 % for Phenion FT. Regarding testosterone biotransformation studies, mass balance was

98.7 ± 7.2 % for monolayer cultures, 98.4 ± 3.2 % (frozen) - 99.9 ± 7.1 % (fresh) for human skin, 93.9 ± 7.6 % for EpiDerm, 93.9 ± 6.9 % for EpiDerm-FT and 94.4 ± 9.3 % for Phenion FT.

With respect to remain in pipette, 5.1 % of PC and 6.3 % of testosterone, respectively, are withhold in the pipette after application. This amount was substracted from the applied amount for calculation of biotransformation experiments.

3.3 Quality of Reconstructed Human Epidermis and Skin

The quality and resiliency of the reconstructed tissues was determined in order to ensure that tissues were of sufficient quality in accordance with demands of OECD guideline 431 and to ensure that test conditions did not cause relevant damages and thus falsify results of biotransformation experiments.
Constructs from each batch left untreated or treated with solvents and PC or testosterone, respectively, (see tbl. 6, chapter 2.10), were analysed for morphology, IL-8 release and LDH leakage into the receptor medium.

3.3.1 Morphology

Untreated RHE and the RHS EpiDerm-FT and Phenion FT (day 0) were of normal morphology. Multiple layers of viable epithelial cells and intact stratum corneum were present (fig. 7 A - C). Constructs from each batch treated with the solvent ethanol and the test compounds PC or testosterone for 24 h were of normal morphology, too (fig. 7 E – G, I - K). No damages due to stress or induced by the test compounds / ethanol were visible. Thus tissues were of sufficient quality with respect to morphology in accordance with OECD 431 and were used in the experiments.
In contrast, AST2000 constructs from several batches showed indentations and pronounced shrinkage. The epidermis was detached from the dermis and fibroblasts were non-homogeneously distributed within the dermal equivalent (fig. 7 D, H). Several batches consisted of 1 - 2 epidermal cell layers only.
Hence, AST2000 failed to meet the requirements of OECD TG 431 (e.g. multiple layers of viable epithelial cells) for *in vitro* reconstructed human skin.

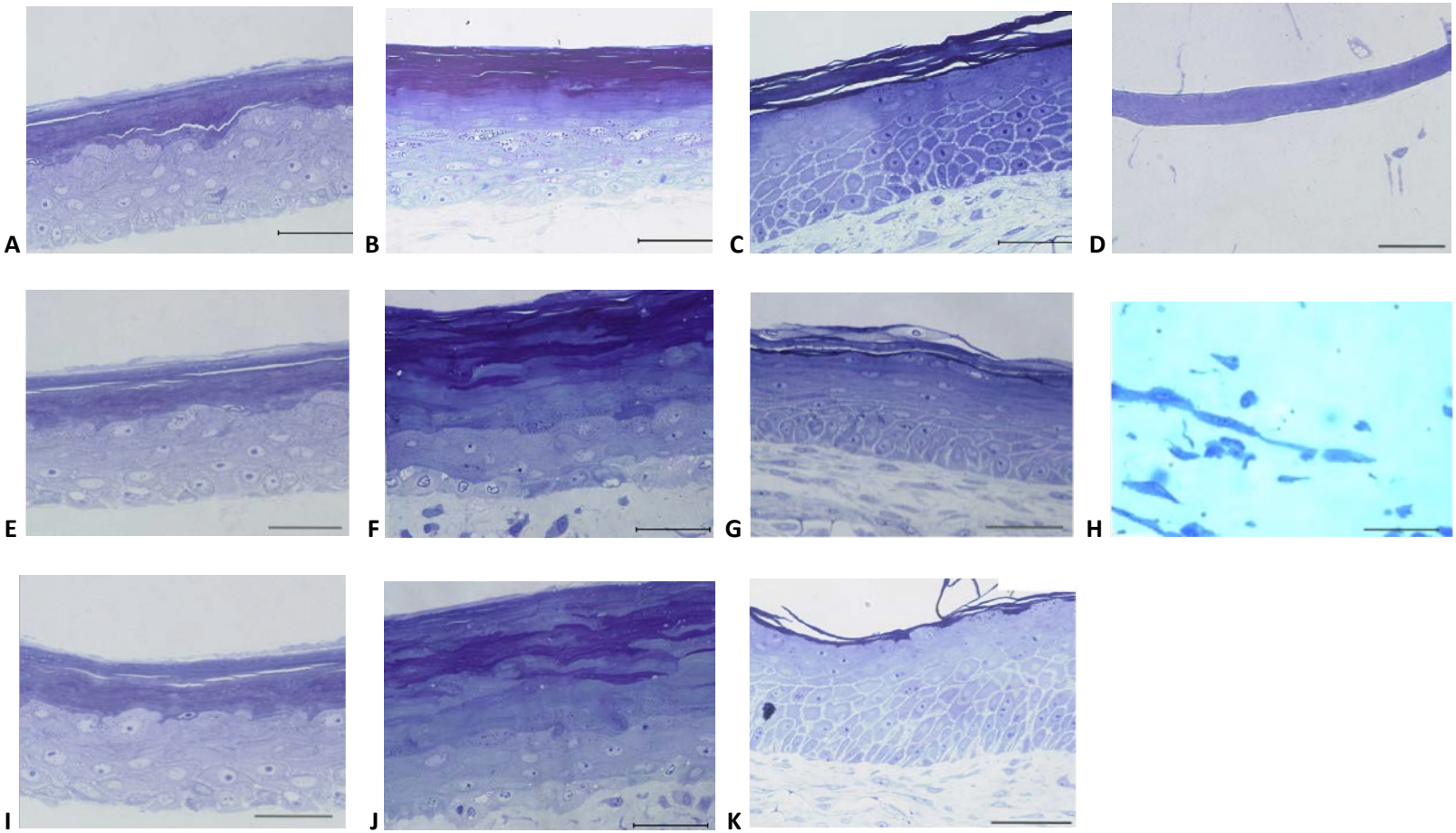

Fig. 7: Morphology of reconstructed tissues after overnight delivery/equilibration (day 0) and after exposure to test compounds prednicarbate (PC) and testosterone (T) for 24 h (day 1). Histological sections (1 - 2 µm) of untreated EpiDerm (A), EpiDerm-FT (B), Phenion FT (C) and AST2000 (D), treated RHE EpiDerm ((E) with PC and (I) with T), treated RHS Epderm-FT ((F) with PC and (J) with T), Phenion FT ((G) after exposure to PC and (K) to T) and AST2000 ((H) after PC exposure) stained with toluidine/pyronine were subjected to microscopy. Representative morphology of at least three different batches is depicted (Scale bar = 50 µm; magnification: 40x).

3.3.2 IL-8 release and LDH leakage

With respsect to RHE and RHS EpiDerm-FT and Phenion FT, after delivery (day 0) and the next day (day 1) as well as following exposure to the test compounds PC or testosterone and solvent ethanol for 24 h there was only minor IL-8 and LDH release. Exposure to ethanol (except for EpiDerm-FT) and PC for 24 h enhanced IL-8 release or LDH leakage less than twofold over baseline. Except for EpiDerm exposed to testosterone for 24 h, IL-8 release and LDH-leakage of the treated tissues exceeded the levels of untreated tissues (day 1) less than twofold (fig. 8), too. These results indicate a sufficient integrity and resiliency of the reconstructed tissues under the applied test conditions.

Contrary, major IL-8 release after delivery of AST2000 (day 0; fig. 8 D) was detected. IL-8 release had declined at day 1. This appears to be linked to the stress induced by shipment. Yet there was also a pronounced induction of IL-8 release and LDH leakage when exposed to ethanol and to the test agent testosterone. The poor resiliency is well in line with poor epidermis formation and keratinocyte differentiation.

Since AST2000 failed to meet the requirements of OECD TG 431 [170] for *in vitro* reconstructed human skin and due to the lack of tolerance to the test agents and their solvents, AST2000 was excluded from the biotransformation studies.

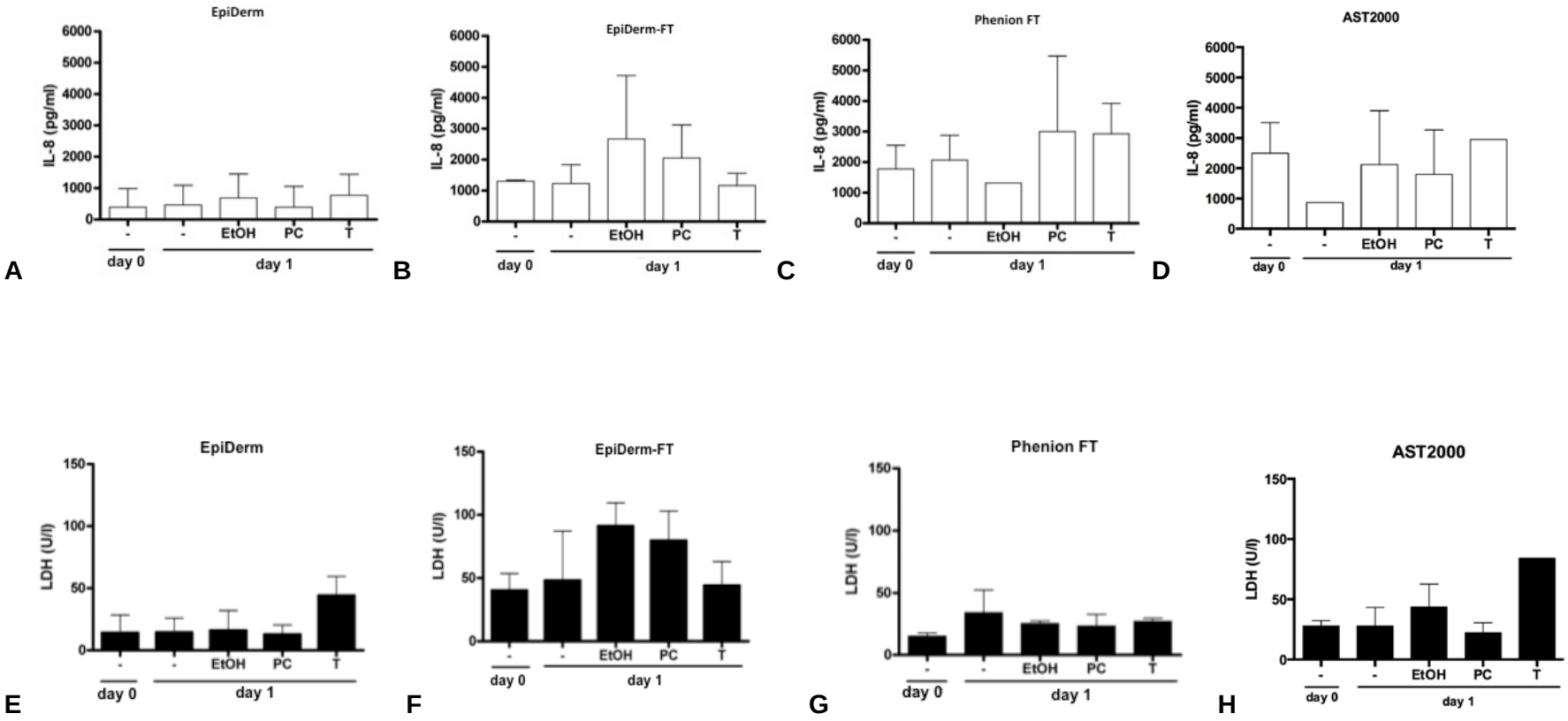

Fig. 8: IL-8 release (pg/ml) and LDH leakage (presented at U/l at 37°C) of native EpiDerm, EpiDerm-FT, Phenion FT and AST2000 after overnight equilibration (day 0) and storage for 24 h (day 1) without (-) and following exposure to solvent ethanol (EtOH; 10 µl/cm^2) and the test compounds prednicarbate (PC; 25 µg/cm^2 in ethanol/PBS) or testosterone (T; 13.7 ng/cm^2 in ethanol) for 24 h (n ≥ 3; mean ± SEM).

3.4 Biotransformation of prednicarbate

3.4.1 Dermal cells

Aiming for a full comparison of cutaneous PC esteratic cleavage the knowledge of PC biotransformation by dermal cells [95] had to completed, the focus being on HaCaT cell line because of the elimination of donor-related variability.

PC biotransformation in NHK and NHDF monolayer cultures is well in accordance with the previous data [95]: In NHK, already within 9 h about 50 % of native PC was transformed to P17EC and to a lesser extent to P21EC and PD (fig. 9 A). The final metabolite PD was first detected after 3 h and after 24 h 50 % of native PC was transformed to this metabolite. PD formation by HaCaT cells was even faster: Already after 9 h the final metabolite achieved 50 % (fig. 9 B). Yet, data variability of HaCaT (CV: 0.069 - 1.1195) compared to the results of NHK (CV: 0.012 - 0.53) was high. Once more only minor PC cleavage was seen in NHDF (fig. 9 C). After 9 h exposure to PC, just 30 % of PC were metabolised with the monoester P17EC being main metabolite (20 % of native PC) followed by low quantities of the final metabolite PD (10 % of native PC). The monoester P21EC was only detected in traces.

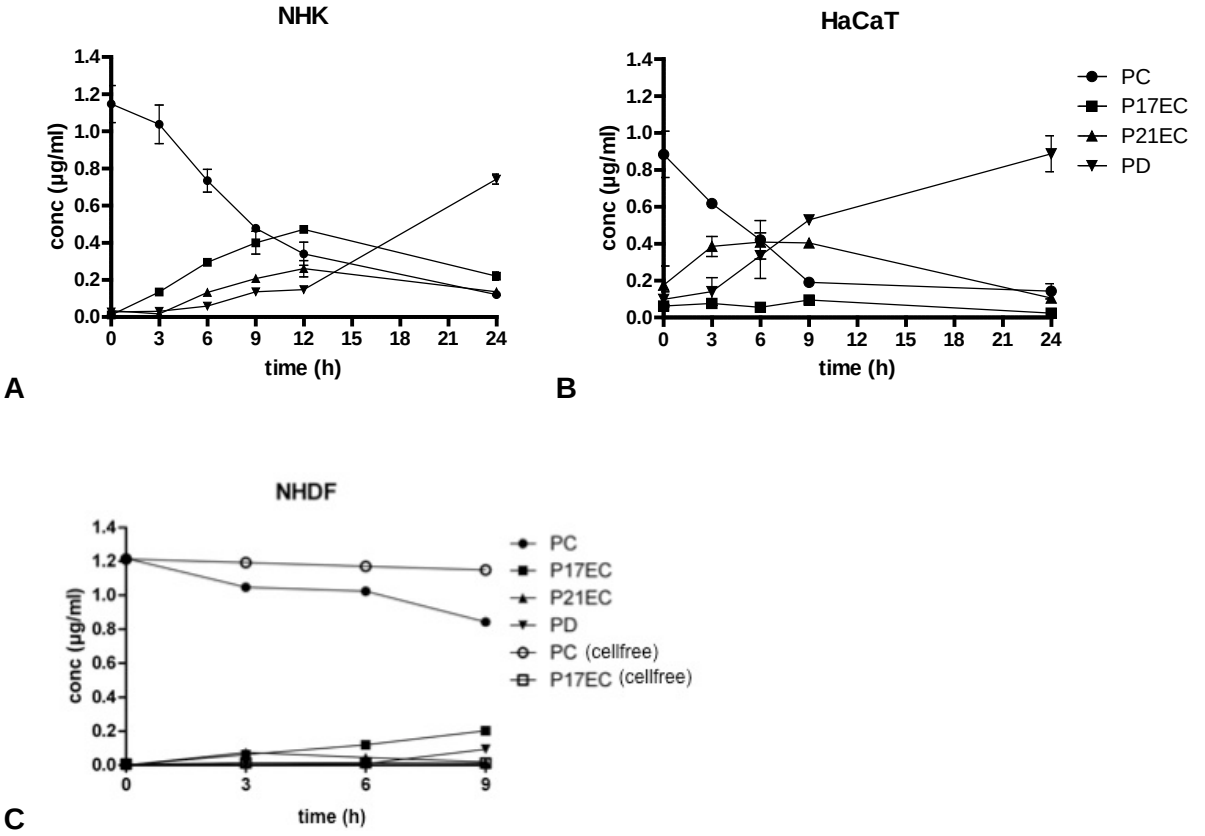

Fig. 9: Biotransformation of PC ($2.5 \cdot 10^{-6}$ M) in normal human keratinocytes (A - NHK, passage 2-3), HaCaT (B, passage 61-65) and normal human dermal fibroblasts (C - NHDF, passage 2-4); mean ± SEM (n= 3).

3.4.2 Native human skin

Before entering into biotransformation experiments for the comparison of PC biotransformation in human skin and the reconstructed tissues, the impact of skin handling and especially the experimental setup was analysed by comparing the standard approach for penetration studies (Franz diffusion cell technique) and the usage of membrane culture inserts representing the standard approach for cultivation of reconstructed tissues (chapter 3.4.2.1). With the well-tolerated approach all further experiments and especially the comparison of biotransformation in human skin and the reconstructed tissues EpiDerm, EpiDerm-FT and Phenion FT were performed (chapter 3.4.2.2, 3.4.4, 3.4.5; 3.5.2, 3.5.4). In addition, influences of skin cryoconservation were analysed by comparing PC biotransformation in human skin from the same donor (in total three different donors) immedietaly after surgery and after cryoconservation for at least 3 months (chapter 3.4.4). To determine whether esteratic activity depends on sex, PC biotransformation in skin from female and male donors was analysed (chapter 3.4.5). Moreover, skin homogenates were treated with enzyme inhibitors for the specification of PC transforming enzymes (chapter 3.4.6).

3.4.2.1 Experimental setup selection: Membrane insert approach vs. Franz cell technique

Franz diffusion cell technique

As the focus is on biotransformation, a well-tolerated exposure is necessary to preserve the viability and integrity of the tissues. For this purpose the influence of the mode of skin mounting on enzyme activity was studied. The extent of PC biotransformation after exposure for 6 h in human skin mounted in Franz diffusion cells was compared to biotransformation of human skin placed in tissue culture inserts. As formulation-related uptake rate was of no interest, a finite-dose approach [35] was choosen which is closer to the clinical situation. After exposure of human skin mounted in Franz diffusion cells (10 $\mu l/cm^2$ of 0.25 % PC), approx. 57 % of the dose were taken up and recovered from tissue (penetrated drug) and medium (permeated drug), respectively (fig. 10). Nearly 40 % of administered PC remained on the skin surface. Native PC was predominantly found within the tissue (42.7 %) and 14.7 % permeated into the medium. Just 6.7 % PC transformation is recognisable with Franz cell technique with P17EC being clearly dominating metabolite (fig. 10 A). P21EC and PD were only detected in traces and only in the tissue.

Membrane insert approach

With resepect to human skin placed in tissue culture inserts for 6 h approx. 54 % of the dose were taken up and recovered from tissue (penetrated drug) and medium (permeated drug), respectively. Thus, penentration and permeation is comparable as seen for human skin mounted in Franz diffusion cells (fig. 10 B). In contrast to 6.7 % PC biotransformation with Franz cell technique, 34.3 % biotransformation was seen following drug exposure in membrane inserts for 6 h (fig. 10 A). Native PC was found in rather high amount within the tissue (41.7 %) as was the first biotransformation product P17EC (12.8 %). 12.1 % of total glucocorticoid permeated into medium, PC being the dominating agent (tbl. 14). PC exceeding the less lipophilic metabolites within the skin is in accordance with previous data when applying PC cream and ointments to human skin and RHE [65, 81, 171]. Moreover, also betamethasone 17-valerate amounts surmount betamethasone amounts in human skin because of a lipophilicity-related distribution [51].

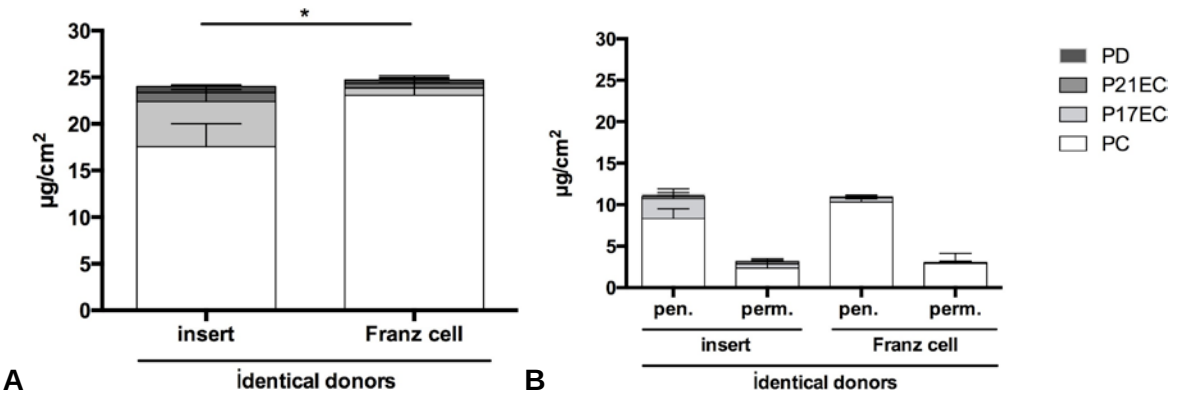

Fig. 10: Comparison of PC biotransformation in cryoconserved human skin from two donors in parallel using the membrane insert approach versus *Franz cell* technique. Tissues were exposed to PC 25 µg/cm² (10 µl/cm²). Data present native PC and metabolites after incubation for 6 h (A) and separated (B) for penetration (tissue) and permeation (medium); * p ≤ 0.05

The biotransformation of human skin ex vivo placed in tissue culture inserts exceeded PC formation using Franz diffusion cells approx. 5fold (fig. 10). This is explainable by the anticipated higher stress level in human skin fixed in Franz cell resulting in a lower enzymatic activity. Thus PC biotransformation is clearly influenced by the experimental setup. In consequence, insert technique (membrane insert approach) was choosen for the comparison of PC and also testosterone biotransformation in human skin compared to reconstructed tissues for all the following experiments.

3.4.2.2 Prednicarbate biotransformation in human skin

Using the improved protocol (membrane insert approach), PC biotransformation in skin of eleven donors in total (fig. 11) was investigated. After exposure of human skin placed in tissue culture inserts for 24 h, 74.5 % of the applied PC dose was taken up and recovered from tissue (penetrated drug) and medium (permeated drug), respectively (fig. 11; 24 h). Nearly 26 % of applied PC remained on the tissue surface; unspecific hydrolytic esterase activity on the skin surface and in the intercellular spaces of the stratum corneum [172] and limited PC stability in aqueous medium after 24 h [65] explain the detection of decomposition products in PBS wash of skin (16% of non-absorbed PC). After 24 h exposure PC and metabolite amounts within the skin (49.6 % of total glucocorticoid) exceeded the permeated amounts recovered from medium (24.8 %).

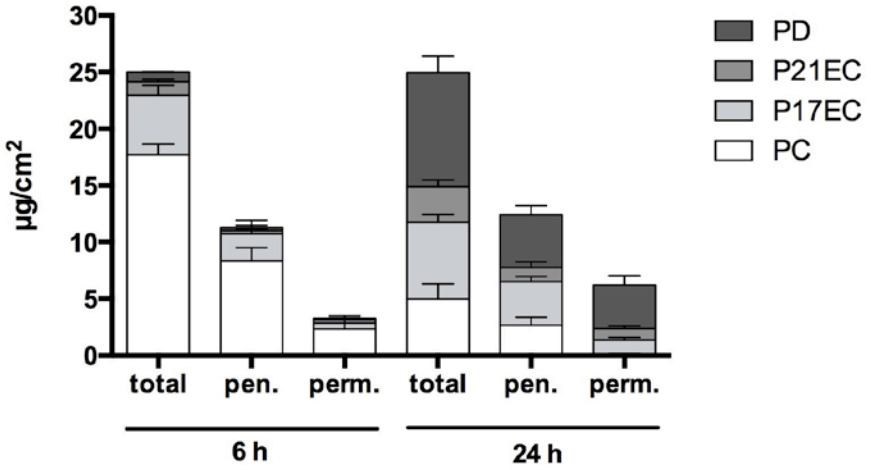

Fig. 11: Biotransformation of prednicarbate (dose: 25 µg/cm², 10 µl/cm²) in freshly excised human skin of 11 female donors (n ≥ 3) after incubation for 6 h and 24 h. Data present total native prednicarbate and metabolite amounts (mean ± SEM, n ≥ 3; total = amounts within PBS wash, tissue, receptor medium and filter) as well as amounts within the tissue (penetration) and the receptor medium (permeation).

Yet, following a 24 h exposure 84 % of absorbed PC is transformed to its metabolites. With focus on tissue, PD and P17EC amounts clearly exceeded P21EC formation (tbl. 14). In medium, main metabolite was PD, too. In total, nearly 44 % of absorbed PC was transformed to PD and approx. 28 % to P17EC after 24 h. Formation to monoester P21EC was just approx. 12 %.

6 h vs. 24 h exposure

Comparing the different exposure times amounts of absorbed glucocorticoid after 24 h exceeded absorption rate after 6 h by approx. 20.5 % (tbl. 14). PC and metabolite amounts

within the skin (49.6 %) exceeded the permeated amounts recovered from medium (24.8 %) as seen after exposure for 6 h (41.7 % penetration, 12.0 % permeation; fig. 11; 6 h). The 4-fold exposure time offers a 2.5 fold increase in biotransformation of absorped PC. After 24 h P17EC formation was twice as high as compared to 6 h exposure and the main metabolite was PD (44 %), whereas formation to other metabolites P21EC and PD was negligible after 6 h (together < 5 %).

Rank-Order			
Matrix	**Absorption** mean ± SEM	**Tissue**	**Medium**
Human Skin (6 h)	54.1 ± 1.3 %	PC>>P17EC>>P21EC~PD	PC>>P17EC>P21EC>PD
Human Skin (24 h)	74.5 ± 3.5 %	PD>P17EC>>PC>P21EC	PD>>P17EC~P21EC>>PC

Tbl. 14: Prednicarbate absorption (% of dose) and rank-order of prednicarbate and metabolites after exposure to human skin for 6 h and for 24 h, respectively.

3.4.3 Reconstructed Human Epidermis and Skin

Reconstructed Human Epidermis (RHE)

Next, PC absorption and biotransformation in comparison to human skin was studied in differentiating keratinocytes forming the RHE EpiDerm when exposed for 6 h (fig. 12) and 24 h (fig. 13), respectively.

6 h exposure

Already after 6 h PC absorption was 71.2 % and most of the drug and its metabolites were recovered from medium (65 % permeation; fig. 12) and thus exceeding absorption and especially permeation of human skin (approx. 54 % absorption, 12 % permeation after 6 h). Almost 96 % of absorbed PC was metabolised by RHE with PD being main metabolite (45.9 % of absorbed PC) and 50.4 % formation of the monosters P17EC (22.9 %) and P21EC (27.5 %). P17EC was found mainly within the tissue whereas P21EC permeated almost completely into the medium. In conclusion, the extent of biotransformation in the RHE

EpiDerm after 6 h exceeded biotransformation in human skin by far and is even more comparable to results obtained with human skin following the 4-fold exposure time (24 h; fig. 11).

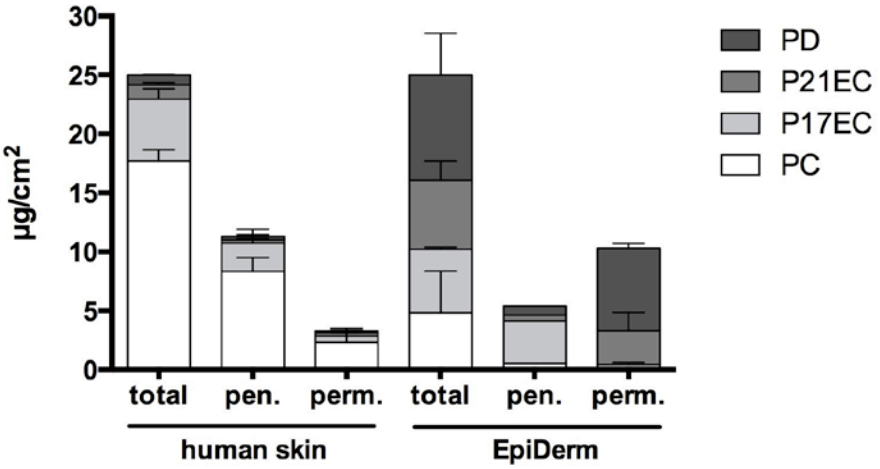

Fig. 12: Biotransformation of prednicarbate (mean ± SEM) using membrane inserts approach in human skin (5 donors) and reconstructed human epidermis EpiDerm (3 batches) exposed to PC 25 µg/cm² for 6 h. Data present total native PC and metabolite amounts (total) as well as amounts within the tissue (penetration) and the receptor medium (permeation).

24 h exposure

The absorption rate after 24 h exposure by RHE was 94 % (fig. 13; tbl. 15) with approx. 90 % permeation. Almost complete PC biotransformation (98 %) in RHE with PD being the clearly dominating glucocorticoid (> 86 % of absorped PC) after exposure for 24 h is close to esteratic cleavage in non-differentiated keratinocytes (fig. 9 A). Because of the still incomplete stratum corneum formation by RHE a significant difference to human skin ex vivo ($p \leq 0.05$ – except for native PC and P21EC in medium; fig. 13) is – at least in part – due to enhanced uptake seen on a regular base with compounds widely varying in molecular weight and lipophilicity [35].

Reconstructed Human Skin

As seen with RHE, PC absorption by RHS EpiDerm-FT and human skin differs significantly (EpiDerm-FT 94 %, human skin 74.5 %; fig. 13, tbl. 15). The absorption by the RHS Phenion FT (90 %) exceeded human skin, too, but with no statistical significance. Metabolites were recovered in higher amounts from medium as compared to human skin ($p \leq 0.05$) when exposing the RHS EpiDerm-FT for 24 h. In total, nearly 95 % of applied glucocorticoid permeated into medium with EpiDerm-FT whereas Phenion FT appears to retain higher glucocorticoid amounts within the tissue (19 % of the dose). This is in line with a higher total

epidermal thickness and cell density of Phenion FT building a reservoir. The same effects were seen after exposure to testosterone (chapter 3.5.3).

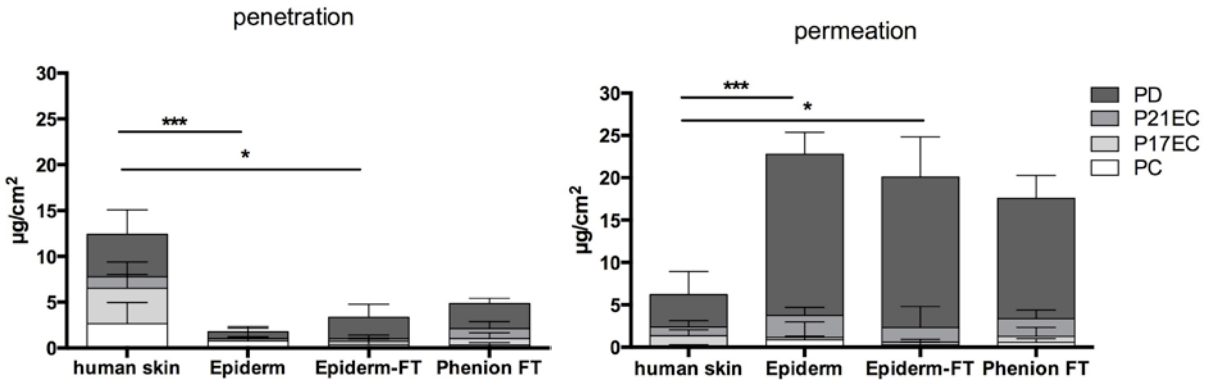

Fig. 13: Biotransformation of prednicarbate (mean ± SEM, separated in tissue (penetration) and medium (permeation)) in directly excised or cryconserved human skin (11 donors; ≤ 3 months) using the membrane inserts approach and reconstructed tissues (at least 3 batches per construct type) exposed to PC 25 µg/cm^2 for 24 h; * p ≤ 0.05 compared to human skin

97.3 % of absorbed PC was transformed to its metabolites in the RHS EpiDerm-FT. The main metabolite after 24 h exposure was PD (> 80% of the applied dose). Amounts of monoesters were low in medium (8.1 % - 11.2 %) and tissue (1.7 % - 5.2 %) of the RHS. With Phenion FT, 95.9 % of absorbed PC was transformed and once more PD was the dominating glucocorticoid (70.3 %; fig. 13). Formation to the monoesters P17EC (6.3 %) and P21EC (14.1 %) was low, too. With respect to biotransformation, no significant differences were seen comparing metabolite formation by the RHS EpiDerm-FT and Phenion FT. Compared to human skin, formation to each metabolite in EpiDerm-FT was significantly increased ($p \leq 0.05$), whereas no significance in biotransformation was observed with Phenion FT. Thus, not only penetration but most interestingly biotransformation in Phenion FT corresponds most closely with human skin.

Rank-Order			
Matrix **24 h**	**Absorption** mean ± SEM	**Tissue**	**Medium**
NHK	-	-	PD>>P17EC>P21EC ~PC
NHDF	-	-	PC>>P17EC>>PD>>P21EC
Human Skin	74.5 ± 0.8 %	PD>P17EC>>PC>P21EC	PD>>P17EC ~ P21EC>>PC
EpiDerm	94.2 ± 0.7 %	PC ~ PD>P17EC>>P21EC	PD>>P17EC>P21EC ~ PC
EpiDerm-FT	93.6 ± 1.8 %	PD>>PC~P17EC>P21EC	PD>>P17EC>P21EC ~ PC
Phenion FT	89.7 ± 1.3 %	PD>>P21EC>PC ~ P17EC	PD>>P21EC>PC>P17EC

Tbl. 15: Prednicarbate absorption (% of applied dose) and rank-order of prednicarbate and metabolites after exposure to human skin (11 donors) and RHE EpiDerm as well as RHS EpiDermFT and Phenion FT (at least 3 batches) for 24 h.

Taken together, the reconstructed tissues are more permeable than native human skin, especially the RHE EpiDerm and the corresponding RHS EpiDerm-FT. PC and metabolites were withhold to a higher extent in the RHS Phenion FT tissues compared to EpiDerm-FT. Thus, Phenion FT mimicks human skin with respect to absorption and especially permeation behaviour to a greater extent than EpiDerm-FT. PC esteratic cleavage predominantly occurs in keratinocytes since biotransformation in NHK/HaCaT exceeded NHDF esteratic activity by far. Furthermore, biotransformation capacity of RHE was slightly less pronounced compared to full thickness reconstructed human skin.

After 24 h exposure, in all tested matrices PD was the dominating metabolite. PD formation reflecting complete PC cleavage and hence the biotransformation by esterases ranked as: RHS ~ RHE > human skin ex vivo. Differences in biotransformation by human skin and the constructs, however, may be masked by differences in drug uptake since absorption of RHE/RHS exceeded penetration and permeation of human skin for at least 14 %.

3.4.4 Influences of cryoconservation on cutaneous biotransformation

For the determination of influcences on esteratic activity due to cryocernservation, human skin from the same donors (in total 3 different female donors) was exposed to PC immediately after surgery (fresh skin) and after cryoconservation for not more than three months. Experiments were performed under equal conditions. Noteworthy, the profile and quantity of native PC and its metabolites (total PC) were almost identical in freshly excised and cryoconserved human skin (24 h exposure; fig. 14). Minor and negligible differences exist just between the proportion of PC penetration and permeation with slightly higher permeation of cryoconserved skin. Since there were no differences between fresh and cryoconserved skin with regard to quantity and profile of PC biotransformation, comparison of human skin and reconstructed tissues was done under consideration of results obtained with fresh and cryoconserved skin (see fig. 13).

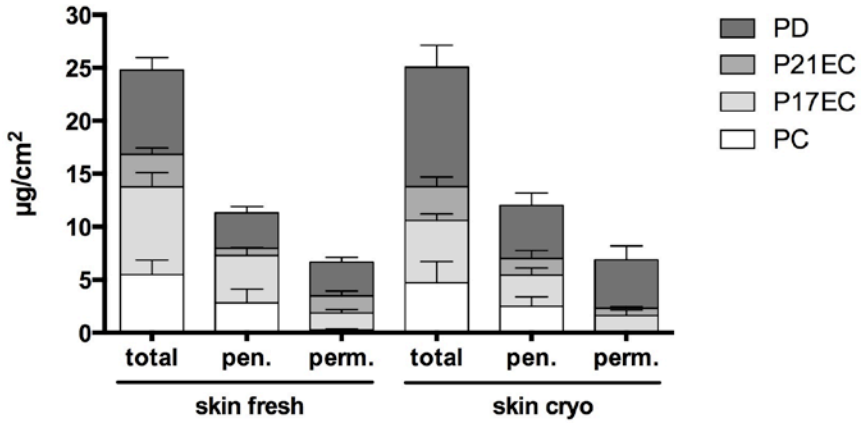

Fig. 14: Prednicarbate biotransformation - effect of storage conditions. Comparison of PC biotransformation in directly excised (skin fresh) and cryoconserved female human skin (2 - 3 months; skin cryo) from the same donor after incubation (in triplicate) in membrane inserts for 24 h. Tissues were exposed to PC 25 µg/cm^2 (10 µl/cm^2). Data present native PC and metabolite amounts (total) and within tissue (penetration) and medium (permeation); mean ± SEM

3.4.5 Determination of sex-specific differences in PC biotransformation

There are well known sex-specific differences in human skin propterties and enzyme expression/activity of steroid transforming enzymes like 17β-HSD [118] in human skin. Thus, the biotransformation by esterases in skin from female donors (n = 8 donors) was compared to male donor tissues (n = 3 donors) in order to determine if this holds true for esterases, too. After 24 h exposure to PC (25 µg/cm^2, 10 µl/cm^2) no differences in PC uptake and biotransformation were observed (fig. 15). The metabolite profile (rank order and amounts)

was very similiar in tissues from both genders with PD being main metabolite (59 % of aborbed PC with female skin/64 % with male skin). Thus, contrary to other steroid transforming enzymes the esterase activity is not depending on sex.

Fig. 15: Prednicarbate biotransformation - evaluation of sex-specific differences. Comparison of PC biotransformation in freshly excised and cryoconserved human skin from female and male donors after incubation (in triplicate) in membrane inserts for 24 h. Tissues were exposed to PC (25 µg/cm^2). Data present native PC and metabolite amounts in PBS wash solution, tissue and medium (n = 8 donors for female skin and n = 3 donors for male skin); mean ± SEM

3.4.6 Esterase inhibition

The choice of feasible inhibitors was based on the structural conditions of PC that are of relevance for metabolism. PC (fig. 3) contains two carboxylic acid groups cleaved by hydrolases. According to the classification of the NC-IUBMB, the family of carboxylic ester hydrolases (EC3.1.1) comprises enzymes probably contributing to PC hydrolysis (carboxylesterases, acetylesterases, acetylcholinesterases and arylesterases). For esterase inhibition experiments, the unspecific serinesterase inhibitor phenylmethanesulfonyl fluoride (PMSF) and two specific carboxylesterase inhibitors (phosphate-based Bis(4-nitro phenyl) phosphate (BNPP) and the phosphate-free inhibitor Benzil), were used. Furthermore, the (acetyl)cholinesterase inhibitor eserin (E) and the specific arylesterase N-ethylmaleimide (NEMI) were tested to proof wether PC is transformed by further esterases with carboxylase activity, too. Skin homogenates (chapter 2.7.3) were exposed to 0.25 % PC alone or in the presence of one of the inidivual inhibitors for 6 h. When incubating skin homogenates with PC 0.25 % alone, 55.8 % ± 6.0 % are transformed to the metabolites P17EC, P21EC and PD (fig. 16 A) with 11.5 % formation to the final metabolite PD (fig. 16 B). As might be expected, no decline in total PC biotransformation was observed in presence of the cholinesterase inhibitor eserin although biotransformation to PD was slightly decreased (fig. 16 B). The arylesterase inhibitor NEMI attained no decline of PC biotransformation certifying that arylesterases are not involved in PC biotransformation. The extent of esterase inhibition varied amongst the other inhibitors. The unspecific serinesterase inhibitor PMSF as single

agent reduces the biotransformation significantly and most effectively (fig. 16 A, 16 B). In presence of PMSF (10^{-3} M), PC biotransformation receded by 28.2 % to 27.6 ± 4.8 % and formation to PD by 10.2 % (remaining PD formation = 1.3 ± 0.3 %; fig. 16 B). The specific carboxylesterase inhibitor BNPP reduces PC biotransformation by 27.1 % (to 28.7 ± 8.9 %) and PD formation by 9.1 % (to 1.5 ± 1.1 %; fig. 16 B), whereas the further carboxylesterase inhibitor Benzil (10^{-7} M) attained no decline in PC biotransformation.

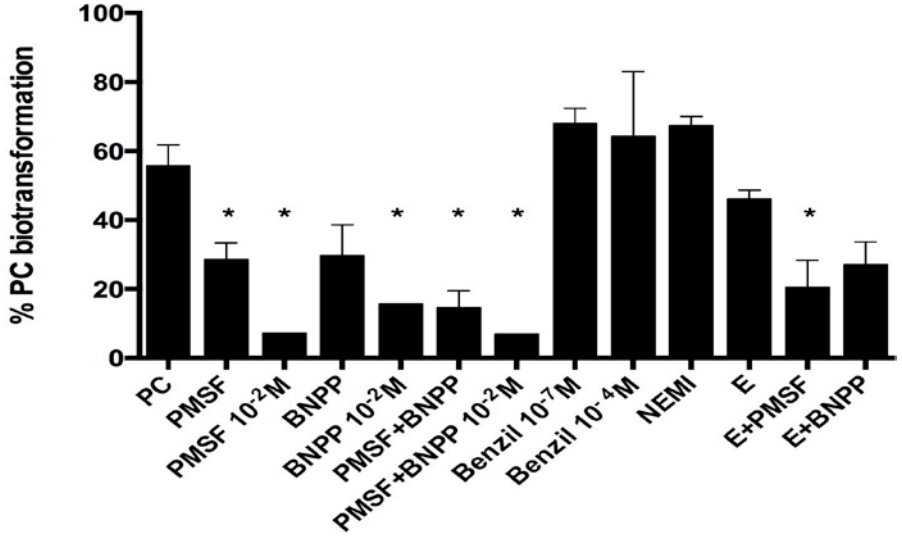

A

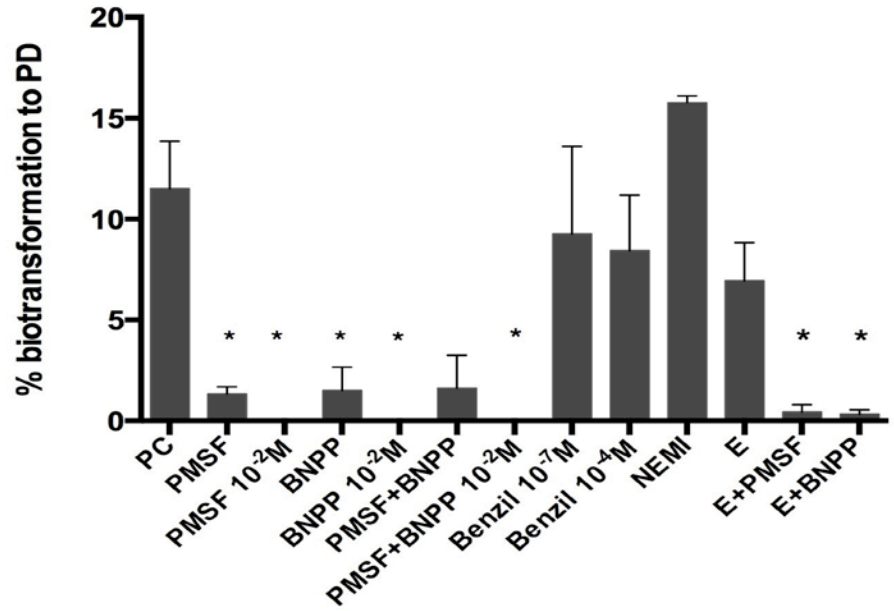

B

Fig.16: Total PC biotransformation (A) and PD formation (B) in % after exposure (6 h) of skin homogenates to prednicarbate (PC; 0.25 %) alone or together with the esterase inhibitors phenylmethanesulfonyl fluoride (PMSF), Bis(4-nitro phenyl) phosphate (BNPP), Benzil, N-ethylmaleimide (NEMI) or the acetylcholine esterase inhibitor eserin (E) alone or in combination (PMSF+BNPP and E+PMSF/E+BNPP). Skin was from 4 female donors, n = 8 individual experiments; mean ± SEM; * p ≤ 0.05 compared to PC exposure without inhibitors.

With combination of PMSF + BNPP as well as with elevated concentrations of PMSF (10^{-2} M) and BNPP (10^{-2} M) alone or in combination (PSMF + BNPP) their inhibition capacity could be increased (fig. 16). With combination of PMSF and BNPP (both 10^{-2} M) total PC biotransformation (fig. 16 A) was reduced to 5 % and PD formation completely eleminated (fig. 16 B). Again no inhibition was achieved with increased concentration of Benzil (10^{-4} M). Thus, Benzil was excluded from further experiments.

With decreased incubation time of 3 h, in presence of the inhibitor BNPP (10^{-3} M) the rate of total PC hydrolysis was diminished as described for 6 h incubation (fig. 17 A) but formation to PD (fig. 17 B) was completely eleminated. When reducing PC concentration (0.125 %) 88.4% were metabolised with 9.2 ± 0.1 % formation to PD (fig. 17 B). PMSF alone (10^{-3} M) reduced biotransformation of PC (0.125 %) by 65.8 % and BNPP alone (10^{-3} M) by 58.1 %. In presence of PMSF + BNPP (both 10^{-3} M) inhibition was again most effectively with only 3.3 ± 0.2 % total PC biotransformation and complete elemination of PD formation (fig. 17 B).

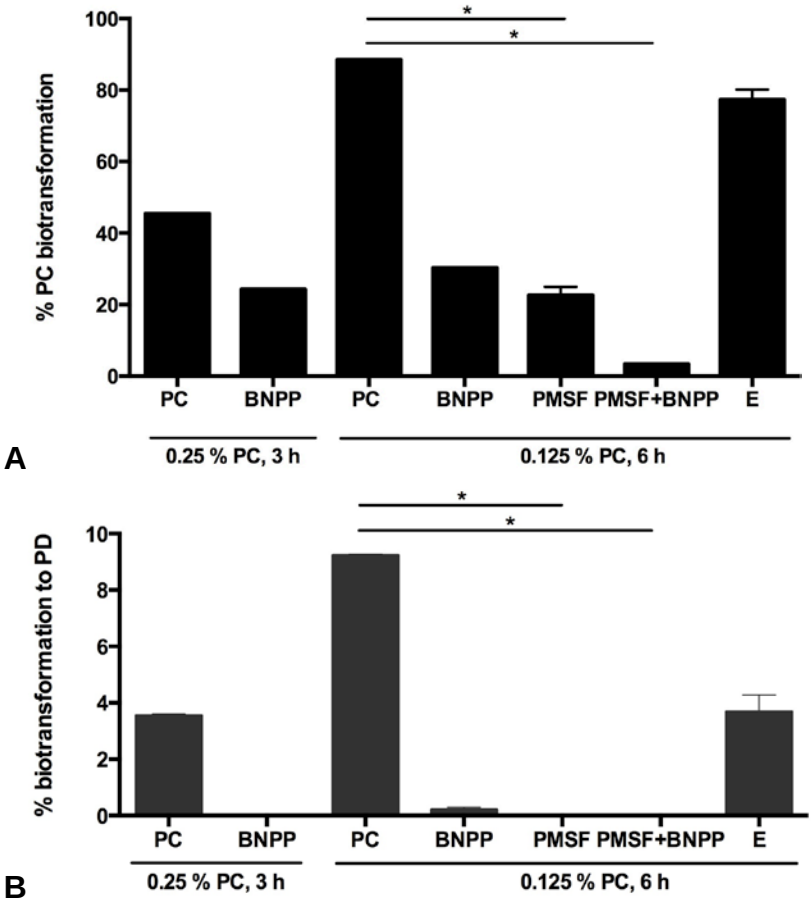

Fig.17: Total PC biotransformation (A) and formation to PD (B) in % after exposure of skin homogenates to prednicarbate (PC; 0.25 % for 3 h and 0.125 % for 6 h, respectively) alone or together with the esterase inhibitors phenylmethanesulfonyl fluoride (PMSF), Bis(4-nitro phenyl) phosphate (BNPP), Benzil, N-ethylmaleimide (NEMI) or the acetylcholine esterase inhibitor eserin (E) alone or in combination (PMSF + BNPP and E + PMSF / E + BNPP). Skin was from 3 female donors, n = 3 individual experiments; mean ± SEM;* p ≤ 0.05 compared to PC exposure without inhibitors.

These results demonstrate that both non specific (serin) esterases and especially carboxylesterases are the dominating enzymes involved in PC biotransformation.

3.5 Biotransformation of testosterone

Next, testosterone was choosen as test compound because of its most complex biotransformation involving several enzymes (fig. 4), the relevance in toxicological testing (OECD suggested reference compound for lipophilic agents) and the transdermal use in hormone replacement therapy. Because of well-known differences in phase I enzyme activity of dermal cells [95, 116], testosterone biotransformation in NHK and NHDF were studied, too. As described for PC, influence of skin cryoconservation on testosterone biotransformation in human skin was analysed (chapter 3.5.4). Furthermore, enzyme gene expression of aromatase and 17β-HSD in monolayers, human skin and the constructs was determined.

3.5.1 Dermal cells

NHK and NHDF were incubated with 5.69 ng/ml (0.0555 MBq/ml) [^{3}H]-T for 24 h in order to evaluate the cell specificity in testosterone biotransformation.

The androgens were detected in high amounts in the medium. Only minor additional amounts were recovered from lysed cell suspension. As to be expected, biotransformation of testosterone in NHK accounted just 14.5 % whereas more than 3-fold amounts of testosterone (55 %) were transformed by NHDF (fig. 18). This is in line with the intensities of enzyme expression in NHK and NHDF (chapter 3.5.5, fig.21; [93]). Dominating metabolite formed by NHK was 4-DIONE (8.6 % of total androgen) followed by AD (2.5 %). These metabolites are formed by 17β-HSD from testosterone and DHT, respectively. AD is also a biotransformation product of 5α-R (from 4-DIONE). DHT as well as 3α-HSD-metabolite amounts (only ADT) were detected in traces. The negligible formation of HOT is in line with the lack of CYP3A4 and only minor CYP3A5 expression in undifferentiated NHK [93]. E_2 is formed in very low amounts, too. No E_1 formation was observed in NHK, possibly due to 17β-HSD type 1 (HSD17B1) expression (chapter 3.5.5; fig. 21) responsible for the transformation of E_1 to E_2 [173]. A further reason for the low estrogen formation can be the negligible aromatase expression (chapter 3.5.5; fig. 21). Thus, 17β-HSD is the clearly dominating androgen metabolizing enzyme in non-differentiated human keratinocytes.

The main metabolite formed by NHDF was AD (25.2 %), followed by 4-DIONE (14.9%) and

DHT (7.4 %), demonstrating high 17β-HSD and 5α-R activities. ADT formation (4.5 %) is result of 3α-HSD activity and expression in NHDF (fig. 18; [93]), although 3-DIOL was not detected. CYP-related formation of HOT and E_2 was low (together 2.7%), too. As androgen recovery by ethyl acetate extraction amounts for at least 98.7 % there is only negligible further phase I metabolism and phase II glucuronidation of the androgens in monolayers of NHK and NHDF, if at all. In fact primary keratinocytes and fibroblasts express an incomplete spectrum of glucurononosyl transferases [46].

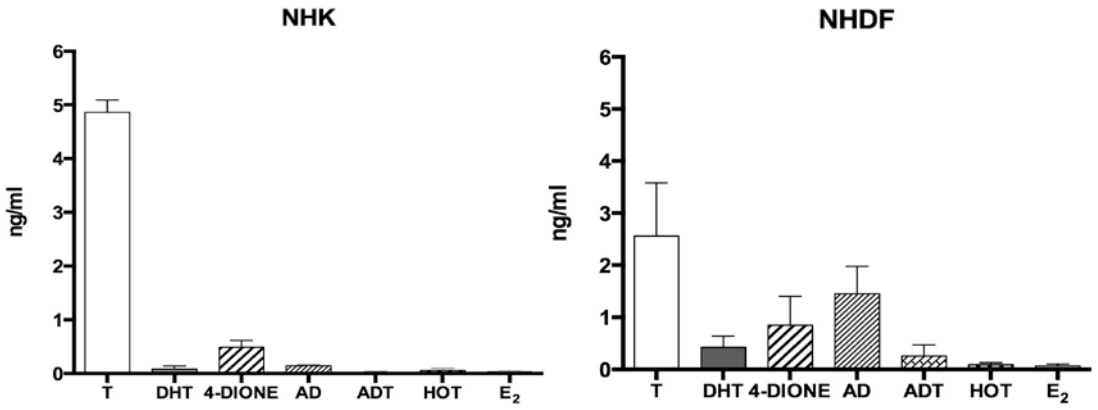

Fig. 18: Biotransformation of testosterone (5.69 ng/ml) in keratinocyte (NHK, passage 2) and fibroblast (NHDF, passage 3) monolayer cultures (mean ± SEM, n ≥ 3 donors) after exposure for 24 h.

The dominating metabolism in the dermal fibroblasts points out the lower epidermal activity of testosterone transformation. This is contrary to PC biotransformation with the epidermis representing the main location of esteratic transformation. These differences demonstrate the need to consider both the biotransformation capacity of the dermal and the epidermal part of (human) skin in drug development and especially toxicological assessment if biotransformation is of relevance.

3.5.2 Native human skin

The biotransformation of testosterone in fresh human skin (n = 5 female donors) was analysed using the membrane insert approach as described (chapter 2.9.1; 3.4.2.1). The finite dose of 13.7 ng/cm^2 was close to those used in penetration studies [35]. Testosterone penetration (fig. 19 B) and permeation (fig. 19 C) was taken into consideration.

As drug amounts removed by skin surface wash after 24 h exposure were below the limit of detection, testosterone well penetrated human skin. Testosterone (and metabolite) recovery from skin and the receptor medium was 99.8 % with 54.9 ± 1.8 % permeation into receptor medium; 43.1 ± 1.2 % of testosterone and its metabolites were recovered from the skin

matrix (fig. 19 B). Native testosterone was the dominating androgen in receptor medium and tissue (48.9 ± 5.8 % of applied testosterone). Contrary to undifferentiated NHK and NHDF, HOT (formed by CYP3A4/5) was the main metabolite (23.1 ± 4.0 %). HOT was found in the skin and in the receptor medium with higher amounts of this polar metabolite in the receptor medium (65.6 ± 4.4 % of total HOT; fig. 19 C). DHT (11.9 ± 1.9 %) and AD (7.4 ± 1.1 %) formation indicate rather high 5α-R activity of human skin from female donors. ADT (4.2 ± 0.6 %) recovery reveals 3α-HSD activity. AD and 4-DIONE (3.2 ± 0.6%) formation proves 17β-HSD activity. E_2 formation (0.1 ± 0.07%), however, was low (fig. 19 A - C) and no E_1 formation was observed indicating low aromatase activity. As seen with NHK and NHDF, according to the almost complete testosterone recovery there is no other phase I or phase II metabolism in fresh female human skin. The obtained metabolite spectrum (fig. 19 A -C) is well in accordance with enzyme expression in human skin (fig. 21).

Taken together, well in accordance with monolayer cell cultures of NHDF (from foreskin), 5α-R and 17β-HSD are relevant enzymes of androgen metabolism in female human skin. Aromatase activity was low with both monolayers and human skin. CYP3A4/5 activity was high in human skin; minor presence of HOT in monolayers obtained from juvenile foreskin indicates a major influence of sex, age and differentiation status of the cells regarding androgen biotransformation.

3.5.3 Reconstructed Human Epidermis and Skin

Reconstructed Human Epidermis

When applying testosterone for 24 h to RHE 89.4 ± 3.2 % of native androgen and metabolites has been recovered from medium and thus permeated the skin (fig. 19 C). The enhanced permeation of the reconstructed tissues is a well-known phenomenon linked to the less developed horny layer barrier of RHE [35, 57] compared to human skin. As with freshly excised female human skin, native testosterone is the most abundant androgen (31.8 ± 3.8 % of applied T) and CYP3A related HOT was the dominating biotransformation product (31.3 ± 4.7 %, fig. 19). In addition, DHT formation was very close to human skin (9.6 ± 2.0 %). Rather high amounts of 4-DIONE (10.5 ± 1.7 %) and ADT (11.2 ± 5.2 %) indicate high 17β-HSD and 3α-HSD activity of RHE, too. Formation of E_2 (3.0 ± 1.0 %) slightly exceeded formation in human skin. In total, 68.2 ± 3.8% of testosterone was transformed by RHE, the metabolite profile of RHE being close to human skin (fig. 19; tbl. 16). The higher biotransformation rate of RHE compared to human skin is due to the well-known poorer barrier function of RHE enabling faster penetration and thus access to the relevant enzymes. Enhanced access of testosterone to androgen metabolising enzymes may overcome the poorer biotransformation capacity of keratinocytes. In addition, keratinocyte differentiation

appears to enhance the expression and functionality of CYP3A4/5 in particular since biotransformation in non-differentiated NHK (fig. 18) was lower compared to RHE formed by differentiated NHK.

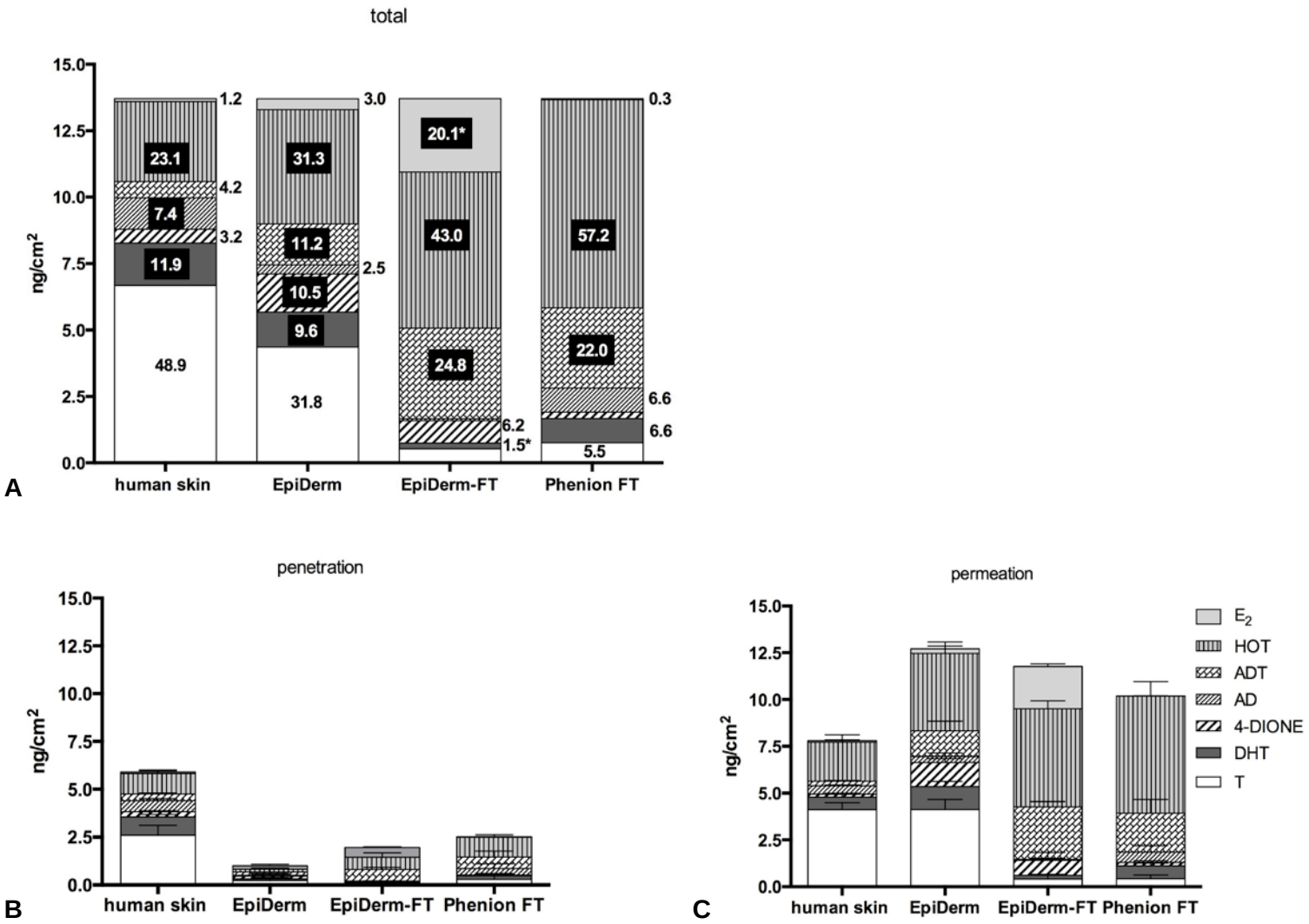

Fig. 19: Biotransformation of testosterone (13.7 ng/cm^2, 10 µl/cm^2) in freshly excised human skin of 5 female donors (membrane inserts), RHE Epiderm as well as RHS Epiderm-FT and Phenion FT (n ≥ 3 batches; each in triplicate) after incubation for 24 h. Data present native testosterone and metabolites (A; total) and separated in penetrated (B; tissue) and permeated (C; receptor medium) amounts; mean (± SEM); * p ≤ 0.05 compared to human skin.

Reconstructed Human Skin

With RHS, permeation rates were 83.1 ± 1.2 % with EpiDerm-FT and 72.3 ± 2.9 % for Phenion FT, respectively. This is in line with the lower permeation of Phenion FT seen after exposure to PC (chapter 3.4.3; tbl. 15) again indicating the skin matrix building a reservoir. The transformation of testosterone in RHS is increased compared to RHE and especially to native human skin (fig. 19). Yet, other than with the non-differentiated NHK and NHDF but in line with human skin (female donors) and RHE dominating metabolite with both RHS is HOT (EpiDerm-FT 43.0 ± 3.2 %; Phenion FT 57.1 ± 6.9 %). Due to the lower expression of CYP3A4 compared to CYP3A5 in RHE/RHS [44, 49, 93, 174] CYP3A5 might be mainly responsible for 6β-hydroxylation of testosterone. Once more, compared to human skin ADT is formed in major amounts by RHS indicating high 3α-HSD activity of EpiDerm-FT (24.8 ± 2.5 %) and Phenion FT (22.0 ± 8.0 %), too. However, the profile of other metabolites varied amongst RHS EpiDerm-FT and Phenion FT (tbl. 16) and human skin, particulary regarding E_2 and DHT formation.

Rank-Order			
Matrix **24 h**	**Absorption** mean ± SEM	**Tissue (penetration)**	**Medium (permeation)**
Human Skin (fresh, female donors)	99.8 ± 3.6 %	T>>HOT>DHT>AD>ADT>4-DIONE>>E_2	T>>HOT>DHT>AD>ADT> 4-DIONE>>E_2
EpiDerm	97.1 ± 0.2 %	T ~ E_2 >HOT ~ 4-DIONE ~ ADT >DHT>AD	T>HOT>>ADT>4-DIONE>DHT>AD ~ E_2
EpiDerm-FT	96.3 ± 0.8 %	HOT>ADT>E_2 >T>>4-DIONE>> AD ~ DHT	HOT>ADT>E_2>4-DIONE> T>DHT>AD
Phenion FT	93.2 ± 0.9 %	HOT>ADT>>AD ~ DHT>T>>4-DIONE ~ E_2	HOT>>ADT>DHT>AD>T>4-DIONE >>E_2

Tbl. 16: Testosterone absorption (% of dose) and rank-order of testosterone and metabolites after exposure (in EtOH; 13.7 ng/cm^2) to female human skin and the reconstructed tissues (EpiDerm, EpiDerm-FT and Phenion FT) for 24 h.

EpiDerm-FT provided particular higher aromatase activity (E_2: 20.1 ± 1.3 %) compared to human skin and Phenion FT ($p < 0.05$). Contrary, the 5α-R formation products DHT (1.5 ± 0.3%; significantly less than in human skin, $p \leq 0.05$) and AD (0.49 ± 0.4 %) are formed in low amounts in EpiDerm-FT. 4-DIONE formation of 6.2 ± 3.1 % reveals 17β-HSD (type 2/4) activity of EpiDerm-FT. The intermediate androgens 4-DIONE, DHT and AD were rapidly metabolised to ADT and E_1 appears to be transformed to E_2 by 17β-HSD, respectively.

With respect to Phenion FT, 5α-R activity considerably preponderates 17β-HSD type 2 oxidation processes and is responsible for the formation of DHT and AD (together 13.3 %), whereas 4-DIONE amounts were low (1.7 ± 0.8 %; fig. 19). Contrary to EpiDerm-FT, E_2 formation was negligible (0.29 ± 0.1 %) but comparable to E_2 formation in human skin (fig. 19). Qualitatively, the biotransformation profile of Phenion FT is most similar to that of human skin (tbl. 16; fig. 19). This holds also true with respect to negligible phase II metabolism as to be derived from almost complete androgen recovery (93.2 %) corresponding to previous observations [99].

In conclusion, the functionality of androgen transforming enzymes in RHS and in particular of Phenion FT is close to female human skin *ex vivo*. Except for lower DHT formation, metabolite spectra are well in accordance (fig. 19; tbl. 16). Biotransformation capacity of androgen related phase I enzymes varies among the investigated tissues and ranked as: RHS > RHE > human skin *ex vivo*. Differences, however, are linked – at least in part – to enhanced androgen access to the enzymes due to the well-known lower barrier function of RHE/RHS. In contrast, differences to the monolayer cultures of undifferentiated NHK and NHDF are present.

3.5.4 Influences of cryoconservation on androgen biotransformation

For the evaluation of influences on cutaneous androgen biotransformation due to cryoconservation, biotransformation studies were repeated with frozen skin (max. 3 months). The skin samples were from the same donors (three identical donors for fresh and frozen skin) and compared to testosterone biotransformation in directly excised (female) human skin. As to be expected (per-)cutaneous absorption of testosterone in cryoconserved and fresh skin was close (98.4 ± 3.2 % vs. 99.9 ± 3.8 %; fig. 20) in line with nearly identical penetration after exposure to PC (chapter 3.4.4). In contrast, other than with freshly excised skin, essentially only native testosterone was detectable in cryoconserved skin and it is the native androgen, too, which is recovered predominantly from the medium (53.5 ± 6.7 % permeation; fig. 20). Only 4-DIONE formation (6.0 ± 5.0 %) exceeded the amount in fresh skin. Other metabolites – merely E_2 and HOT - were only detected in traces indicating a

major decline of 5α-R, 3β-HSD and CYP3A4/5 activity and less decline of 17β-HSD activity. Thus, cryoconservation of human skin is not an option when aiming for an analysis of androgen metabolism.

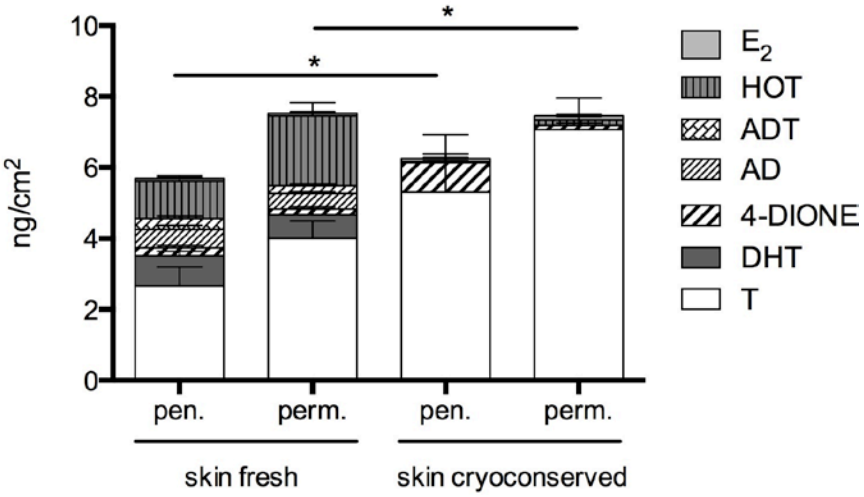

Fig. 20: Biotransformation of testosterone in female human skin, fresh and cryoconserved (skin from 3 identical donors) after incubation with testosterone (in EtOH; 10 µl/cm²; 13.7 ng/cm², 10.69 ng) for 24 h in membrane inserts; mean ± SEM; * p ≤ 0.05.

3.5.5 Gene expression

In addition, relative gene expression of enzymes involved in androgen metabolism - aromatase (CYPA19A1) and 17β-HSD type 1 and 3 (HSD17B1/HSD17B3) - was analysed by PCR in monolayer cultures (NHK, HaCaT and NHDF), human skin and the reconstructed tissues. The reconstructed tissue Phenion FT was separated in epidermis and dermis for separate analysis of gene expression in both strata.

Aromatase (CYP19A1)

In NHK (and HaCaT) no CYP19A1 expression was detected. Contrary, moderate expression was observed in NHDF (fig. 21). This is well in accordance with moderate E_2 formation in NHDF (fig. 18), whereas E_2 and E_1 as biotransformation products of CYP19A1 were not detected in NHK. Contrary to human skin and the RHE EpiDerm, CYP19A1 is expressed in both RHS. With respect to Phenion FT, CYP19A1 is mainly expressed in the dermis and was found in the epidermis just in 1 of 3 batches. This is in line with detection of E_2 in both RHS and especially in EpiDerm-FT, whereas E_2 formation was low in human skin and the RHE EpiDerm (fig. 19). The lack of CYP19A1 gene expression in NHK and the RHE EpiDerm reveales that CYP19A1 is mainly located in the dermis and not in the epidermis. The higher

expression level of CYP19A1 in the dermis of Phenion FT compared to the epidermis underlines these findings.

17β-Hydroxysteroid dehydrogenase (HSD17B1 and HSD17B3)

HSD17B1 and HSD17B3 are expressed in monolayer cultures of NHK, HaCaT and NHDF with slightly higher expression of HSD17B1 in NHK and of HSD17B3 in HaCaT. HSD17B3 was found just in one of three probes of NHK. HSD17B3 is also expressed in human skin, the RHE EpiDerm (just 1 of 3 batches) and both RHS. HSD17B1 is only expressed in human skin, EpiDerm and Phenion FT but not in the RHS EpiDerm-FT.

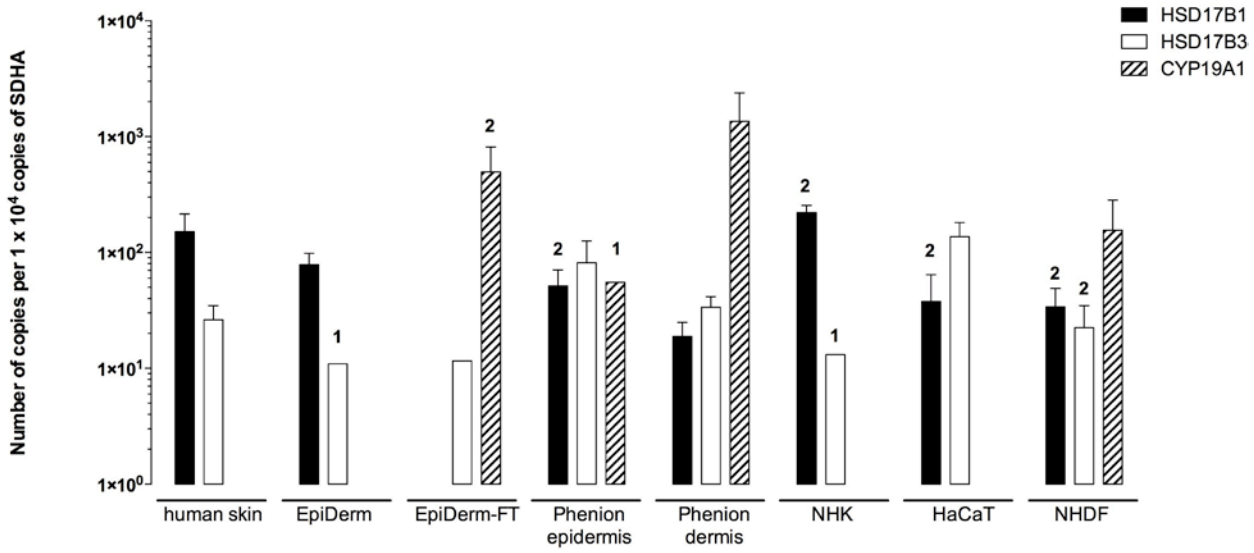

Fig. 21: Gene expression of enzymes involved in androgen metabolism (HSD17B1/3: *17β-hydroxysteroid dehydrogenase;* CYP19A1*: aromatase)* in human skin, EpiDerm, EpiDerm-FT, Phenion FT (separated in epidermis and dermis) as well as monolayer cells (NHK, HaCaT and NHDF). "1" or "2" indicates that mRNA expression was detected in one or two of the three donors; mean ± SEM, n = 3.

4 Final Discussion

4 Final Discussion

Over the last years several reconstructed human epidermis and full thickness skin models have been developed to replace animals in *in vitro* toxicological assays and more recently in non-clinical drug research. Predictive non-clinical testing for local biotransformation may increase efficiency of drug development by the early exclusion of non-suitable compounds and enhancement of formulation development can be an option, too. Reconstructed human epidermis is OECD adopted for testing of e.g. corrosivity and irritancy [175, 176] and appears suitable for the estimation of percutaneous absorption, too [35].Cutaneous biotransformation can influence dermal absorption and toxicity of topically applied substances, for example by CYP-related formation of mutagenic and sensitising products. This is of relevance e.g. in genotoxicity analysis [177, 178]. PC cleavage to P17EC enhances the risk of skin atrophy. Therefore biotransformation in the skin is of relevance for agents making contact with the skin. Sufficient knowledge of biotransformation capacity is a prerequisite for toxicity evaluation. Furthermore, a reconstructed tissue reflecting human skin not only with regard to morphological properties but also to biotransformation capability is required. Thus, the aim of the present thesis was to characterize the extent of biotransformation in the reconstructed epidermis EpiDerm and full thickness human skin (EpiDerm-FT, AST2000 and Phenion FT) in comparison to excised human skin and monolayer cell cultures in view of their qualification for the determination of dermal toxicity and sensitization. For a first approach the current study focuses on the esteratic cleaved prednisolone diester prednicarbate used for inflammatory skin diseases [83, 85, 96] and the oxidative/reductive transformed androgen testosterone. For this, the first step was to identify suitable and less stressful experimental test conditions. For (separation and) quantification of testosterone and its metabolites an analytical method was developed. In addition, knowledge of dermal biotransformation was expanded by determination of influences like sex, cryoconservation (of human skin), gene expression analysis and enzyme inhibition.

In detail, the presented thesis consists of the following purposes:

4.1 Development and *in house* validation of HPLC-radiodetection for quantification of testosterone and biotransformation products

For the separation and quantification of testosterone and its metabolites after extraction from the biological matrices (receptor medium, tissues, cell lysates, wash solution) an hplc-method was established based on previously described HPLC methods [166, 179, 180]. Most of these hplc methods require a gradient elution or complex mobile phases with

tetrahydrofuran (THF) as solvent [179]. THF generates peroxides causing oxidation of components in biological samples [166]. This oxidation can falsify biotransformation results, especially since testosterone is enzymatically oxidated in the skin. Thus, THF as solvent was avoided and replaced by acetonitrile. Furthermore, isocratic elution was preferred since stable baseline is easier to achieve as with gradient elution [180]. Radiodetection enables the quantification of the applied testosterone concentrations and its formed metabolites. Furthermore, radio-HPLC prevents detection of endogenous androgens and estrogens. Since not all anticipated metabolites were available as radioactively labelled reference compound, separation and determination of retention times was initially analysed via UV-detection and verified with the available radio-labelled compounds. In addition, with radiodetection the lower limit of quantification could be decreased from 10^{-6} M with UV-detection to $1.8 \cdot 10^{-9}$ M. Decrease in testosterone concentration is of high relevance since solubility of the lipophilic compound in the receptor medium [32] is limited and addition of solubilizers like BSA or tensides (Igepal®) influences tissue permeability and viability [32, 138, 139]. Optimation of separation was achieved by increasing the ratio of acetonitrile and temperature. Sufficient separation was achieved with a reversed-phase column (RP-18) under isocratic conditions (acetonitrile/water 60:40 v/v; flow rate 1 ml/min) within 30 min at constant 25° C avoiding direct light. In fact, column temperature can influence run time, viscosity of the mobile phase and separation efficiency. Hence, temperature should be maintained at a constant level. However, a disadvantage of isocratic elution is the longer elution and separation time compared to previously described hplc analsis with only approx. 15 min run time for sufficient separation [180].

For the *in house* validation, baseline separation (retention times, retention factors, separation factors and resolution), selectivity as well as linearity and repeatability (inter-/intra-day variability) were determined and revealed validity and repeatability of this method and thus the obtained results. Just separation of E_1 from E_2 was marginally acceptable. Therefore it cannot be completely ruled out that the lack of E_1 formation might be a result of overlapping signals (chapter 3.1). Furthermore, this method does not allow detection of very hydrophilic compounds like glucuronidated metabolites. However, since glucuronlystranferases are expressed only slightly in dermal cells and recovery by ethyl acetate extraction was almost complete (chapter 3.2), essential glucuronidation is not expected.

No interfering peaks were seen in the chromatogram e.g. due to impurities, medium compounds or solvents when analysing blank samples. Thus, sufficient selectivity of this method is given. The extraction from biological materials with ethyl acetate appears to improve selectivity. Furthermore, extraction with ethyl acetate offers nearly quantitative recovery whereas extraction by chloroforme was insufficient. This is in line with studies of various solvents for extraction of testosterone and its metabolites from cell microsomes with

ethyl acetate being the most effective extraction solvent [166].
An internal standard was added to all samples before extraction to determine the extraction efficiency of each experiment and for the detection of analysis errors during the analytical process. Physico-chemical properties of an internal standard should be close to the compound under evaluation without interferiences regarding chemical reactions or identical retention times. Corticosterone fulfills these requirements and is suitable for the hplc-analysis due to comparable efficient extraction by ethyl acetate and being well separated from testosterone and its metabolites. This is in line with previously described methods using corticosterone as internal standard for quantitative analysis of testosterone biotransformation [166].

4.2 Evaluation of reconstructed tissue quality and resiliency to experimental conditions

An intact diffusion barrier during the test is a basic prerequisite for meaningful results. Therefore, the determination of skin integrity before and during testing is required [29].The quality of the reconstructed tissues in accordance with the demands of OECD Test Guideline 431 (OECD TG 431) for testing in RHE was verified by studying tissue morphology of untreated reconstructs and sensitivity to test agents under the anticipated less stressful test conditions in membrane inserts. OECD TG 431 specifies criteria which reconstructed human epidermis/skin have to be met to represent an acceptable test matrix. The most important structural and functional requirements are a multilayered stratum corneum, presence of a functional barrier and sufficient tissue viability [170]. The RHE EpiDerm and the RHS EpiDerm-FT and Phenion FT revealed no morphological abnormalities after delivery or exposure to test compounds and their solvents, respectively (fig. 8). A multilayered stratum corneum and functional barrier could be determined with a higher total epidermal thickness and cell density of Phenion FT building a reservoir. Contrary, the RHS AST2000 failed to meet the requirements. Formation of only a few keratinocyte layers and detachment of the epidermis from the dermis even after arrival of the tissues was described earlier [181]. Thus, AST2000 was excluded from biotransformation experiments since a functional barrier was not present. This can lead to overestimation of biotransformation capacity since topically applied compounds can permeate easier [182] and gain more access to enzymes.
In addition, IL-8 and LDH-release as markers for cell damage and stress proved resiliency to the application of test compounds (PC/testosterone) and the solvent ethanol (fig. 11), respectively, again with highest sensitivity of AST2000 except for ethanol application leading to highest sensitivity of EpiDerm-FT. This can be caused by the lower barrier function of the EpiDerm-FT compared to the Phenion FT and human skin (chapter 3.4.3; 3.5.3). The

standard approach for cell viability is the 3-(4,5-dimethylthiazol-2-yl)-2,5-diphenyl tetrazolium bromide (MTT-)reduction assay [183]. However, the MTT assay is standardised for evaluation of only major changes in viability but not minor damages of cell integrity [32, 63] to the test compounds, their solvents or the tissue handling. The suitability of IL-8 relase and LDH leakage as a measurement for cell integrity of reconstructed tissues has been shown [184, 185]. Furthermore, correlation of IL-8 release between reconstructed tissues and human skin has been shown [186] as well as correlation between IL-8 release and results derived from the MTT assay [184].

The high resilience to PC exposure is in line with preserved tissue integrity after exposure to various PC formulations [65, 66]. LDH leakage of untreated Phenion FT and after exposure to the test compounds and their solvents corresponds with the values described by the manufacturer (27 U/l). Exposure to triton 1% for 24 h results in 100-fold increase of LDH leakage (information by the manufacturer Henkel AG, Germany).

In summary, sufficient developed strata and cell viability given RHE EpiDerm/RHS EpiDerm-FT and Phenion FT are reflecting the prerequisites laid down by the OECD TG 431. The experimental conditions did not cause relevant tissue damage influencing cell viability what might lead to lower enzymatic activity. Thus, with these matrices (EpiDerm, EpiDerm-FT and Phenion FT) PC and testosterone biotransformation was investigated.

4.3 Influences of experimental setup - *Franz cell technique vs. membrane approach*

As the focus was on biotransformation, it was aimed for a well-tolerated exposure of the tissues and thus initially the influence of the mode of skin mounting on enzyme activity was studied.

The Franz cell technique represents a frequently used method for *in vitro* studies of percutaneous absorption. The method described in OECD TG 428 is considered to be the standard method [28]. In previous studies this approach was used for biotransformation experiments, too [43, 65]. The skin is mounted and clamped between a donor and receptor chamber with stratum corneum exposed to the air and the dermis in contact with the receptor medium. This method was compared to an experimental setup using tissue culture inserts e.g. used for generation of reconstructed tissues. The results of biotransformation with these described methods (fig. 10) in skin of identical donors exhibited a significant lower formation with Franz cell technique compared to PC exposure in membrane inserts. Thus, esteratic biotransformation is clearly influenced by the experimental setup. This is explainable by the anticipated higher stress level in human skin fixed in a Franz cell resulting in a lower enzymatic activity. Interestingly, no differences in penetration and permeation were seen in

accordance with comparison of various experimental setups described previously [32, 187]. For example, there are no significant differences in testosterone and caffeine penetration/permeation between static Franz cells and flow-through cells [32, 187]. Regarding flufenamic acid penetration, no differences were seen between an in-house perfusion model (*Saarbrücker perfusion model*, [188]) compared to Franz diffusion cells. Also with the RHS EpiSkin no differences in absorption of six different substances were found between the Franz cell approach or usage of RHS in their inserts [64]. Penetration and permeation therefore appear insensitive towards external (mechanical) influences due to differences in the experimental setup. The standard approach for absorption testing by mounting the skin to Franz cells [35, 189], however, clearly leads to stress inducing decline of esterase activity (fig. 10). Hence exerted distension and pressure on tissues when mounting in Franz cells cause damage and decline of tissue viability probably responsible for the decline of enzyme activity. The degradation of enzyme activity due to the experimental setup can falsify results of biotransformation since underestimation of the extent of biotransformation becomes possible. In consequence, the toxicity of substances with dermal absorption or bioactivation of prodrugs in the skin can be underestimated using stress inducing experimental setups. Thus, biotransformation is strongly influenced by the experimental setup just as described for other external factors (e.g. concentration or vehicles of test compounds [190], properties of receptor solution [139]. This asks for standardized test conditions if biotransformation is of relevance.

A further advantage of the membrane insert approach compared to Franz cell technique alongside preservation of cell integrity/viability is a lower preparation time and material consumption.

Taken together, an essential result of this thesis is a new, for the tissues less stressful environment for biotransformation studies using the membrane approach with tissue culture inserts. The Franz-cell approach is suitable for studies only when viability and biotransformation is of no relevance.

4.4 Biotransformation in human skin *ex vivo* and reconstructed tissues under consideration of gene expression

The main focus of this thesis was on the comparative characterization of biotransformation capacity of reconstructed tissues: Esteratic cleavage of the double ester PC and phase I oxidation/reduction of testosterone in RHS composed of differentiating NHK and NHDF embedded into a collagen matrix was compared to human skin ex-vivo and also RHE formed by differentiating NHK without dermal equivalent. Well-known differences in the esteratic [95], oxidative/reductive [116] and also phase II enzyme expression and activity [46] and

hence biotransformation capacity between the dermal cells ask for the comparison of the constructs. This holds true the more since RHS has gained interest with respect to *in vitro* evaluation of the anti-inflammatory and atrophogenic effects of topical glucocorticoids including PC [164, 191, 192], too. For example, higher esterase [95, 193] and CYP3A4/CYP3A5 [78, 109] activity in the epidermis rather than in the dermis were described previously. In contrast, 5α-R type 2 was only detected in fibroblasts [116]. Interestingly, CYP3A activity and expression in NHK was negligible compared to HaCaT cells [47, 93]. Furthermore, increase in CYP3A4 mRNA expression corresponds with cell differentiation [78, 133]. This is why biotransformation in RHE/RHS was compared to human skin under consideration of differences in gene expression (fig. 21) and biotransformation in human skin-derived cell cultures (NHK, NHDF) and the keratinocyte-based HaCaT cell line (fig. 9; 18).

The present data point out that RHE and RHS once more proved overpredictive with respect to skin penetration and permeation especially of more hydrophilic metabolites into the receptor media. This is in line with penetration studies of both test compounds PC and testosterone [10, 32, 43] and various hydrophilic and lipophilic test compounds [163]. The higher permeability of RHE/RHS might be explained mainly by differences in the ultrastructural morphology like cellular density and cellular organization in the epidermal layers [41]. Hyperproliferation and insufficient formation of free fatty acids and polar ceramides (e.g. ceramides 5 and 6) was oberved [41, 194]. The still incomplete stratum corneum formation of the constructs may favour biotransformation within the tissues by faciliating the access to the metabolizing enzymes localized within the skin matrix. On the other hand, due to the less developed barrier applied solvents and test compounds can achieve the viable epidermis faster and to a greater extent. This can lead to higher sensitivity of the constructs compared to human skin and decreased cell viablility and thus biotransformation. The latter can be excluded here as experimental conditions did not cause relevant tissue damages influencing cell viability (fig. 8). However, higher absorption by the skin constructs was taken into account by relating metabolite formation to the amount of absorbed PC and testosterone, respectively.

The metabolite profiles of PC and the rank order of PC and metabolites in the tested RHE/RHS, however, are close to human skin ex vivo making reconstructed tissues suitable for biotransformation studies of prodrugs requiring activation by esterases in the skin. These finding is in line with conclusions based on bioconversion of naltrexone esters in the RHE EpiDerm compared to human skin [163]. However, quantitative differences in PC hydrolysis and thus higher formation of the metabolites in RHE/RHS (EpiDerm and EpiDerm-FT, $p<0.05$ compared to human skin) can be due to the enhanced uptake or distribution (tbl. 15) as described for other ester-prodrugs in RHE, too [10, 163]. Furthermore, esterase activity is

linked to mechanical stress (chapter 3.4.2.2). Thus, it cannot completely ruled out that the transport after surgery and preparation caused a decrease in cell viability and hence in biotransformation of PC in human skin. The similar metabolic profiles of PC in RHE and RHS (fig. 13) do further confirm a more pronounced ester cleavage in the epidermis as compared to the dermis [193]. This result is strongly supported by comparable PD formation in RHE and non-differentiated keratinocytes (fig. 9; 13) and also FDA hydrolysis obtained with an FDA-assay by Franzisca Marie Bätz [195]. The assay protocol makes use of tissue homogenates. Hence, the results of FDA-assay are not influenced by differences in skin penetration. Because of the previously described higher esterase formation in epidermal cells compared to dermal cells [95], PC hydrolysis in un-differentiated keratinocytes exceeded esteratic hydrolysis in fibroblasts by far. This corresponds well with FDA hydrolysis [195] in NHK and NDHF, too. Furthermore, since PD formation in NHK is well in accordance with formation in RHE it can be assumed that there are no differences in esterase activity due to cell differentiation.

The HaCaT cell line seems to be slightly more active regarding PC cleavage than NHK with a faster PD formation (fig. 9 A and 9 B). Of particular note is the high variability and - contrary to PC cleavage - the less efficient FDA cleavage [195] of HaCaT cells. These differences in PC and FDA ester cleavage and also the high variability are probably based on donor-specific genetic susceptibility, different HaCaT subclones [47], the old age of the donor (62 years old male donor) and especially different passages: Differences in the activity of e.g. N-acetylation were related to different HaCaT subclones [196]. While biotransformation of PC was studied in cultured HaCaT cells from passage 61 to 66, FDA assay was based on passages 39 to 58 [195]. Increasing passaging of the cell culture is accompanied by redifferentiation of the cell line. Additionally, there is a well-known linear correlation between the increasing passaging of HaCaT cells and augmented tumour formation [197]. Moreover, expression of arylesterase in HaCaT is lower than the expression level in NHK [93] and contrary to PC FDA is substrate of arylesterases [195]. Thus, FDA is probably mainly cleaved by other esterases and/or by other isoforms of the carboxylesterases to a relevant extent.

No significant differences in PC biotransformation were found between both RHS. However, PC uptake and biotransformation of the RHS Phenion FT is less pronounced compared to the EpiDerm-FT and most similar to human. This might be due to the higher total epidermis thickness and cell density of Phenion FT building a reservoir more similar to human skin. These differences are probably based on the different methods of the EpiDerm-FT and Phenion FT tissue construction. The EpiDerm-FT consists of fibroblasts embedded in a rigid collagen gel (on special membrane filters) coated with keratinocytes. Contrary, the dermal compartiment of the Phenion FT is based on a characteristic porous structure with regions of

lower density faciliating mobility and cell division of the embedded fibroblasts ([71]; information by the manufacturer Henkel AG). Importantly, PC biotransformation in the reconstructed tissues and human skin corresponds also with enzyme activities dervived by the ready-to-use FDA assay for cleavage of the model dye FDA [195]. The non-linear relation is probably result of a major FDA cleavage by arylesterases as described, whereas PC is mainly metabolised by carboxylesterases like other glucocorticoid esters e.g. betamethasone 17-valerate [86]. Furthermore, as stated above the FDA assay is irrespective of penetration and is based on skin homogenates enhancing access to enzymes. Thus, RHS is recommended for further studies on ester drugs or esterificated prodrugs to support the relation reported here. Since enzymes involved in the activation of ester drugs/produgs are present in RHE/RHS and biotransformation of PC in the constructs corresponce well with human skin RHE/RHS appear suitable to replace human and animal skin for pharmacological and toxicological testing.

Regarding testosterone bioconversion, the influence of dermal biotransformation on skin penetration [65, 70] may violate the suitability of testosterone as penetration standard due to intensive biotransformation. The enzymes responsible for activation and deactivation of testosterone are expressed in NHK (5α-R, 17β-HSD, 3α-HSD [100, 116]), human skin (5α-R, 17β-HSD, 3β-HSD, CYP3A4/CYP3A5 [47, 100]) and also skin appendages [198]. In RHE [47, 49, 199, 200] expression of 5α-R, 17β-HSD and 3β-HSD was demonstrated, too. Expression levels of the enzymes within the skin and thus the extent of androgen metabolism and the testosterone metabolite profile strongly depend on skin site [99, 198, 201], sex with higher male activity, age [99, 102, 116], differentiation status of dermal cells and culture conditions [110, 136, 140, 202]. Bioconversion in hair follicles and sebaceous/sweat glands is of relevance, too, since contrary to human skin reconstrcucted tissues do not dispose skin appendages [41]. Moreover, human skin often is from female donors whereas monolayer cell cultures are derived from juvenile foreskin. Furthermore, the RHE and RHS are often built from cells isolated from foreskin. This was true with RHE EpiDerm and RHS EpiDerm-FT and Phenion FT, too. There are well-known differences in enzyme expression and distribution between cells of genital and non-genital origin [103].

The higher biotransformation activity and metabolite profile of foreskin-derived dermal fibroblasts compared to keratinocytes (fig. 18) close to previous data [116, 203] indicates the accurateness of the obtained results with this new approach of radio-HPLC analysis. Enzyme expression levels of 17β-HSD and especially 4-DIONE and AD as main metabolites in NHK are in accordance with previous data [47, 116, 140], too. Since 5α-R type 2 is not expressed in NHK but in NHDF [116], DHT was dominantly found in NHDF (fig. 18). In addition, the formation of AD in both NHK and NHDF confirms that 4-DIONE offers a higher substrate specifity for 5α-R than testosterone [140]. Again 3-DIOL was not detected in NHK and NHDF

obviously due to high activity of 17β-HSD responsible for the fast oxidation of DHT to AD as described previously [140]. In line with localization of aromatase in the dermis and not in the epidermis [128] no aromatase expression and metabolism was observed in NHK (fig. 18 and 21) contrary to NHDF. Finally, relevant phase II biotransformation was not observed as primary keratinocytes and fibroblasts express an incomplete spectrum of glucurononosyl transferases [46]. In particular UGT2B7 [113] relevant for hydroxy-steroid (e.g. ADT) glucuronidation is not expressed. UGT2B17 involved in conjugation of ADT and DHT [204] is only slightly expressed in RHE and RHS [48]. Yet, undifferentiated cells from foreskin forming the NHDF and NHK monolayers are not appropriate for testing testosterone biotransformation in human skin especially due to considerable differences in the phase I metabolite profiles and enzyme expression (fig. 18, 19 and 21). There is also the fact that 17β-HSD products AD and 4-DIONE are main metabolites in the NHDF and NHK monolayer cultures, whereas human skin ex vivo transforms testosterone in particular into HOT by CYP related hydroxylation and 5α-R activated DHT. DHT and ADT are formed in relevant amounts by NHDF and human skin (fig. 18; 19) but only negligible amounts by NHK.

Contrary to monolayers of NHK and NHDF testosterone metabolism in RHE and RHS is rather close to fresh human skin (fig. 19; tbl. 16). This is in line with comparable mRNA expression of involved phase I enzymes like 17β-HSD, 5α-R and CYP3A5 [44, 45, 48]. Noticeable differences - especially compared to human skin - mainly regard E_2 and also DHT formation (fig. 19). Differences by the constructs can be due to varying culture conditions according to manufacturer´s instructions since e.g. glucocorticoids induce aromatase expression [105] and hydrocortisone is a frequent additive in culture media. E_2 formation is particularly pronounced in EpiDerm-FT ($p \leq 0.05$ compared to human skin) and less so in Phenion FT and human skin *ex-vivo* as well as in the RHE EpiDerm. The latter is in line with the lack of aromatase expression in the epidermis [128] and as described for NHK. The lack of E_1 formation in all constructs can be explained by 17β-HSD type 1 expression catalyzing the irreversible conversion of E_1 to E_2 (fig.4; 21). In addition, a higher affinity of testosterone to aromatase than of 4-DIONE appears possible. EpiDerm-FT and Phenion FT differ with respect to DHT formation, once more the latter construct being closer to human skin (fig. 19; $p \leq 0.05$ compared to human skin). Except for differences in E_2 and DHT formation, testosterone metabolite profiles in the constructs (and especially Phenion FT) are very close to freshly excised human skin. This holds true despite of the fact, that RHE and RHS are grown from foreskin derived cells whereas excised skin was from females undergoing cosmetical surgery. This demonstrates that in particular the cell differentiation (probably due to differences in cell culture conditions) and tissue handling influence the metabolic profile of testosterone. The expression of a comprehensive spectrum of enzymes involved in dermal oxidative and reductive bioconversion including activation and also inactivation of exogenous

compounds close to human skin [48] make RHE and RHS a suitable matrix for preclinical studies. Importantly, the intense testosterone metabolism in human RHE and RHS does not impair the suitability of the androgen as a penetration standard. This becomes obvious since penetration in fresh human skin and in cryoconserved and hence enzyme deprived human skin ex vivo without relevant biotransformation was similar. Furthermore, both with finite-dose and infinite-dose studies in RHE and RHS penetration data are in correspondence with data derived from cryoconserved human skin [35, 63].

More importantly, the comparable enzyme expression is of high relevance for evaluation of potential toxic reactions in RHE/RHS instead of human skin. Especially the CYP3A and more the CYP3A5 expression in human skin is of relevance. Besides CYP1A1, CYP3A5 appears to be involved in sensitization, e.g. by the activation of geraniol into geranial and neral which are the active forms of the potent contact allergen [67]. Moreover, dermal CYPs activate dapsone, sulphonamide antibiotics and nevirapine [178] as well as diphenylthiourea which are potent skin sensitizer [68], too. Additionally, CYP related metabolism of polycyclic aromatic hydrocarbons was described ([47] and references therein). The cutaneous activation of e.g. benzo[a]pyrene contributes to genotoxicity of the carcinogen [205]. In line with CYP3A4/5 expression in differentiated tissues (human skin and RHE/RHS) only [93], HOT is the dominating metabolite in native human and reconstructed epidermis (EpiDerm) and skin (RHS EpiDerm-FT, Phenion FT (fig. 19). In fact, enzyme expression levels of CYP3A4 and especially CYP3A5 in human skin compared to all constructs analysed here is very close [93] once more indicating that CYP enzymes are mainly localized in the epidermis [78] obviously maintaining the epidermal barrier function. Previous results are ambiguous with respect to CYP3A4/5 expression and activity in undifferentiated keratinocytes. A few studies described some CYP3A4 and/or CYP3A5 expression at the mRNA and protein level and activity in non-differentiated keratinocytes fibroblasts, Langerhans cells [110], and the keratinocyte-based cell line HaCaT [47], whereas others demonstrated a lack of CYP3A activities and expression in NHK [47, 110, 152] and NHDF [93]. Obviously, the CYP3A4/5 mRNA expression level and functionality significantly depends on cellular differentiation and cell culture conditions as observed here and described previously [78, 132]. The duration of air exposure is essential for the final differentiation of cell layers [5, 40, 41]. Furthermore, rising CYP expression levels corresponds with increasing maturity of the reconstructed tissues [49]. Thus, enzymes studied here are also involved in the adverse drug reactions and hence RHE/RHS contrary to monolayer cultures appear suitable to replace human skin for sensitizing and genotoxic analysis of compounds undergoing dermal biotransformation. These findings are in line with very similar activation and genotoxicity of benzo[a]pyrene in EpiDerm and EpiDerm-FT compared to human skin [205]. Finally, it is important to mention that the reproducibility of PC and testosterone biotransformation in at least 3 batches of RHE

and RHS was good (fig. 12; 13; 19) indicating sufficient quality of these constructs and low donor-related variability.

To summarize the results for PC and testosterone biotransformation, reconstructed human epidermis and especially reconstructed full thickness human skin revealed a biotransformation capacity close to native human skin but demonstrated that culture condition and skin handling ask for standardization since enzyme expression and biotransformation can easily be influenced by various endogenous and exogenous factors like culture conditions, cell origin or skin handling. Thus, RHS should be used for further studies on other substances with dermal absorption and ester drugs/prodrugs to support - or falsify - the relation reported here.

4.6 Influences of cryoconservation on cutaneous biotransformation

In addition, biotransformation in freshly excised versus cryoconserved human skin was compared since little is known about enzyme stability of previously frozen skin compared to fresh human skin. Therefore, skin samples from the same donors where analysed after surgery (within 12 hours after storage at 4° C) and after cryoconservation (storage at -20° C for a maximum of three months). The essential benefit of cryoconservation lies in the possibility for repeatable testing of the same charge (or donor) for intraindividual comparisons. In addition, skin can be stored to compensate the limited availability of human skin for further experiments. It could be demonstrated that lipid composition and barrier function of the skin during cryoconservation remains stable within a time period of 12 months [206]. Since penetration is a passive process through the non-viable barrier [18], the stratum corneum, for analysis of penetration cryoconserved skin is an option. Cryoconservation did not influence penetration of several compounds (e.g. di-n-butylphthalate (DBP)), caffeine and testosterone) compared to fresh skin [32, 76, 190, 207] up to 30 days. Afterwards the permeation increases constantly [208].

With respect to esteratic activity, cryoconservation appears to preserve enzyme activity of human skin as to be derived from essentially unchanged PC cleavage compared to directly excised skin from the same donor (fig. 14). This is in line with results of biotransformation in fresh and previously frozen rat skin indicating a strong robustness of esterases [209]. Furthermore, there were no differences in biotransfomation of the ester DBP, mainly hydrolysed by carboxylesterases, too, in fresh and previously frozen skin of rabbit, guinea-pig and hairy rat [76]. Furthermore, it could be demonstrated that esteratic cleavage of benzyl acetate was present in frozen human and rat skin [210]. However, the knowledge of esterase stability is limited; differences in the various members of the carboxylic ester hydrolase family and isoforms cannot be excluded currently. A major decline of esterase activity in pig skin by storage > 6 months [211] may be an overestimation due to non-

intraindividual comparison.
In contrast, cryoconservation of skin resulted in nearly unchanged testosterone (fig. 20) whereas approx. 50 % of applied testosterone was transformed to its metabolites with fresh human skin (fig. 19). All the enzymes involved in testosterone transformation degrade rapidly. This is well in accordance with previous observations in skin, [33] rat liver parenchymal cells [131] and hepatocytes [130]. A few studies detected an increased LDH release into culture media linked to damages in cell integrity after skin freezing [212]. Further studies described a considerable decrease in skin viability [213] within 24 h after freezing. However, a high variability in skin viability and biotransformation was seen [15, 214] when freezing skin for longer storage. Furthermore, pH values of previously frozen and thawed skin increases [214]. It cannot be ruled out that the alteration of pH values influences steroidogenic enzyme activity as enzymes exhibit a specific and occasionally narrow pH optimum (e.g. 5α-R type 2; [99]). Thus, cryoconservation of human skin is not an option when aiming for an analysis of androgen metabolism.
These significant differences in robustness of steroidogenic enzymes compared to esterases towards cryoconservation and high variability of skin viability [214] after freezing demonstrate the need for further analysis of general enzyme stability. It is further noticeable that viable skin is an essential prerequisite for biotransformation studies. Contrary, for penetration studies previously frozen skin is an option again demonstrated by nearly identical penetration rates of both test compounds PC and testosterone. Regarding permeation across cryopreserved hairless rat skin, freezing of the skin for 180 days with 10 % glycerol results in considerable less increase in permeation rates as compared to freezing without glycerol [208]. If freezing with glycerol acts also cryoprotective towards biotransformation, should also be investigated with a large sample size.

4.5 Sex-specifity of cutaneous esteratic activity

There are well-known gendered differences in physiological skin properties like thickness of epidermis and dermis [215], collagen density [3] acidity of the skin [215, 216]. In fact, female epidermis is thicker whereas male dermis is thicker [215, 216]. Thus, penetration and permeation can be influenced due to differences in the epidermal/dermal thickness. Furthermore, due to the less pronounced epidermal barrier topically applied substances can gain more access to (epidermal) enzymes of male skin probably leading to enhanced biotransformation. The differences in skin properties are mainly due to unequal hormonal influences of androgens and estrogens [216]. Varying cutaneous expression/activity and substrate affinity of steroidogenic enzymes like 17β-HSD and 5α-R [118, 125, 198] in female and male human skin are to be expected probably leading to unequal metabolic profiles of

topically applied substrates. The esteratic cleavage in female and male human skin was compared to proof whether there are sex-related differences in cutaneous esteratic activity, too.

It could be shown however, that contrary to steroidogenic enzymes esteratic activity depends not on sex since no differences neither in metabolic profile nor in extent of hydrolysis were observed in breast and abdomen skin from male or female donors (fig. 15). This significantly facilitates the evaluation of hydrolytic enzyme activity by far since it makes no difference whether reconstructed tissue is based on cells of male or female donors.

At the same time, however, it is equally obvious that in contrast androgen transformation can be influenced by sex and age since involved enzymes are responsible for the endogenous synthesis and inactivation of female or male sex hormones with intracrine and paracrine actions. Regarding hepatical metabolism, there is some evidence for females having lower activity of CYP1A2, CYP2E1 and UGT but higher activity of CYP3A4, CYP2A6, and CYP2B6 [217]. If this holds true for dermal CYP enzymes is obviously unknown at present. The general knowledge of sex differences in cutaneous biotransformation is mearge and significantly more research is needed. Thus, when interpreting outcomes of toxicity evaluation it must be taken into consideration if biotransformation results might be influenced by sex-specific characteristics.

4.6 Enzyme inhibition

Skin homogenisation enables the release of esterases localised in the cytosolic compartiment and endoplasmatic reticulum [88]. The results of esterase inhibition in human skin demonstrated that carboxylesterases and unspecific serine esterases are mainly responsible for the hydrolysis of PC (fig. 16; 17). Almost complete inhibition of PC formation to the monoesters and complete deletion of PD formation was achieved with combination of the specific carboxylesterase inhibitor BNPP and the unspecific serine esterase inhibitor PMSF. PMSF itself is unstable and hydrolysed rapidly at pH 8 [218]. Thus experiments were conducted with reduced incubation periods, increased inhibitor and reduced substrate (PC) concentrations leading to an enhanced inhibitory effect. Further studies on the time and concentration dependence of the inhibitors are desirable. In fact, BNPP revealed a time- and concentration-dependent inhibitory effect [219, 220] .

Taking enzyme expression into account it can be assumed that CE2 mainly contributes to PC formation since CE2 expression exceeded CE1 expression in human skin and cultured keratinocytes [93]. Furthermore, CE1 is not expressed in HaCaT [92] metabolizing PC in relevant amounts (fig. 9 B). In contrast, CE1 expression in fibroblasts exceeded expression levels of keratinocytes by far [93] but PC biotransformation in fibroblasts is negligible (fig. 9 C). Furthermore, CE1 shows a higher substrate specifity for esters with a small alcohol

group. Contrary, CE2 mainly hydrolyses substrates with large alcohol and small acyl group [221]. This is certainly the case for PC (for structure see fig. 3) and also methylprednisolone 21-hemisuccinate with well-known higher affinity to CE2 [88]. Furthermore, betamethasone 17-valerate was transformed intensively in small intestine microsomes where CE2 dominates compared to liver microsomes with CE1 dominance [86].

Interestingly, esteratic cleavage of the monosters P17EC and P21EC to PD was slightly deminished in presence of the cholinesterase inhibitor eserine, whereas bioconversion of PC to these monoesters was not decreased (fig. 16). In fact, hydrolysis of prednisolone monoesters like prednisolone senesyonate and geranate were completely inhibited by cholinesterase inhibitors indicating that these enzymes are responsible for bioconversion of prednisolone *monoesters* only [222]. Thus, cholinesterases may contribute to bioconversion of only PC intermediates (prednisolone monoesters P17EC and P21EC) to PD to a minor extent and probably exhibit a low substrate specifity. Arylesterases are not involved in PC formation since no decrease in biotransformation to the monoesters and the final metabolite PD was observed in presence of the effective arylesterase inhibitor NEMI [223]. Due to the almost complete inhibition with serin esterase inhibitors it can be concluded that other esterases with carboxylase activity like acetylesterases or alcohol dehydrogenase [220] do not contribute to PC or PD monoester hydrolysis.

However, further experiments with specific inhibitors and a wide range of concentrations and test durations are required to support or falsify the relations described here.

Due to a poor substrate specifity and excistence of several isoenzymes with varying substrate specifities esterases are responsible for intensive biotransformation of topically applied esters/ester-prodrugs in human skin. This is of high relevance for activation/inactivation and thus efficacy within the skin. To enhance the (pro-)drug development, esterase isoenzymes and especially their substrate specifity needs to be identified. Targeted inhibition of defined enzymes can enhance efficacy of esterificated (pro-)drugs, too.

5 Prospects

5 Prospects

Besides the commercially available reconstructed human epidermis and full thickness skin evaluated in this thesis regarding their biotransformation capacity, further commercially available reconstructed tissues like SkinEthic™ are recently described with respect to morphology offering similar architectural structure compared to human skin, too. The knowledge of their biotransformation capacity is limited. Moreover, RHE like EpiDerm are adopted for skin absorption and toxicity testing of substances (probably) exposed to human skin. Although reconstructed epidermis and skin are useful tools for absorption and hazard assessment, further improvement like refinement of lipid composition to represent native human skin barrier to a greater extent can be done. Furthermore, incorporation of e .g. blood vessels into reconstructed skin would enhance the comparison of transport processes within the skin. Reconstructed tissues with embedded immunocompetent cells or mimicking skin diseases like atopic dermatitis and psoriasis vulgaris or imitating wounded skin are under development. These reconstructed tissues can be used for the evaluation of drug efficacy and safety but also for a more detailed characterization of the disease and healing processes e.g. by analysis of differences and changes in gene expression or levels of proinflammatory cytokines. For example, proinflammatoric genes are highly expressed as well as chemokine receptors in skin of atopic patients. However, such reconstructed tissues also have to be evaluated with respect to biotransformation capacity to determine if they are able to metabolize compounds exposed to skin similar to native human skin. This is of relevance because e.g. barrier function is decreased in atopic patients or wounded skin leading to increased permeability and thus probably enhanced activation or (de)toxification in the skin. Furthermore, enzme expression and functionality can be influenced in lesional keratinocytes of e.g. atopic patients due to filaggrin deficiency.

To complement the results obtained in this thesis, the mRNA and protein expression levels of the involved enzymes in the reconstructed tissues and human skin should be examined in total. To identify and differentiate the specific isoenzyme(s) responsible for biotransformation further experiments with more specific inhibitors are required. Sufficient knowledge of isoenzyme substrate specifity can enhance efficacy of substances undergoing (carboxylesterase-mediated) hydrolysis by selective preservation of endogenous ester cleavage with specific inhibitors.

Furthermore, for a broader and sufficient knowlegde of metabolism within the skin the biotransformation of further substances and enzyme activity of a wide spectrum of phase I/phase II enzymes should be examined. Comparison between human skin and

reconstructed tissues should be done, too. Only in this way it will be possible to make a judgement on whether reconstructed tissues in general are able to replace human and animal skin in toxicity testing and to identify a skin model representing human skin to a full extent. In addition, biotransformation should be assessed in both male and female human skin in order to exclude possible sex related differences. This is neccessary since RHE/RHS are based on cells of male origin and differences in enzyme expression level and biotransformation profile in skin of male and female donors have been demonstrated.

The results of this thesis illustrate that reconstructed human epidermis and skin in principle are useful in *in vitro* tests despite of the well-known less pronounced barrier function. Reconstructed tissues representing viable test matrices enable standardized simultaneous determination of dermal biotransformation and its impact on absorption of topically applied substances in a simple way. However, to obtain reliable data test protocols have to be standardized to minimize influences on biotransformation due to e.g. varying culture conditions and experimental setup. The composition of cell culture media and duration of cultivation can influence cell differentiation and enzyme expression level of e.g. CYP enzymes. These enzymes are responsible for sensitization and genotoxicity of carcinogens and thus are involved in the adverse drug reactions.

In large scale trials data reproducibility must be confirmed for broad acceptance of reconstructed skin-based *in vitro* toxicity tests and proof of test validity. Moreover, for capturing the predictive capacity of reconstrcuted human skin in carcinogen risk assessment, a larger number of chemicals need to be assessed.

6 Summary / Zusammenfassung

6 Summary

6.1 Summary

Reconstructed human epidermis and full thickness skin initially created to substitute seriously wounded skin are of high interest in *in vitro* tests as alternative to animal experiments and to compensate the limited availability of human skin for this purpose. Reconstructed human epidermis is OECD adopted for testing of e.g. corrosivity and irritancy [175, 176] and appears suitable for the estimation of percutaneous absorption of compounds, too. However, for regulatory acceptance and broader use in particular in preclinical drug development an ideal construct should mimick morphology and present a barrier but also biotransformation capacity close to human skin. Biotransformation of substances with dermal absorption can influence penenetration and permeation [33, 65] and thus the effects of the applied compound. Cutaneous biotransformation may not only lead to formation of the active form of pro-drugs influencing drug absorption and efficacy [65], but also CYP related formation of mutagenic and sensitising products [177, 178]. Therefore biotransformation in the skin is of relevance and we need to understand biotransformation activities in human skin as well as RHE/RHS.

For a first approach into biotransformation capacity of RHE/RHS the current thesis focuses on the prednisolone diester prednicarbate used for inflammatory skin diseases [83, 85, 96] to unravel the potential of reconstructed tissues for the investigation of ester-prodrugs. Furthermore, the OECD adopted test compound testosterone was choosen because of the most complex biotransformation involving several enzymes. Esteratic cleavage and androgen (de-)activation in RHS composed of differentiated NHK and NHDF embedded into a collagen matrix are compared to human skin ex-vivo and RHE formed by differentiated NHK without dermal equivalent. Well-known differences in the esteratic [95], oxidative/reductive [116] and phase II enzyme activity [46] biotransformation capacity of dermal cells ask for the comparison of the constructs.

For separation and quantification of testosterone and its metabolites an hplc assay with radiodetection and corticosterone as internal standard was established and *in-house* validated. Determination of retention times, retention factors, separation factors, resolution as well as linearity and inter-/intraday-variability revealed that the results obtained with this method were reliable and valid. The lower limit of quantification (LOQ) was 0.0075 MBq/ml (0.7 ng).

The quality of the reconstructed tissues in accordance with OECD TG 431 requirements and resiliency to test compounds and solvents was determined. No morphological abnormalities and sufficient cell viability of the RHE EpiDerm and RHS EpiDerm-FT and Phenion FT were

detected. In contrast, the AST2000 failed to meet the requirements and was excluded from the biotransformation experiments.

Because of the still incomplete stratum corneum formation by RHE/RHS a significant difference in extent of permeation and biotransformation compared to human skin ex vivo is - at least in part - due to enhanced uptake seen on a regular base with compounds widely varying in molecular weight and lipophilicity [35].
However, no qualitative differences in the metabolic profile of PC were seen in the RHE EpiDerm and both RHS (EpiDerm-FT and Phenion FT) compared to human skin demonstrating that PC esteratic cleavage predominantly occurs in the epidermal layers. In fact, experiments performed within this thesis verified that PC cleavage in NHK exceeded hydrolysis in NHDF by far [95]. To complete the knowledge on PC biotransformation by dermal cells, the focus was on HaCaT cell line because of the elimination of donor-related variability. It could be demonstrated that the proportion of ester hydrolysis is very similar to NHK, although PD formation in HaCaT was even faster.

Qualitatively, the biotransformation profile of testosterone in RHE and RHS, especially Phenion FT, was very similar to human skin, too. Differences in the quantitative formation of testosterone metabolites (HOT, E_2) in human skin and the reconstructed tissues as well as undifferentiated cell cultures are due to differences in culture conditions and differentiation status of epidermal cells with well-known influences on enzyme expression and activity. Considerably lower formation in RHE confirmed the general higher androgen formation in the dermis. This is confirmed by the more pronounced expression of relevant enzymes and especially testosterone formation in NHDF compared to oxidative/reductive biotransformation in NHK.

In addition, it could demonstrated that the experimental setup influences the extent of biotransformation. It was shown that PC transformation following drug exposure in membrane inserts was three times higher compared to results obtained using Franz cell technique. This is explainable by the anticipated higher stress level in human skin fixed in Franz cell resulting in a lower enzymatic activity. Thus, all experiments were conducted using the membrane insert approach.
Furthermore, influence of skin cryoconservation on biotransformation was analysed. Noteworthy, profile and quantity of native PC and its metabolites were almost identical in freshly excised and cryoconserved human skin. In contrast, cryoconservation leads to almost complete degradation of steroidogenic enzymes. Thus, skin viability is relevant for the majority of dermal enzymes and freezing of skin not an option when biotransformation is investigated. Interestingly, there is no difference in esteratic cleavage of PC in female and male skin enhancing esterdrug/prodrug development and toxicity analysis since activation in

human skin is irrelevant of sex. With targeted enzyme inhibition it was shown that PC is mainly hydrolysed by carboxylesterases and unspecific serin esterases in human skin.

Taken together, in this thesis it has been demonstrated that reconstructed human epidermis and especially reconstructed full thickness human skin exerts a biotransformation capacity and enzyme expression profile close to human skin although RHE and RHS once more proved overpredictive with respect to skin penetration. Given this result verified in studies on a large scale of further subjects of phase I and phase II metabolism, reconstructed human skin may find its use as validated and accepted standard in *in vitro* tests for pharmacological and toxicological testing in particular for preclinical drug development, thereby reducing animal experiments and eliminating species-related differences.

6.2 Zusammenfassung

Ziel dieser Dissertation war es, rekonstruierte humane Epidermis- sowie humane Vollhautmodelle hinsichtlich ihrer Biotransformationsleistung untereinander sowie insbesondere gegenüber menschlicher Haut *ex vivo* vergleichend zu charakterisieren. Rekonstruierte Hautmodelle - initial zur Versorgung schwerer Hautwunden entwickelt - haben in den vergangenen Jahren als Ersatzmethoden zum Tierversuch, bzw. zur Kompensation schwer verfügbarer Humanhaut *ex vivo*, bei der pharmakologischen bzw. toxikologischen Prüfung von Substanzen mit dermaler Absorption (Kosmetika, Pestizide, Arzneimittel zur (trans-)dermalen Applikation), an Bedeutung gewonnen, insbesondere auch in der präklinischen Entwicklung. Zur Bestimmung der perkutanen Absorption sowie zur Prüfung der Hautirritation/-korrosion sind diese Hautmodelle zum Teil bereits validiert und von der OECD als Testmatrices akzeptiert [28, 170]. Der kutane Metabolismus hat jedoch einen entscheidenden Einfluss auf das Absorptionsverhalten [65], auf die Aktivierung/Deaktivierung in der Haut und somit auf die Wirkung und Toxizität einer Substanz. Daher ist neben einer vergleichbaren morphologischen Struktur sowie Barriereeigenschaft rekonstruierter Hautmodelle ebenso eine vergleichbare Biotransformationsleistung von entscheidender Bedeutung, um ein *in-vitro*-Testsystem zu etablieren, dass die menschliche Haut bezüglich Barriereeigenschaft und metabolischer Fähigkeiten hinreichend widerspiegelt und somit einen sicheren, reproduzierbaren und wissenschaftlich basierten Einsatz als Ersatzmethode für Toxizitätsprüfungen ermöglicht.

Die Biotransformation in den rekonstuierten Häuten im Vergleich zu Humanhaut *ex vivo* wurde anhand des Glucocorticoids Prednicarbat, ein Doppelester des antiinflammatorisch wirkenden Prednisolons [83, 96], sowie des Androgens Testosteron untersucht, der einem komplexen Metabolisierungsprozess, an dem zahlreiche Enzyme beteiligt sind, unterliegt.

Diese Substanzen werden dermal bzw. transdermal appliziert. Testosteron findet darüber hinaus als anerkannter OECD-Standard häufige Anwendung in Penetrationsstudien [28]. Zunächst wurde eine HPLC-Methode mit Corticosteron als interner Standard [224] zur Trennung sowie zur quantitativen Bestimmung von Testosteron und der entsprechenden Metabolite nach Extraktion aus den verschiedenen biologischen Matrices entwickelt und durch Ermittlung insbesondere der Retentionszeiten, der Auflösung, des Kapazitätsverhältnisses und des Trennfaktors als Maß für die Trennleistung sowie der Linearität und Inter-/Intraday-Variabilitäten hausintern validiert. Der Einsatz eines Radiodetektors ermöglichte eine Nachweisgrenze von 0.0075 MBq/ml (0,7 ng). Für die Testsubstanz Prednicarbat konnte eine bereits etablierte HPLC-UV/Vis-Methode verwendet werden [65, 95].

Die rekonstruierten Gewebe wurden histologisch hinsichtlich der Qualität nach Anlieferung sowie der Einfluss der experimentellen Bedingungen (wie Lösungsmittel, Konzentrationen, Inkubationsdauer) auf Qualität und Zellintegrität untersucht. Für das Epidermismodell sowie die rekonstriuerten Vollhautmodelle EpiDerm-FT und Phenion FT wurden keine Auffälligkeiten, die zu einem Ausschluss aus den Versuchen geführt hätten, festgestellt. Dagegen erfüllt ein Konstrukt (AST2000) aufgrund fehlender Barriereeigenschaften die Anforderungen an rekonstruierte Haut nicht. Es wurde daher von weiteren Versuchen ausgeschlossen.

Ein Vergleich unterschiedlicher Versuchsbedingungen ergab, dass der Einsatz in der Franz-Diffusions-Zelle, eine etablierte *in vitro* Methode zur Bestimmung der kutanen Absorption, einen erhöhten mechanischen Stress der Haut verursacht und somit aufgrund einer möglichen Enzymschädigung eine geringere Biotransformation mit sich zieht. Für den weiteren experimentellen Vergleich der Biotransformation wurde daher ein schonender Einsatz des humanen und rekonstruierten Hautmaterials im Gewebe-Einsatz durchgeführt.

Hinsichtlich der Esterhydrolyse ergab sich qualitatitv ein sehr ähnliches Profil der untersuchten rekonstruierten humanen Epidermis- und Vollhautmodelle gegenüber Humanhaut. Auffällig waren im Vergleich zur Humanhaut jedoch eine quantitativ erhöhte Esterhydrolyse sowie eine deutlich erhöhte Permeation beider Testsubstanzen, bzw. insbesondere der entsprechenden Metabolite, in das Rezeptormedium. Diese ist auf die bekannte geringer ausgeprägte Barrierefunktion rekonstruierter Haut zurückzuführen. Vergleicht man die Vollhautmodelle untereinander, sind sowohl das Ausmaß der hydrolytischen Prednicarbat-Biotransformation als auch der Permeation sehr ähnlich. Die unwesentlich geringere Biotransformation in der rekonstruierten Epidermis gegenüber den Vollhautmodellen demonstriert die wesentliche Beteiligung der Keratinozyten an der Esterhydrolyse.

Die rekonstruierten Hautmodelle weisen auch für Testosteron ein gegenüber Humanhaut sowie untereinander ein vergleichbares Metabolitenprofil auf, wobei jedoch quantitative Unterschiede (hauptsächlich in der Bildung der Metabolite Estradiol und Dihydrotestosteron), die sich im Wesentlichen auf bekannte Einflussfaktoren wie Kulturbedingungen des biologischen Materials und Differenzierungsgrade zurückführen lassen, beobachtet wurden.

Aufgrund der bekannten Unterschiede in der Enzymausstattung und -aktivität kutaner Zellen wurde die Biotransformation der Testsubstanzen zusätzlich in Monolayer-Kulturen dermaler Zellen (NHK/NHDF) untersucht. Es konnte bestätigt werden, dass die Esterase-Aktivität epidermaler Keratinozyten wesentlich ausgeprägter ist als die der humanen dermalen Fibroblasten [95]. Darüber hinaus wurde, um die Kenntnisse der dermalen Prednicarbatumwandlung abzurunden, erstmals die Biotransformation in der immortalisierten Keratinozyten-Zelllinie (HaCaT) untersucht. Es zeigte sich, dass die Esterase-Aktivität dieser Zelllinie mit der normaler humaner Keratinozyten nahezu vergleichbar ist, jedoch ein 50%-iger Umsatz bereits in kürzerer Zeit erfolgte.
Bezüglich der Biotransformation von Testosteron zeigte sich erwartungsgemäß [116] ein umgekehrtes Bild; hier konnte eine deutlich erhöhte Biotransformation nach Inkubation der dermalen Zellen (NHDF) bestätigt werden.
Auch für Testosteron konnten durch die Ergebnisse der Monolayerkulturen und der rekonstruierten Epidermis im Vergleich zur rekonstruierten Vollhaut die Unterschiede der Biotransformation von Testosteron in Epidermis und Dermis mit stärkerer Beteiligung des dermalen Hautkompartiments bestätigt werden. Es konnte ebenfalls bestätigt werden, dass der Differenzierungsgrad einen erheblichen Einfluss auf die CYP-Aktivität ausübt, da CYP-abhängige Biotransformationen in der Haut bzw. den Hautmodellen im Vergleich zur undifferenzierten Zellkultur deutlich erhöht waren. Dies stimmt mit Genexpressionuntersuchungen in Monolayerkulturen und Haut bzw. rekonstruierten Hautmodellen mit dem Ergebnis einer zunehmenden Genexpression bei höherem Differenzierungsgrad überein.
Auch der Einfluss der Kryokonservierung hinsichtlich der Biotransformationseigenschaften des Hautmaterials (Humanhaut *ex vivo*) wurde untersucht. Hinsichtlich der Esterase-Aktivität konnte eine Stabilisierung durch den Einfrierprozess über einen Zeitraum von bis zu drei Monaten gezeigt werden, wohingegen eine nahezu vollständige Degradierung der androgen-transformierenden Enzyme festgestellt wurde. Somit ist die Viabilität der Haut eine wichtige Voraussetzung für die Mehrheit dermaler Enzyme des Fremdstoffwechsels.
Bezüglich der Esterhydrolyse konnten keine geschlechtsspezifischen Unterschiede hinsichtlich der dermalen Biotransformationsleistung festgestellt werden. Dies macht die Untersuchung von (Ester-) Prodrugs einfacher, da ein geschlechtsspezifischer Unterschied hinsichtlich der Biotransformationsergebnisse ausgeschlossen werden kann. Des Weiteren

konnte mit Hilfe von Enzyminhibitionsversuchen gezeigt werden, dass an der Esterhydrolyse des Doppelesters neben Carboxylesterasen hauptsächlich unspezifische Serinesterasen beteilgt sind.

Zusammenfassend konnte hiermit durch den direkten Vergleich der Biotransformationsleistung rekonstruierter Epidermis- bzw. Vollhautmodelle mit humaner Haut *ex vivo* gezeigt werden, dass die untersuchten Hautmodelle für beide Testsubstanzen ein mit der humanen Haut vergleichbares Biotransformations- und enzymexpressionsprofil aufweisen und somit - nach hinreichender Validierung - als *in vitro*-Testmatrix zur Arzneistoffentwicklung, insbesondere in der präklinischen Phase, und Toxizitätsprüfung geeignet scheinen. Es ist jedoch zu berücksichtigen, dass aufgrund der verminderten Barrierefunktion dieser Testmatrices eine erhöhte und beschleunigte Penetration applizierter Substanzen in die Haut erfolgt und somit das Ausmaß der Biotransformation im Vergleich zu exzidierter Humanhaut erhöht ist.

7 References

7 References

1. Walters, K.A., *Dermatological and Transdermal Formulations, Drugs and the Pharmaceutical Sciences.* Marcel Dekker Inc., New York, 2002.
2. Merk, H.F., et al., *Molecular pathways in dermatotoxicology.* Toxicol Appl Pharmacol, 2004. **195**(3): p. 267-77.
3. Tur, E., *Physiology of the skin--differences between women and men.* Clin Dermatol, 1997. **15**(1): p. 5-16.
4. Simpson, C.L., D.M. Patel, and K.J. Green, *Deconstructing the skin: cytoarchitectural determinants of epidermal morphogenesis.* Nat Rev Mol Cell Biol, 2011. **12**(9): p. 565-80.
5. Bouwstra, J.A. and M. Ponec, *The skin barrier in healthy and diseased state.* Biochim Biophys Acta, 2006. **1758**(12): p. 2080-95.
6. Fritsch, P., *Dermatologie, Venerologie.* Verlag Springer 2003. **3. Auflage**.
7. Bouwstra, J.A., et al., *Structure of the skin barrier and its modulation by vesicular formulations.* Prog Lipid Res, 2003. **42**(1): p. 1-36.
8. Schreiner, V., et al., *Barrier characteristics of different human skin types investigated with X-ray diffraction, lipid analysis, and electron microscopy imaging.* J Invest Dermatol, 2000. **114**(4): p. 654-60.
9. Bouwstra, J.A. and P.L. Honeywell-Nguyen, *Skin structure and mode of action of vesicles.* Adv Drug Deliv Rev, 2002. **54 Suppl 1**: p. S41-55.
10. Gysler, A., et al., *Skin penetration and metabolism of topical glucocorticoids in reconstructed epidermis and in excised human skin.* Pharm Res, 1999. **16**(9): p. 1386-91.
11. Zouboulis, C.C., *Acne and sebaceous gland function.* Clin Dermatol, 2004. **22**(5): p. 360-6.
12. Pochi, P.E. and J.S. Strauss, *Endocrinologic control of the development and activity of the human sebaceous gland.* J Invest Dermatol, 1974. **62**(3): p. 191-201.
13. Jacobi, U., et al., *Gender-related differences in the physiology of the stratum corneum.* Dermatology, 2005. **211**(4): p. 312-7.
14. Ohman, H. and A. Vahlquist, *In vivo studies concerning a pH gradient in human stratum corneum and upper epidermis.* Acta Derm Venereol, 1994. **74**(5): p. 375-9.
15. Van Gele, M., et al., *Three-dimensional skin models as tools for transdermal drug delivery: challenges and limitations.* Expert Opin Drug Deliv, 2011. **8**(6): p. 705-20.
16. Moser, K., et al., *Passive skin penetration enhancement and its quantification in vitro.* Eur J Pharm Biopharm, 2001. **52**(2): p. 103-12.
17. Lademann, J.O., N.; Richter, H.; Jacobi, U.; Schaefer, H.; Blume-Peytavi, U.; Sterry, W., *Follikuläre Penetration- Ein entscheidender Penetrationsweg von topische applizierten Substanzen.* Haut 2003, 2003. **54**: p. 321-323.
18. Farahmand, S. and H.I. Maibach, *Estimating skin permeability from physicochemical characteristics of drugs: a comparison between conventional models and an in vivo-based approach.* Int J Pharm, 2009. **375**(1-2): p. 41-7.
19. Williams, A.C., *Transdermal and Topical Drug Delivery*2003: Pharmaceutical Press.
20. Barry, B.W., *Drug delivery routes in skin: a novel approach.* Adv Drug Deliv Rev, 2002. **54 Suppl 1**: p. S31-40.
21. Ghafourian, T., et al., *Validated models for predicting skin penetration from different vehicles.* Eur J Pharm Sci, 2010. **41**(5): p. 612-6.
22. Magnusson, B.M., et al., *Molecular size as the main determinant of solute maximum flux across the skin.* J Invest Dermatol, 2004. **122**(4): p. 993-9.
23. Magnusson, B.M., W.J. Pugh, and M.S. Roberts, *Simple rules defining the potential of compounds for transdermal delivery or toxicity.* Pharm Res, 2004. **21**(6): p. 1047-54.
24. Storm, J.E., et al., *Metabolism of xenobiotics during percutaneous penetration: role of absorption rate and cutaneous enzyme activity.* Fundam Appl Toxicol, 1990. **15**(1): p. 132-41.

25. Patil, S., et al., *Epidermal enzymes as penetration enhancers in transdermal drug delivery?* J Pharm Sci, 1996. **85**(3): p. 249-52.
26. Baron, J.M. and H.F. Merk, *Drug metabolism in the skin.* Curr Opin Allergy Clin Immunol, 2001. **1**(4): p. 287-91.
27. OECD, *Guideline 404 for testing of chemicals. Adopted on 22th April 2002.*
28. OECD, *Test Guideline 428: Skin absorption: In vitro Method. Adopted on 13th April 2004*.
29. OECD, *Guidance Document No. 28 for the conduct of skin absorption studies. Adopted at 35th Joint Meeting August 2003.*
30. Ackermann, K., et al., *The Phenion full-thickness skin model for percutaneous absorption testing.* Skin Pharmacol Physiol, 2010. **23**(2): p. 105-12.
31. Schmook, F.P., J.G. Meingassner, and A. Billich, *Comparison of human skin or epidermis models with human and animal skin in in-vitro percutaneous absorption.* Int J Pharm, 2001. **215**(1-2): p. 51-6.
32. Schreiber, S., et al., *Reconstructed epidermis versus human and animal skin in skin absorption studies.* Toxicol In Vitro, 2005. **19**(6): p. 813-22.
33. Kao, J., F.K. Patterson, and J. Hall, *Skin penetration and metabolism of topically applied chemicals in six mammalian species, including man: an in vitro study with benzo[a]pyrene and testosterone.* Toxicol Appl Pharmacol, 1985. **81**(3 Pt 1): p. 502-16.
34. Godin, B. and E. Touitou, *Transdermal skin delivery: predictions for humans from in vivo, ex vivo and animal models.* Adv Drug Deliv Rev, 2007. **59**(11): p. 1152-61.
35. Schäfer-Korting, M., et al., *The use of reconstructed human epidermis for skin absorption testing: Results of the validation study.* Altern Lab Anim, 2008. **36**(2): p. 161-87.
36. Kandarova, H., et al., *Assessment of the human epidermis model SkinEthic RHE for in vitro skin corrosion testing of chemicals according to new OECD TG 431.* Toxicol In Vitro, 2006. **20**(5): p. 547-59.
37. Liebsch, M. and H. Spielmann, *Currently available in vitro methods used in the regulatory toxicology.* Toxicol Lett, 2002. **127**(1-3): p. 127-34.
38. Bell, E., et al., *The reconstitution of living skin.* J Invest Dermatol, 1983. **81**(1 Suppl): p. 2s-10s.
39. Parenteau, N.L., et al., *Epidermis generated in vitro: practical considerations and applications.* J Cell Biochem, 1991. **45**(3): p. 245-51.
40. Ponec, M., *Skin constructs for replacement of skin tissues for in vitro testing.* Adv Drug Deliv Rev, 2002. **54 Suppl 1**: p. S19-30.
41. Ponec, M., et al., *Characterization of reconstructed skin models.* Skin Pharmacol Appl Skin Physiol, 2002. **15 Suppl 1**: p. 4-17.
42. Netzlaff, F., et al., *The human epidermis models EpiSkin, SkinEthic and EpiDerm: an evaluation of morphology and their suitability for testing phototoxicity, irritancy, corrosivity, and substance transport.* Eur J Pharm Biopharm, 2005. **60**(2): p. 167-78.
43. Schäfer-Korting, M., et al., *Reconstructed human epidermis for skin absorption testing: results of the German prevalidation study.* Altern Lab Anim, 2006. **34**(3): p. 283-94.
44. Hu, T., et al., *Xenobiotic metabolism gene expression in the EpiDermin vitro 3D human epidermis model compared to human skin.* Toxicol In Vitro, 2010. **24**(5): p. 1450-63.
45. Luu-The, V., et al., *Steroid metabolism and profile of steroidogenic gene expression in Episkin: high similarity with human epidermis.* J Steroid Biochem Mol Biol, 2007. **107**(1-2): p. 30-6.
46. Götz, C., et al., *Xenobiotic metabolism capacities of human skin in comparison with a 3D-epidermis model and keratinocyte-based cell culture as in vitro alternatives for chemical testing: phase II enzymes.* Exp Dermatol, 2012. **21**(5): p. 364-9.
47. Götz, C., et al., *Xenobiotic metabolism capacities of human skin in comparison with a 3D epidermis model and keratinocyte-based cell culture as in vitro alternatives for chemical testing: activating enzymes (Phase I).* Exp Dermatol, 2012. **21**(5): p. 358-63.

48. Luu-The, V., et al., *Expression profiles of phases 1 and 2 metabolizing enzymes in human skin and the reconstructed skin models Episkin and full thickness model from Episkin.* J Steroid Biochem Mol Biol, 2009. **116**(3-5): p. 178-86.
49. Neis, M.M., et al., *Expression and induction of cytochrome p450 isoenzymes in human skin equivalents.* Skin Pharmacol Physiol, 2010. **23**(1): p. 29-39.
50. Bando, H., et al., *Effects of skin metabolism on percutaneous penetration of lipophilic drugs.* J Pharm Sci, 1997. **86**(6): p. 759-61.
51. Kubota, K., J. Ademola, and H.I. Maibach, *Metabolism of topical drugs within the skin, in particular glucocorticoids.* Curr Probl Dermatol, 1993. **21**: p. 61-6.
52. Kubota, K., J. Ademola, and H.I. Maibach, *Simultaneous diffusion and metabolism of betamethasone 17-valerate in the living skin equivalent.* J Pharm Sci, 1995. **84**(12): p. 1478-81.
53. Svensson, C.K., *Biotransformation of drugs in human skin.* Drug Metab Dispos, 2009. **37**(2): p. 247-53.
54. Jäckh, C., et al., *Characterization of enzyme activities of Cytochrome P450 enzymes, Flavin-dependent monooxygenases, N-acetyltransferases and UDP-glucuronyltransferases in human reconstructed epidermis and full-thickness skin models.* Toxicol In Vitro, 2011. **25**(6): p. 1209-14.
55. Küchler, S., et al., *Hallmarks of atopic skin mimicked in vitro by means of a skin disease model based on FLG knock-down.* Altern Lab Anim, 2011. **39**(5): p. 471-80.
56. Roguet, R. and H. Schaefer, *Overview of in vitro cell culture technologies and pharmaco-toxicological applications.* Toxicol In Vitro, 1997. **11**(5): p. 591-9.
57. Netzlaff, F., et al., *Permeability of the reconstructed human epidermis model Episkin in comparison to various human skin preparations.* Eur J Pharm Biopharm, 2007. **66**(1): p. 127-34.
58. OECD, *Draft proposal Test Guideline 439: In vitro skin irritation: Reconstructed human epidermal test method. Adopted 2010*
59. Eskes, C., et al., *The ECVAM international validation study on in vitro tests for acute skin irritation: selection of test chemicals.* Altern Lab Anim, 2007. **35**(6): p. 603-19.
60. Gerner, I., M. Liebsch, and H. Spielmann, *Assessment of the eye irritating properties of chemicals by applying alternatives to the Draize rabbit eye test: the use of QSARs and in vitro tests for the classification of eye irritation.* Altern Lab Anim, 2005. **33**(3): p. 215-37.
61. OECD, *Test Guideline 432: In vitro 3T3 NRU phototoxicity test. Adopted on 13th April 2004.*
62. Ackermann, K., et al., *The Phenion full-thickness skin model for percutaneous absorption testing.* Skin Pharmacol Physiol, 2010. **23**(2): p. 105-12.
63. Schäfer-Korting, M., et al., *Reconstructed epidermis and full-thickness skin for absorption testing: influence of the vehicles used on steroid permeation.* Altern Lab Anim, 2008. **36**(4): p. 441-52.
64. Gregoire, S., et al., *Improvement of the experimental setup for skin absorption screening studies with reconstructed skin EPISKIN.* Skin Pharmacol Physiol, 2008. **21**(2): p. 89-97.
65. Lombardi Borgia, S., et al., *In vitro skin absorption and drug release - a comparison of six commercial prednicarbate preparations for topical use.* Eur J Pharm Biopharm, 2008. **68**(2): p. 380-9.
66. Santos Maia, C., et al., *Drug targeting by solid lipid nanoparticles for dermal use.* J Drug Target, 2002. **10**(6): p. 489-95.
67. Hagvall, L., et al., *Cytochrome P450-mediated activation of the fragrance compound geraniol forms potent contact allergens.* Toxicol Appl Pharmacol, 2008. **233**(2): p. 308-13.
68. Samuelsson, K., et al., *Diphenylthiourea, a common rubber chemical, is bioactivated to potent skin sensitizers.* Chem Res Toxicol, 2011. **24**(1): p. 35-44.
69. Ott, H., et al., *Cutaneous metabolic activation of carvoxime, a self-activating, skin-sensitizing prohapten.* Chem Res Toxicol, 2009. **22**(2): p. 399-405.

70. Hu, T., et al., *Dermal penetration and metabolism of p-aminophenol and p-phenylenediamine: application of the EpiDerm human reconstructed epidermis model.* Toxicol Lett, 2009. **188**(2): p. 119-29.
71. Mewes, K.R., et al., *Elastin expression in a newly developed full-thickness skin equivalent.* Skin Pharmacol Physiol, 2007. **20**(2): p. 85-95.
72. Ponec, M., et al., *Lipid and ultrastructural characterization of reconstructed skin models.* Int J Pharm, 2000. **203**(1-2): p. 211-25.
73. Kuijpers, A.L., et al., *Skin-derived antileukoproteinase (SKALP) and epidermal fatty acid-binding protein (E-FABP): two novel markers of the psoriatic phenotype that respond differentially to topical steroid.* Acta Derm Venereol, 1997. **77**(1): p. 14-9.
74. Pannatier, A., et al., *The skin as a drug-metabolizing organ.* Drug Metab Rev, 1978. **8**(2): p. 319-43.
75. Oesch, F., et al., *Drug-metabolizing enzymes in the skin of man, rat, and pig.* Drug Metab Rev, 2007. **39**(4): p. 659-98.
76. Beydon, D., J.P. Payan, and M.C. Grandclaude, *Comparison of percutaneous absorption and metabolism of di-n-butylphthalate in various species.* Toxicol In Vitro, 2010. **24**(1): p. 71-8.
77. Zouboulis, C.C., *Human skin: an independent peripheral endocrine organ.* Horm Res, 2000. **54**(5-6): p. 230-42.
78. Swanson, H.I., *Cytochrome P450 expression in human keratinocytes: an aryl hydrocarbon receptor perspective.* Chem Biol Interact, 2004. **149**(2-3): p. 69-79.
79. Baron, J.M., et al., *Expression of multiple cytochrome p450 enzymes and multidrug resistance-associated transport proteins in human skin keratinocytes.* J Invest Dermatol, 2001. **116**(4): p. 541-8.
80. Sugibayashi, K., T. Hayashi, and Y. Morimoto, *Simultaneous transport and metabolism of ethyl nicotinate in hairless rat skin after its topical application: the effect of enzyme distribution in skin.* J Control Release, 1999. **62**(1-2): p. 201-8.
81. Gysler, A., et al., *Skin penetration and metabolism of topical glucocorticoids in reconstructed epidermis and in excised human skin.* Pharm Res, 1999. **16**(9): p. 1386-91.
82. Lange, K., et al., *Cutaneous inflammation and proliferation in vitro: differential effects and mode of action of topical glucocorticoids.* Skin Pharmacol Appl Skin Physiol, 2000. **13**(2): p. 93-103.
83. Schäfer-Korting, M., et al., *Glucocorticoids for human skin: new aspects of the mechanism of action.* Skin Pharmacol Physiol, 2005. **18**(3): p. 103-14.
84. Schäfer-Korting, M., et al., *Prednicarbate activity and benefit/risk ratio in relation to other topical glucocorticoids.* Clin Pharmacol Ther, 1993. **54**(4): p. 448-56.
85. Wohlrab, J., et al., *Hydrocortisone aceponate activity and benefit/risk ratio in relation to reference topical glucocorticoids.* Skin Pharmacol Physiol, 2010. **23**(4): p. 177-82.
86. Imai, T., et al., *Substrate specificity of carboxylesterase isozymes and their contribution to hydrolase activity in human liver and small intestine.* Drug Metab Dispos, 2006. **34**(10): p. 1734-41.
87. Zhang, W., G. Xu, and H.L. McLeod, *Comprehensive evaluation of carboxylesterase-2 expression in normal human tissues using tissue array analysis.* Appl Immunohistochem Mol Morphol, 2002. **10**(4): p. 374-80.
88. Hosokawa, M., *Structure and catalytic properties of carboxylesterase isozymes involved in metabolic activation of prodrugs.* Molecules, 2008. **13**(2): p. 412-31.
89. Hicks, L.D., et al., *Analysis of the inhibition of mammalian carboxylesterases by novel fluorobenzoins and fluorobenzils.* Bioorg Med Chem, 2007. **15**(11): p. 3801-17.
90. Kitano, Y., *Hydrolysis of hydrocortisone 17-butyrate 21-propionate by cultured human keratinocytes.* Acta Derm Venereol, 1986. **66**(2): p. 98-102.
91. Herrmann, W.P. and J. Habbig, *Immunological demonstration of multiple esterases in human eccrine sweat.* Br J Dermatol, 1976. **95**(1): p. 67-70.
92. Zhu, Q.G., et al., *Stereoselective characteristics and mechanisms of epidermal carboxylesterase metabolism observed in HaCaT keratinocytes.* Biol Pharm Bull, 2007. **30**(3): p. 532-6.

93. Bätz, F., *Vergleich der kutanen Expression von Esterasen in rekonstruierter humaner Vollhaut bzw. Epidermis und Humanhaut ex vivo*, 2013: Dissertation Freie Universität Berlin.
94. Prusakiewicz, J.J., C. Ackermann, and R. Voorman, *Comparison of skin esterase activities from different species.* Pharm Res, 2006. **23**(7): p. 1517-24.
95. Gysler, A., et al., *Prednicarbate biotransformation in human foreskin keratinocytes and fibroblasts.* Pharm Res, 1997. **14**(6): p. 793-7.
96. Schackert, C., H.C. Korting, and M. Schäfer-Korting, *Qualitative and quantitative assessment of the benefit-risk ratio of medium potency topical corticosteroids in vitro and in vivo: characterisation of drugs with an increased benefit-risk ratio.* BioDrugs, 2000. **13**(4): p. 267-77.
97. Schäfer-Korting, M., Schmid, M.-H. and Korting, H.C., *Drug Safety.* 1996. **14**: p. 375-385.
98. Gupta, A.K. and M. Chow, *Prednicarbate (Dermatop): profile of a corticosteroid.* J Cutan Med Surg, 2004. **8**(4): p. 244-7.
99. Chen, W., D. Thiboutot, and C.C. Zouboulis, *Cutaneous androgen metabolism: basic research and clinical perspectives.* J Invest Dermatol, 2002. **119**(5): p. 992-1007.
100. Fritsch, M., C.E. Orfanos, and C.C. Zouboulis, *Sebocytes are the key regulators of androgen homeostasis in human skin.* J Invest Dermatol, 2001. **116**(5): p. 793-800.
101. Turgeon, D., et al., *Relative enzymatic activity, protein stability, and tissue distribution of human steroid-metabolizing UGT2B subfamily members.* Endocrinology, 2001. **142**(2): p. 778-87.
102. Zouboulis, C.C., et al., *Sexual hormones in human skin.* Horm Metab Res, 2007. **39**(2): p. 85-95.
103. Chen, W., et al., *Evidence of heterogeneity and quantitative differences of the type 1 5alpha-reductase expression in cultured human skin cells--evidence of its presence in melanocytes.* J Invest Dermatol, 1998. **110**(1): p. 84-9.
104. Thiboutot, D., et al., *Activity of 5-alpha-reductase and 17-beta-hydroxysteroid dehydrogenase in the infrainfundibulum of subjects with and without acne vulgaris.* Dermatology, 1998. **196**(1): p. 38-42.
105. Svenstrup, B., et al., *Comparison of the effect of cortisol on aromatase activity and androgen metabolism in two human fibroblast cell lines derived from the same individual.* J Steroid Biochem, 1990. **35**(6): p. 679-87.
106. Hughes, S.V., et al., *1,25-dihydroxyvitamin D3 regulates estrogen metabolism in cultured keratinocytes.* Endocrinology, 1997. **138**(9): p. 3711-8.
107. Rink, J.D., et al., *Cellular characterization of adipose tissue from various body sites of women.* J Clin Endocrinol Metab, 1996. **81**(7): p. 2443-7.
108. Katiyar, S.K., M.S. Matsui, and H. Mukhtar, *Ultraviolet-B exposure of human skin induces cytochromes P450 1A1 and 1B1.* J Invest Dermatol, 2000. **114**(2): p. 328-33.
109. Janmohamed, A., et al., *Quantification and cellular localization of expression in human skin of genes encoding flavin-containing monooxygenases and cytochromes P450.* Biochem Pharmacol, 2001. **62**(6): p. 777-86.
110. Saeki, M., et al., *mRNA expression of multiple cytochrome p450 isozymes in four types of cultured skin cells.* Int Arch Allergy Immunol, 2002. **127**(4): p. 333-6.
111. Sieben, S., et al., *Multiple cytochrome P450-isoenzymes mRNA are expressed in dendritic cells.* Int Arch Allergy Immunol, 1999. **118**(2-4): p. 358-61.
112. Sultan, C., et al., *[Metabolism of dihydrotestosterone in cultured skin fibroblasts: reduction to 5 alpha-androstane-3 alpha, 17 beta-diol].* C R Seances Soc Biol Fil, 1983. **177**(1): p. 83-92.
113. Küchler, S., et al., *3D-wound healing model: influence of morphine and solid lipid nanoparticles.* J Biotechnol, 2010. **148**(1): p. 24-30.
114. van Ingen, I.L., M.M. Jansen, and P. Barrera, *Topical opioids for painful ulcers in systemic sclerosis.* Ann Rheum Dis, 2008. **67**(3): p. 427.
115. Arver, S., et al., *Long-term efficacy and safety of a permeation-enhanced testosterone transdermal system in hypogonadal men.* Clin Endocrinol (Oxf), 1997. **47**(6): p. 727-37.

116. Münster, U., et al., *Testosterone metabolism in human skin cells in vitro and its interaction with estradiol and dutasteride.* Skin Pharmacol Appl Skin Physiol, 2003. **16**(6): p. 356-66.
117. Kaufman, K.D., *Androgen metabolism as it affects hair growth in androgenetic alopecia.* Dermatol Clin, 1996. **14**(4): p. 697-711.
118. Hikima, T., et al., *Comparison of skin distribution of hydrolytic activity for bioconversion of beta-estradiol 17-acetate between man and several animals in vitro.* Eur J Pharm Biopharm, 2002. **54**(2): p. 155-60.
119. Setlur, S.R., et al., *Genetic variation of genes involved in dihydrotestosterone metabolism and the risk of prostate cancer.* Cancer Epidemiol Biomarkers Prev, 2010. **19**(1): p. 229-39.
120. Zhao, Y., C.R. Mendelson, and E.R. Simpson, *Characterization of the sequences of the human CYP19 (aromatase) gene that mediate regulation by glucocorticoids in adipose stromal cells and fetal hepatocytes.* Mol Endocrinol, 1995. **9**(3): p. 340-9.
121. Cheung, C., et al., *Species variations in cutaneous alcohol dehydrogenases and aldehyde dehydrogenases may impact on toxicological assessments of alcohols and aldehydes.* Toxicology, 2003. **184**(2-3): p. 97-112.
122. Garrigue, J.L., et al., *In vitro genotoxicity of para-phenylenediamine and its N-monoacetyl or N,N'-diacetyl metabolites.* Mutat Res, 2006. **608**(1): p. 58-71.
123. Harris, I.R., et al., *Comparison of activities dependent on glutathione S-transferase and cytochrome P-450 IA1 in cultured keratinocytes and reconstructed epidermal models.* Skin Pharmacol Appl Skin Physiol, 2002. **15 Suppl 1**: p. 59-67.
124. Courchay, G., et al., *Messenger RNA expression of steroidogenesis enzyme subtypes in the human pilosebaceous unit.* Skin Pharmacol, 1996. **9**(3): p. 169-76.
125. Thiboutot, D., et al., *Androgen metabolism in sebaceous glands from subjects with and without acne.* Arch Dermatol, 1999. **135**(9): p. 1041-5.
126. Sawaya, M.E. and V.H. Price, *Different levels of 5alpha-reductase type I and II, aromatase, and androgen receptor in hair follicles of women and men with androgenetic alopecia.* J Invest Dermatol, 1997. **109**(3): p. 296-300.
127. Sawaya, M.E. and N.S. Penneys, *Immunohistochemical distribution of aromatase and 3B-hydroxysteroid dehydrogenase in human hair follicle and sebaceous gland.* J Cutan Pathol, 1992. **19**(4): p. 309-14.
128. Inoue, T., et al., *The role of estrogen-metabolizing enzymes and estrogen receptors in human epidermis.* Mol Cell Endocrinol, 2011. **344**(1-2): p. 35-40.
129. Ngawhirunpat, T., et al., *Age difference in simultaneous permeation and metabolism of ethyl nicotinate in rat skin.* Biol Pharm Bull, 2001. **24**(4): p. 414-7.
130. Swales, N.J., T. Johnson, and J. Caldwell, *Cryopreservation of rat and mouse hepatocytes. II. Assessment of metabolic capacity using testosterone metabolism.* Drug Metab Dispos, 1996. **24**(11): p. 1224-30.
131. Utesch, D., et al., *Characterization of cryopreserved rat liver parenchymal cells by metabolism of diagnostic substrates and activities of related enzymes.* Biochem Pharmacol, 1992. **44**(2): p. 309-15.
132. Ahmad, N., R. Agarwal, and H. Mukhtar, *Cytochrome P-450-dependent drug metabolism in skin.* Clin Dermatol, 1996. **14**(4): p. 407-15.
133. Du, L., et al., *Effects of the differentiated keratinocyte phenotype on expression levels of CYP1-4 family genes in human skin cells.* Toxicol Appl Pharmacol, 2006. **213**(2): p. 135-44.
134. Guo, J.F., et al., *Levels of cytochrome P-450-mediated aryl hydrocarbon hydroxylase (AHH) are higher in differentiated than in germinative cutaneous keratinocytes.* J Invest Dermatol, 1990. **94**(1): p. 86-93.
135. Mowszowicz, I., et al., *Testosterone 5 alpha-reductase activity of skin fibroblasts. Increase with serial subcultures.* Mol Cell Endocrinol, 1980. **17**(1): p. 41-50.
136. Gingras, S., et al., *Characterization and modulation of sex steroid metabolizing activity in normal human keratinocytes in primary culture and HaCaT cells.* J Steroid Biochem Mol Biol, 2003. **87**(2-3): p. 167-79.

137. Stillman, S.C., B.A. Evans, and I.A. Hughes, *Androgen dependent stimulation of aromatase activity in genital skin fibroblasts from normals and patients with androgen insensitivity.* Clin Endocrinol (Oxf), 1991. **35**(6): p. 533-8.
138. Haberland, A., et al., *Albumin effects on drug absorption and metabolism in reconstructed epidermis and excised pig skin.* ALTEX, 2003. **20**(1): p. 3-9.
139. Haberland, A., et al., *The impact of skin viability on drug metabolism and permeation -- BSA toxicity on primary keratinocytes.* Toxicol In Vitro, 2006. **20**(3): p. 347-54.
140. Sonoda, T., et al., *Testosterone metabolism by cultured human beard outer root sheath cells in comparison with epidermal keratinocytes.* J Dermatol Sci, 1993. **6**(3): p. 214-8.
141. Van Neste, D., et al., *Finasteride increases anagen hair in men with androgenetic alopecia.* Br J Dermatol, 2000. **143**(4): p. 804-10.
142. Dumont, M., et al., *Characterization, expression, and immunohistochemical localization of 3 beta-hydroxysteroid dehydrogenase/delta 5-delta 4 isomerase in human skin.* J Invest Dermatol, 1992. **99**(4): p. 415-21.
143. Sansone, G. and R.M. Reisner, *Differential rates of conversion of testosterone to dihydrotestosterone in acne and in normal human skin--a possible pathogenic factor in acne.* J Invest Dermatol, 1971. **56**(5): p. 366-72.
144. Jewell, C., et al., *Specificity of procaine and ester hydrolysis by human, minipig, and rat skin and liver.* Drug Metab Dispos, 2007. **35**(11): p. 2015-22.
145. Sloan, K.B., *Prodrug: Topical and Ocular Drug Delivery.* Marcel Dekker Inc., New York., 1992.
146. Kellner, H.M., et al., *[Pharmacokinetics and biotransformation following topical use of the local corticoid prednicarbate].* Z Hautkr, 1986. **61 Suppl 1**: p. 18-40.
147. Gysler, A., U. Konigsmann, and M. Schafer-Korting, *[Tridimensional skin models recording percutaneous absorption].* ALTEX, 1999. **16**(2): p. 67-72.
148. Barth, J., et al., *Studies on the pharmacokinetics and metabolism of prednicarbate after cutaneous and oral administration.* Skin Pharmacol, 1993. **6**(3): p. 179-86.
149. Tojo, K., K. Yamada, and T. Hikima, *Diffusion and metabolism of prednisolone farnesylate in viable skin of the hairless mouse.* Pharm Res, 1994. **11**(3): p. 393-7.
150. Boogaard, P.J., et al., *Metabolic inactivation of 2-oxiranylmethyl 2-ethyl-2,5-dimethylhexanoate (C10GE) in skin, lung and liver of human, rat and mouse.* Xenobiotica, 1999. **29**(10): p. 987-1006.
151. Kao, J. and J. Hall, *Skin absorption and cutaneous first pass metabolism of topical steroids: in vitro studies with mouse skin in organ culture.* J Pharmacol Exp Ther, 1987. **241**(2): p. 482-7.
152. Rolsted, K., et al., *Evaluation of cytochrome P450 activity in vitro, using dermal and hepatic microsomes from four species and two keratinocyte cell lines in culture.* Arch Dermatol Res, 2008. **300**(1): p. 11-8.
153. Luu-The, V., *Analysis and characteristics of multiple types of human 17beta-hydroxysteroid dehydrogenase.* J Steroid Biochem Mol Biol, 2001. **76**(1-5): p. 143-51.
154. Steinsträsser, I. and H.P. Merkle, *Dermal metabolism of topically applied drugs: pathways and models reconsidered.* Pharm Acta Helv, 1995. **70**(1): p. 3-24.
155. Hueber, F., et al., *Percutaneous absorption of estradiol and progesterone in normal and appendage-free skin of the hairless rat: lack of importance of nutritional blood flow.* Skin Pharmacol, 1994. **7**(5): p. 245-56.
156. Scott, R.C., M. Walker, and P.H. Dugard, *A comparison of the in vitro permeability properties of human and some laboratory animal skins.* Int J Cosmet Sci, 1986. **8**(4): p. 189-94.
157. Scott, R.C., et al., *Further validation of an in vitro method to reduce the need for in vivo studies for measuring the absorption of chemicals through rat skin.* Fundam Appl Toxicol, 1992. **19**(4): p. 484-92.
158. Barbero, A.M. and H.F. Frasch, *Pig and guinea pig skin as surrogates for human in vitro penetration studies: a quantitative review.* Toxicol In Vitro, 2009. **23**(1): p. 1-13.
159. Jacobi, U., et al., *Porcine ear skin: an in vitro model for human skin.* Skin Res Technol, 2007. **13**(1): p. 19-24.

160. Baynes, R.E., K.B. Halling, and J.E. Riviere, *The influence of diethyl-m-toluamide (DEET) on the percutaneous absorption of permethrin and carbaryl.* Toxicol Appl Pharmacol, 1997. **144**(2): p. 332-9.
161. Schlupp, P., et al., *Drug release and skin penetration from solid lipid nanoparticles and a base cream: a systematic approach from a comparison of three glucocorticoids.* Skin Pharmacol Physiol, 2011. **24**(4): p. 199-209.
162. Mitriaikina, S. and C.C. Müller-Goymann, *Comparative permeation studies of nondiluted and diluted betamethasone-17-valerate semisolid formulations through isolated human stratum corneum and artificial skin construct.* Skin Pharmacol Physiol, 2009. **22**(3): p. 142-50.
163. Hammell, D.C., et al., *Bioconversion of naltrexone and its 3-O-alkyl-ester prodrugs in a human skin equivalent.* J Pharm Sci, 2005. **94**(4): p. 828-36.
164. Weindl, G., F. Castello, and M. Schäfer-Korting, *Evaluation of anti-inflammatory and atrophogenic effects of glucocorticoids on reconstructed human skin.* Altern Lab Anim, 2011. **39**(2): p. 173-87.
165. Varani, J., et al., *All-trans retinoic acid and extracellular Ca2+ differentially influence extracellular matrix production by human skin in organ culture.* Am J Pathol, 1993. **142**(6): p. 1813-22.
166. Baltes, M.R., J.G. Dubois, and M. Hanocq, *Ethyl acetate extraction procedure and isocratic high-performance liquid chromatographic assay for testosterone metabolites in cell microsomes.* J Chromatogr B Biomed Sci Appl, 1998. **706**(2): p. 201-7.
167. U.S. Department of Health and Human Services, F.a.D.A., *Guidance for Industry, Bioanalytical Method Validation* 2001.
168. (ICH), I.C.o.H., *Validation of Analytical Methods: Methodology. ICH Q2 B*, 1996.
169. Shah, V.P., et al., *Bioanalytical method validation--a revisit with a decade of progress.* Pharm Res, 2000. **17**(12): p. 1551-7.
170. OECD, *Test Guideline 431: In vitro skin corrosion: Human Skin Model Test. Adopted on 13th April 2004*.
171. Brinkmann, I. and C. Müller-Goymann, *Prednicarbate permeation through artificial skin construct from different formulations and their dilutions*, in *Inernational Meeting on Pharmaceutics, Biopharmaceutics and Pharmaceutical Technology*, B. Proc Int Meeting Pharm, Pharm Tech, Editor 2004: Nuremberg.
172. Beisson, F., et al., *Use of the tape stripping technique for directly quantifying esterase activities in human stratum corneum.* Anal Biochem, 2001. **290**(2): p. 179-85.
173. Luu-The, V., *Assessment of steroidogenesis and steroidogenic enzyme functions.* J Steroid Biochem Mol Biol, 2013.
174. Yengi, L.G., et al., *Quantitation of cytochrome P450 mRNA levels in human skin.* Anal Biochem, 2003. **316**(1): p. 103-10.
175. OECD, *Test Guideline 431: In vitro skin corrosion: Human Skin Model Test.* Adopted on 13th April 2004, 431.
176. OECD, *Draft Proposal Test Guideline 439: In vitro skin irritation: Reconstructed human epidermis test method. .* Adopted 2010, 439.
177. Lavergne, S.N., B.K. Park, and D.J. Naisbitt, *The roles of drug metabolism in the pathogenesis of T-cell-mediated drug hypersensitivity.* Curr Opin Allergy Clin Immunol, 2008. **8**(4): p. 299-307.
178. Andreu, I., C. Mayorga, and M.A. Miranda, *Metabolomics in drug intolerance.* Curr Drug Metab, 2009. **10**(9): p. 947-55.
179. Sanwald, P., et al., *Isocratic high-performance liquid chromatographic method for the separation of testosterone metabolites.* J Chromatogr B Biomed Appl, 1995. **672**(2): p. 207-15.
180. Li, H. and R.J. Letcher, *A high-performance-liquid-chromatography-based method for the determination of hydroxylated testosterone metabolites formed in vitro in liver microsomes from gray seal (Halichoerus grypus).* J Chromatogr Sci, 2002. **40**(7): p. 397-402.

181. Schoepe, S., *Investigations of in vitro Test Systems for the Detection of Glucocorticoid-induced Skin Atrophy as a Tool in Drug Discovery*, 2009: Dissertation Freie Universität Berlin.
182. Simonsen, L. and A. Fullerton, *Development of an in vitro skin permeation model simulating atopic dermatitis skin for the evaluation of dermatological products.* Skin Pharmacol Physiol, 2007. **20**(5): p. 230-6.
183. Page, M., et al., *Optimization of the tetrazolium-based colorimetric assay for the measurement of cell number and cytotoxicity.* Int J Immunopharmacol, 1988. **10**(7): p. 785-93.
184. Coquette, A., et al., *Analysis of interleukin-1alpha (IL-1alpha) and interleukin-8 (IL-8) expression and release in in vitro reconstructed human epidermis for the prediction of in vivo skin irritation and/or sensitization.* Toxicol In Vitro, 2003. **17**(3): p. 311-21.
185. Medina, J., et al., *Assessment of the phototoxic potential of compounds and finished topical products using a human reconstructed epidermis.* In Vitr Mol Toxicol, 2001. **14**(3): p. 157-68.
186. de Brugerolle de, F., et al., *Predictivity of an in vitro model for acute and chronic skin irritation (SkinEthic) applied to the testing of topical vehicles.* Cell Biol Toxicol, 1999. **15**(2): p. 121-35.
187. van de Sandt, J.J., et al., *In vitro predictions of skin absorption of caffeine, testosterone, and benzoic acid: a multi-centre comparison study.* Regul Toxicol Pharmacol, 2004. **39**(3): p. 271-81.
188. Wagner, H., et al., *Drug distribution in human skin using two different in vitro test systems: comparison with in vivo data.* Pharm Res, 2000. **17**(12): p. 1475-81.
189. OECD, *Test Guideline 428: Skin absorption: in vitro Method.* Adopted on 13th April 2004, 428.
190. Wagner, H., et al., *Effects of various vehicles on the penetration of flufenamic acid into human skin.* Eur J Pharm Biopharm, 2004. **58**(1): p. 121-9.
191. Schoepe, S., et al., *Identification of novel in vitro test systems for the determination of glucocorticoid receptor ligand-induced skin atrophy.* Skin Pharmacol Physiol, 2010. **23**(3): p. 139-51.
192. Zöller, N.N., et al., *Evaluation of beneficial and adverse effects of glucocorticoids on a newly developed full-thickness skin model.* Toxicol In Vitro, 2008. **22**(3): p. 747-59.
193. Sugibayashi, K., et al., *Utility of a three-dimensional cultured human skin model as a tool to evaluate the simultaneous diffusion and metabolism of ethyl nicotinate in skin.* Drug Metab Pharmacokinet, 2004. **19**(5): p. 352-62.
194. Bouwstra, J.A., et al., *Characterization of stratum corneum structure in reconstructed epidermis by X-ray diffraction.* J Lipid Res, 1995. **36**(3): p. 496-504.
195. Bätz, F.M., et al., *Esterase activity in excised and reconstructed human skin - Biotransformation of prednicarbate and the model dye fluorescein diacetate.* Eur J Pharm Biopharm, 2013. **84**(2): p. 374-85.
196. Bonifas, J., et al., *Evaluation of cytochrome P450 1 (CYP1) and N-acetyltransferase 1 (NAT1) activities in HaCaT cells: implications for the development of in vitro techniques for predictive testing of contact sensitizers.* Toxicol In Vitro, 2010. **24**(3): p. 973-80.
197. Boukamp, P., et al., *Sustained nontumorigenic phenotype correlates with a largely stable chromosome content during long-term culture of the human keratinocyte line HaCaT.* Genes Chromosomes Cancer, 1997. **19**(4): p. 201-14.
198. Thiboutot, D., et al., *Activity of the type 1 5 alpha-reductase exhibits regional differences in isolated sebaceous glands and whole skin.* J Invest Dermatol, 1995. **105**(2): p. 209-14.
199. Bernard, F.X., et al., *Expression of type 1 5alpha-reductase and metabolism of testosterone in reconstructed human epidermis (SkinEthic(R)): a new model for screening skin-targeted androgen modulators.* Int J Cosmet Sci, 2000. **22**(6): p. 397-407.

200. Luu-The, V., et al., *Characterization, expression, and immunohistochemical localization of 5 alpha-reductase in human skin.* J Invest Dermatol, 1994. **102**(2): p. 221-6.
201. Eicheler, W., et al., *Immunohistochemical evidence for differential distribution of 5 alpha-reductase isoenzymes in human skin.* Br J Dermatol, 1995. **133**(3): p. 371-6.
202. Du, L., et al., *Differentiation-specific factors modulate epidermal CYP1-4 gene expression in human skin in response to retinoic acid and classic aryl hydrocarbon receptor ligands.* J Pharmacol Exp Ther, 2006. **319**(3): p. 1162-71.
203. Maudelonde, T., et al., *Studies of androgen metabolism and action in cultured hair and skin cells.* J Steroid Biochem, 1986. **24**(5): p. 1053-60.
204. Belanger, A., et al., *Inactivation of androgens by UDP-glucuronosyltransferase enzymes in humans.* Trends Endocrinol Metab, 2003. **14**(10): p. 473-9.
205. Brinkmann, J., et al., *Metabolically competent human skin models: activation and genotoxicity of benzo[a]pyrene.* Toxicol Sci, 2013. **131**(2): p. 351-9.
206. Bronaugh, R.L., R.F. Stewart, and M. Simon, *Methods for in vitro percutaneous absorption studies. VII: Use of excised human skin.* J Pharm Sci, 1986. **75**(11): p. 1094-7.
207. Harrison, S.M., B.W. Barry, and P.H. Dugard, *Effects of freezing on human skin permeability.* J Pharm Pharmacol, 1984. **36**(4): p. 261-2.
208. Babu, R.J., et al., *The influence of various methods of cold storage of skin on the permeation of melatonin and nimesulide.* J Control Release, 2003. **86**(1): p. 49-57.
209. Hewitt, P.G., J. Perkins, and S.A. Hotchkiss, *Metabolism of fluroxypyr, fluroxypyr methyl ester, and the herbicide fluroxypyr methylheptyl ester. I: during percutaneous absorption through fresh rat and human skin in vitro.* Drug Metab Dispos, 2000. **28**(7): p. 748-54.
210. Garnett, A., *Investigation of the in vitro percutaneous absorption and skin metabolism of benzyl acetate and related compounds*, 1992: PhD Thesis University of London, UK.
211. Abdulmajed, K., C. McGuigan, and C.M. Heard, *Topical delivery of retinyl ascorbate co-drug. 5. In vitro degradation studies.* Skin Pharmacol Physiol, 2006. **19**(5): p. 248-58.
212. Wester, R.C., et al., *Human cadaver skin viability for in vitro percutaneous absorption: storage and detrimental effects of heat-separation and freezing.* Pharm Res, 1998. **15**(1): p. 82-4.
213. Castagnoli, C., et al., *Evaluation of donor skin viability: fresh and cryopreserved skin using tetrazolioum salt assay.* Burns, 2003. **29**(8): p. 759-67.
214. Messager, S., et al., *Assessment of skin viability: is it necessary to use different methodologies?* Skin Res Technol, 2003. **9**(4): p. 321-30.
215. Dao, H., Jr. and R.A. Kazin, *Gender differences in skin: a review of the literature.* Gend Med, 2007. **4**(4): p. 308-28.
216. Giacomoni, P.U., T. Mammone, and M. Teri, *Gender-linked differences in human skin.* J Dermatol Sci, 2009. **55**(3): p. 144-9.
217. Anderson, G.D., *Gender differences in pharmacological response.* Int Rev Neurobiol, 2008. **83**: p. 1-10.
218. James, G.T., *Inactivation of the protease inhibitor phenylmethylsulfonyl fluoride in buffers.* Anal Biochem, 1978. **86**(2): p. 574-9.
219. Eng, H., et al., *Utility of the carboxylesterase inhibitor bis-para-nitrophenylphosphate (BNPP) in the plasma unbound fraction determination for a hydrolytically unstable amide derivative and agonist of the TGR5 receptor.* Xenobiotica, 2010. **40**(6): p. 369-80.
220. Hewitt, P.G., J. Perkins, and S.A. Hotchkiss, *Metabolism of fluroxypyr, fluroxypyr methyl ester, and the herbicide fluroxypyr methylheptyl ester. II: in rat skin homogenates.* Drug Metab Dispos, 2000. **28**(7): p. 755-9.
221. Imai, T., *Human carboxylesterase isozymes: catalytic properties and rational drug design.* Drug Metab Pharmacokinet, 2006. **21**(3): p. 173-85.

222. Hikima, T. and K. Tojo, *Binding of prednisolone and its ester prodrugs in the skin.* Pharm Res, 1997. **14**(2): p. 197-202.
223. Lorentz, K., W. Wirtz, and T. Weiss, *Continuous monitoring of arylesterase in human serum.* Clin Chim Acta, 2001. **308**(1-2): p. 69-78.

8 Curriculum vitae

8 Curriculum Vitae

Der Lebenslauf ist in der Online-Version aus Gründen des Datenschutzes nicht enthalten.

9 Eidesstattliche Erklärung

9 Eidesstattliche Erklärung

Hiermit bestätige ich, Wiebke Antonia Klipper, dass ich die vorliegende Arbeit selbstständig angefertigt habe. Ich versichere, dass ich ausschließlich die angegebenen Quellen und Hilfen in Anspruch genommen habe.

Berlin, den _____

Wiebke Antonia Klipper